# Manual for Using Fluorescent Microspheres to Measure Regional Organ Perfusion

Fluorescent Microsphere Resource Center
University of Washington
Division of Pulmonary and Critical Care Medicine
Box 356522
Seattle, WA 98195-6522
U.S.A.

Revised: Dec 31, 2015

Telephone: (206) 543-3166
Facsimile: (206) 685-8673
Email: glenny@u.washington.edu
Internet: http://fmrc.pulmcc.washington.edu/

# Table of Contents

# 1 The Fluorescent Microsphere Resource Center (FMRC)

## Purpose of the FMRC and this Manual

The Fluorescent Microsphere Resource Center (FMRC) developed from the need to identify and develop nonradioactive methods for measuring regional organ blood flow. This manual is intended to serve as a practical reference for scientists who are beginning to use fluorescent microspheres to measure regional organ perfusion.

### The Fluorescent Microsphere Resource Center

The purpose of the FMRC is to provide a forum to exchange information among scientists regarding new methods for measuring regional organ blood flow as well as to continue the development of new methods.

Since its introduction by Rudolf and Heyman (1967), measurement of regional organ blood flow using radio-labeled microspheres has become the gold standard. However, there are increasing concerns regarding health and environmental hazards and expense associated with special handling, disposal and limited shelf-life.

Techniques using fluorescent microspheres to measure regional organ blood flow have only recently been developed and validated against traditional radioactive methods (Glenny, et al. 1993; Prinzen, et al. 1994; Van-Oosterhout, et al. 1995). Fluorescent methodologies are evolving rapidly and are currently being used world-wide. The FMRC serves as a focal point for compilation and dissemination of information regarding fluorescent technology.

The FMRC is a nonprofit organization located at the University of Washington. It is supported as a core facility by multiple investigators in the Division with grants from the NIH. Funds from private industry also support the FMRC with the understanding that these funds will be used to promote the advancement of the scientific process rather than exploitation of commercial interests.

### The FMRC Manual

This manual serves as a primer and practical reference for scientists planning to use fluorescent microspheres to measure regional organ perfusion. The manual includes information on all aspects of fluorescent microsphere techniques related to the measurement of regional organ perfusion. Information about the physical properties of fluorescent microspheres, their preparation and injection, and techniques for their recovery are provided. The manual also includes a short tutorial on the principles and measurement of fluorescence. The specifics of using a spectrophotometer are addressed. The manual is

continually revised and updated based on comments, requests, and contributions from users. For this manual to serve its intended purpose, feedback from users is essential. We need to know what works and what does not. Please let us know about sections of the manual that are not clear.

A secondary purpose of this manual is to answer frequently-asked questions (FAQ's). If an answer cannot be found in the manual, personnel at the FMRC or users of the FMRC list server will respond to specific questions.

# Obtaining Information from the FMRC

Distribution of information on fluorescent microsphere methods is accomplished through the following modalities:

- **Electronic mail**. Personnel at the FMRC answer this mail and return requested information and manuals. Electronic mail should be sent to:

  glenny@u.washington.edu

- The FMRC has a **home page** on the internet. This web site is updated regularly and provides a convenient interface to browse through FMRC information or download pertinent files. The web site includes recent announcements, the latest manuals and current WINFAC analysis software. Documents are available in Adobe Acrobat™ PDF format for easy viewing and printing. High-quality images of fluorescent microspheres are also available through the web site. The FMRC home page is:

  http://fmrc.pulmcc.washington.edu/

- A **FAX** machine receives requests and transmits information to those scientists who do not have access to the Internet. The fax number is: (206) 685-8673.

- Requests for information or questions can also be answered through **postal mail**. The FMRC may be contacted at the following address:

  Fluorescent Microsphere Resource Center
  University of Washington
  Box 356522
  Seattle, WA 98195-6522
  USA

- Scientists are encouraged to **visit** the FMRC Laboratory. Visitors are welcome to participate in experiments or simply observe. Scientists may conduct their own experiments if previously cleared by the University of Washington Animal Care Committee.

# References

Glenny, R. W., S. Bernard and M. Brinkley. Validation of fluorescent-labeled microspheres for measurement of regional organ perfusion. *J Appl Physiol*. 74:2585-97, 1993.

Prinzen, F. W. and R. W. Glenny. Developments in non-radioactive microsphere techniques for blood flow measurement. *Cardiovasc Res*. 28:1467-75, 1994.

Rudolph, A. M. and M. A. Heymann. The circulation of the fetus in utero. Methods for studying distribution of blood flow, cardiac output and organ blood flow. *Circ Res*. 21:163-84, 1967.

van Oosterhout, M. F., H. M. Willigers, R. S. Reneman and F. W. Prinzen. Fluorescent microspheres to measure organ perfusion: validation of a simplified sample processing technique. *Am J Physiol*. 269:H725-33, 1995.

# 2 Tutorial on Fluorescence and Fluorescent Instrumentation

## Brief Tutorial on Fluorescence

Fluorescence occurs when a molecule absorbs light photons from the u.v.-visible light spectrum, known as excitation, and then rapidly emits light photons as it returns to it's ground state. Fluorimetry characterizes the relationship between absorbed and emitted photons at specified wavelengths. It is a precise quantitative analytical technique that is inexpensive and easily mastered. This chapter outlines the basic concepts and theories on instrument setup and fluorescent dyes in solution.

All chemical compounds absorb energy which causes excitation of electrons bound in the molecule, such as increased vibrational energy or, under appropriate conditions, transitions between discrete electronic energy states. For a transition to occur, the absorbed energy must be equivalent to the difference between the initial electronic state and a high-energy state. This value is constant and characteristic of the molecular structure. This is termed the excitation wavelength. If conditions permit, an excited molecule will return to ground state by emission of energy through heat and/or emission of energy quanta such as photons. The emission energy or wavelength of these quanta are also equivalent to the difference between two discrete energy states and are characteristic of the molecular structure.

Fluorescence occurs when a molecule absorbs photons from the u.v.-visible light spectrum (200-900 nm), causing transition to a high-energy electronic state and then emits photons as it returns to its initial state, in less than $10^{-9}$ sec. Some energy, within the molecule, is lost through heat or vibration so that emitted energy is less than the exciting energy; i.e., the emission wavelength is always longer than the excitation wavelength. The difference between the excitation and emission wavelengths is called the Stokes shift.

Fluorescent compounds or fluorophors can be identified and quantified on the basis of their excitation and emission properties. Figure 2-1 shows the excitation and emission spectra of a yellow-green fluorescent dye (Molecular Probes, Inc.). The excitation spectra is determined by measuring the emission intensity at a fixed wavelength, in this case 506 nm, while varying the excitation wavelength. The emission spectra is determined by measuring the variation in emission intensity wavelength for a fixed excitation wavelength, in this case 495 nm.

As shown in Figure 2-1, this dye has a detectable emission intensity for a broad excitation range (440-492 nm). Maximum emission occurs at a unique excitation wavelength of 495 nm. Emitted light is detected for a broad wavelength range (492–600 nm), however, when excited at 495 nm, maximum emission occurs at 506 nm. The excitation and emission properties of a compound are fixed, for a given instrument and environmental condition, and can be used for identification and quantification.

The principal advantage of fluorescence over radioactivity and absorption spectroscopy is the ability to separate compounds on the basis of either their excitation or emission spectra, as opposed to a single spectra. This advantage is further enhanced by commercial fluorescent dyes that have narrow and

distinctly separated excitation and emission spectra. Table 2-1 lists excitation and emission wavelength pairs which cause maximum emission for 10 common fluorescent dyes.

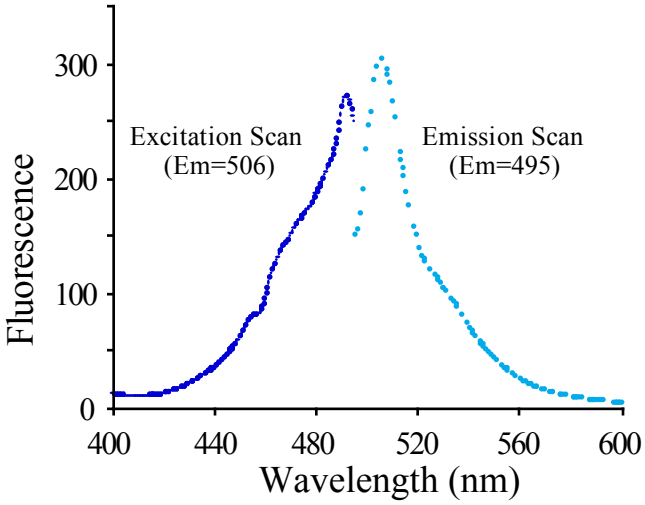


Figure 2-1

Excitation and emission spectra of a yellow-green fluorescent dye (Molecular Probes, Inc.). The Stokes shift of this dye is relatively small (11 nm). In theory, peak intensity of the excitation and emission scans should be equivalent.

Although, maximum emission occur only for specific excitation and emission wavelength pairs, the magnitude of fluorescent intensity is dependent on both intrinsic properties of the compound and on readily controlled experimental parameters, including intensity of the absorbed light and concentration of the fluorophor in solution.

The intensity of emitted light, F, is described by the relationship

$$F = \phi I_0(1-e^{-\varepsilon bc}) \quad (1)$$

where $\phi$ is the quantum efficiency, $I_0$ is the incident radiant power, $\varepsilon$ is the molar absorptivity, $b$ is the path length of the cell, and $c$ is the molar concentration of the fluorescent dye (Guilbault, 1990) .

The quantum efficiency is the percentage of molecules in an excited electronic state that decay to ground state by fluorescent emission; i.e., rapid emission of a light photon in the range of 200-900 nm. This value is always less than or equal to unity and is characteristic of the molecular structure. The quantum efficiency for some fluorescent dyes is presented in Table 2-1. A high efficiency is desirable to produce a higher relative emission intensity. All non-fluorescent compounds have a quantum efficiency of zero.

The intensity of the excitation light, which impinges on the sample, depends of the source type, wavelength and other instrument factors. The light source, usually mercury or xenon, has a characteristic spectrum for emission intensity relative to wavelength. The properties and advantages of sources are discussed below in the Instrumentation Section.

For dilute concentrations, where $\varepsilon bc < 0.05$, equation (1) reduces to the form:

$$F = k\phi I_0 \varepsilon bc \quad (2)$$

Table 2-1
Excitation/Emission Wavelengths and Quantum Efficiencies of Fluorescent Dyes in 2-ethoxyethyl acetate

| Color | Excitation Wavelength ($l_{ex}$, nm) | Emission Wavelength ($l_{em}$, nm) | Quantum Efficiency |
|---|---|---|---|
| Blue | 360 | 423 | 0.7 |
| Blue-Green | 430 | 467 | 0.7 |
| Green | 445 | 492 | 0.7 |
| Yellow-Green | 485 | 506 | 0.9 |
| Yellow | 517 | 524 | 0.9 |
| Orange | 534 | 552 | 0.9 |
| Orange-Red | 553 | 569 | 0.9 |
| Red | 566 | 598 | 0.9 |
| Crimson | 610 | 635 | 0.4 |
| Scarlet | 646 | 680 | 0.1 |

If $\phi$, $I_0$, $\varepsilon$ and $b$ remain constant, the relationship between the fluorescence intensity and dye concentration is linear (Guilbault, 1990).

At high dye concentrations or short path lengths, fluorescence intensity relative to dye concentration decreases as a result of "quenching". As the concentration of molecules in a solution increases, probability increases that excited molecules will interact with each other and lose energy through processes other than fluorescent emission. Any process that reduces the probability of fluorescent emission is known as quenching. Other parameters that can cause quenching include presence of impurities, increased temperature, or reduced viscosity of the solution media (Guilbault, 1990).

# Introduction to Experimentation

A schematic representation of a fluorimeter is shown in Figure 2-2. The light source produces light photons over a broad energy spectrum, typically ranging from 200 to 900 nm. Photons impinge on the excitation monochromator, which selectively transmits light in a narrow range centered about the specified excitation wavelength. The transmitted light passes through adjustable slits that control magnitude and resolution by further limiting the range of transmitted light. The filtered light passes into the sample cell causing fluorescent emission by fluorphors within the sample. Emitted light enters the emission monochromator, which is positioned at a 90º angle from the excitation light path to eliminate background signal and minimize noise due to stray light. Again, emitted light is transmitted in a narrow range centered about the specified emission wavelength and exits through adjustable slits, finally entering the photomultiplier tube (PMT). The signal is amplified and creates a voltage that is proportional to the measured emitted intensity. Noise in the counting process arises primarily in the PMT. Therefore, spectral resolution and signal to noise is directly related to the selected slit widths.

Since source intensity may vary over time, most research grade fluorimeters are equipped with an additional "reference PMT" which measures a fraction of the source output just before it enters the excitation monochromator, and used to ratio the signal from the sample PMT.

Not all fluorimeters are configured as described above. Some instruments employ sets of fixed band-pass filters rather than variable monochromators. Each filter can transmit only a select range of wavelengths. Units are usually limited to 5 to 8 filters and are therefore less flexible. Fiber optics are also employed for "surface readers", to transmit light from the excitation monochromators to the sample surface and then transport emitted light to the emission monochromators. This setup has the advantage of speed, but has the disadvantages of increased signal to noise, due to the inline geometry, and smaller path length which increase the probability of quenching.

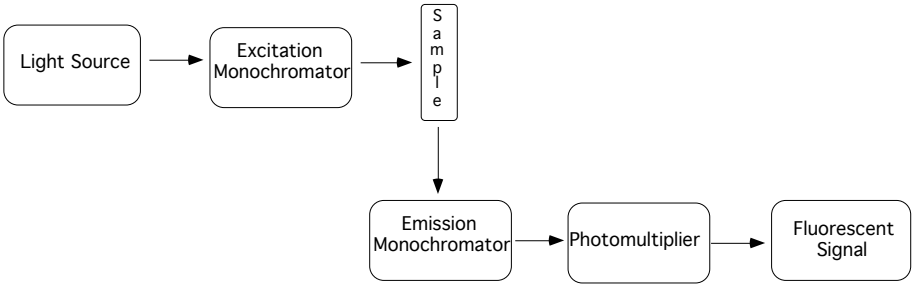


Figure 2-2 Top:

Schematic representation of a fluorescence spectrophotometer. The excitation and emission monochromators are variable band-pass filters.

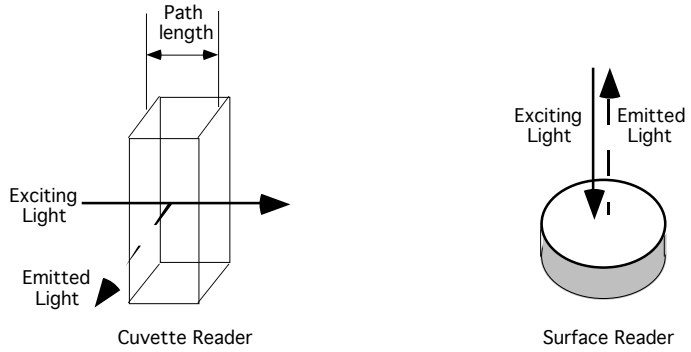


Figure 2-2 Bottom:

Two methods of measuring fluorescence. The cuvette reader excites the sample over the entire path length and reads the emitted light at right angles. The surface reader excites the sample from the top and reads the emitted light returning along the same path direction.

Fluorescent methods have three significant advantages over absorption spectroscopy. First, two wavelengths are used in fluorimetry, but only one in absorption spectroscopy. Emitted light from each fluorescent color can be easily separated because each color has unique and narrow excitation spectra. This selectivity can be further enhanced by narrowing the slit width of the emission monochromator so that only emitted light within a narrow spectral range is measured. Multiple fluorescent colors within a single sample can quantified by sequential measurement of emitted intensity using a set of excitation and emission wavelength pairs specific for each color. The second advantage of fluorescence over absorption spectroscopy is low signal to noise, since emitted light is read at right angles to the exciting light. For absorption spectrophotometry, the excitation source, sample and transmitted light are configured in line, so that the absorption signal is the small difference between the exciting light and the transmitted light, both of which are quite intense. The third advantage is that fluorescent methods have a greater range of linearity. Because of these differences, the sensitivity of fluorescence is approximately 1,000 times greater than absorption spectrophotometric methods (Guilbault, 1990).

A major disadvantage of fluorescence is the sensitivity of fluorescence intensity to fluctuations in pH and temperature. However, pH effects can be eliminated by using nonaqueous solvents, and normal room temperature fluctuations do not significantly affect the fluorescence intensities of commercial dye solutions.

It is important to consider interactions between different types of compounds in a given solution. For instance, one potential problem with neighboring fluorescent colors is that the emitted photons from one compound may cause excitation of a compound that fluoresces at a longer excitation wavelength, causing a reduction in the observed emitted intensity. This would be greatest when the emission wavelength overlaps the excitation wavelengths of two colors. An example is shown in Figure 2-3, where the emission light from the red dye is measured in a solution containing increasing concentrations of crimson dye. It was found that the decrease in red emission intensity was less than 3% for crimson concentrations that were almost three-fold greater than the red microspheres. Potential interactions should be considered when choosing combinations of colors for use in experiments requiring multiple fluorescent microspheres. Future quantification of absorption and emission effects caused by companion dyes will enable us to apply a mathematical correction matrix to reduce a source of error and allow greater flexibility in choice of color combinations.

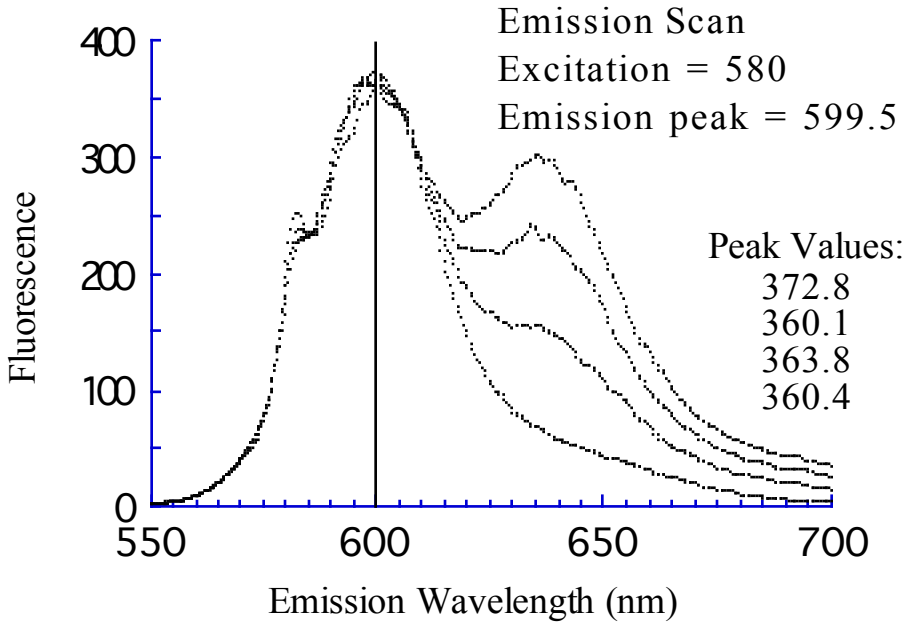


Figure 2-3

Emission spectra of mixtures of red and crimson fluorescent dye (at an excitation wavelength of 580 nm). Per ml of solvent, 2,500 red microspheres were present together with 0, 2,000, 4,000 or 6,000 crimson microspheres. With increasing crimson concentration the reading for red decreases (<3%) due to absorption of the emitted red fluorescence by the crimson (see text). Note that the emission signal at 640 nm (peak of crimson emission) is not read when the sample is excited at 580 nm.

A significant problem can arise when absorption of excited or emitted light from a fluorescent dye occurs in the presence of non-fluorescent substances, significantly decreasing the fluorescence signal and causing erroneous results. Nonfluorescent dyes commonly used for vital stains in tissue samples absorb light from 400- to 680-nm wavelengths. Absorption curves of five commonly used nonfluorescent dyes are shown in Figure 2-4. These dyes significantly interfere with excited and/or emitted light from the dyes in the fluorescent microspheres. Users should check vital dyes to see if they fluoresce and when they do not, assume they can be used in conjunction with fluorescent dyes without considering the absorption characteristics of vital dyes. A simple method is used to determine if a substance interferes with your fluorescence signal. Make a fluorescent sample containing the fluorescent dyes of interest and read them at the appropriate excitation and emission wavelengths. Add the vital dye or other substance to the solution and reread the fluorescence, taking into account any dilution that may have occurred. If the fluorescent signals are the same, your vital dye probably does

not affect your fluorescence signal. **Note:** It is best to test this with fluorescence signals and vital dye concentrations in the ranges commonly encountered.

Many fluorescent compounds interact with the excitation light to decompose or otherwise change their structure. To minimize this possibility, an excitation energy of the longest wavelength that results in a detectable fluorescent emission may be more suitable than employing peak excitation energy (Guilbault, 1990).

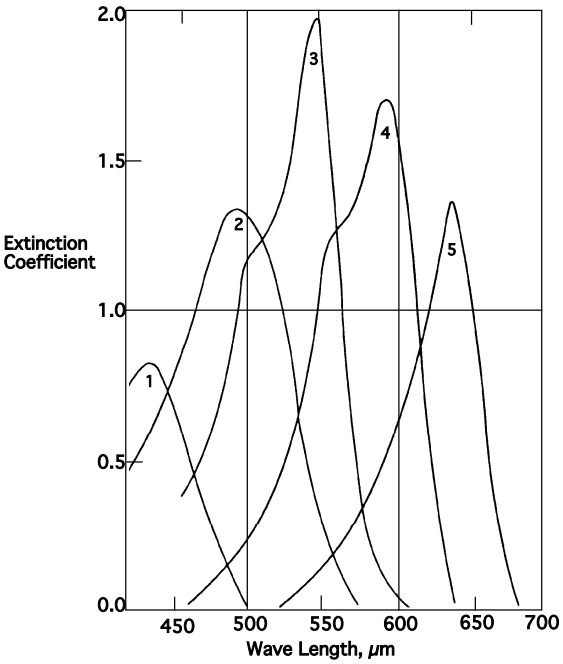


Figure 2-4:

**Absorption spectra** of five different dyes: 1) Tartrazine (yellow); 2) orange G; 3) fuchsin (red); 4) crystal violet; and 5) Neptune blue BG (patent blue V).

# Fluorescence Instrumentation

## Perkin-Elmer LS-50B

To obtain accurate data, it is necessary to understand several key aspects of fluorescence spectrophotometry and how these pertain to use of the LS-50B.

All fluorescence instruments contain three basic elements: a source of light, a sample holder, and a detector (Figure 2-2). To be of analytical utility, a system must be equipped with adjustable monochromators that can accurately select excitation and emission wavelengths. It is also essential to monitor and correct any fluctuations in source intensity. The Perkin-Elmer Models LS-50 and LS-50B Luminescence Spectrometer measure the fluorescence intensity of samples in either a continuous scan over a range of wavelengths or at select excitation and emission wavelength pairs. Blood flow analysis data require accurate detection of fluorescence intensities for a sample containing multiple fluorophores. This can be accomplished accurately and rapidly by using a wavelength program that performs serial intensity measurements on a single sample at predefined excitation and emission wavelength pairs.

## The Xenon Source

The LS-50B employs a pulsed xenon source that produces a high output using a low voltage, 9.9 watts, resulting in longer lamp life with minimal ozone and heat production. Equally important, the pulsed source reduces potential photobleaching of the sample, during analysis, by several orders of magnitude over continuous sources. The xenon flash lamp produces a 10-µsec pulse of radiation in 16 msec. In fluorescence mode, the photomultiplier tube detector is gated for an 80-msec period in synchronization with the lifetime of the lamp pulse.

## Photomultiplier Tube

A photomultiplier dark current is acquired prior to the onset of each lamp pulse and is subtracted from that pulse for correction of phototube dark current. The instrument measures and corrects every flash of the lamp to improve sensitivity at low levels of fluorescence, making it possible to measure samples in room light, thus freeing the user from working through septa in light-tight compartments.

## Determining Fluorescence Ratios (LS-50B)

Intensity of emitted light depends on a number of factors, including intensity of incident exciting light (the more powerful the exciting light, the stronger the emitted fluorescence intensity). All light sources currently used in fluorescence instrumentation lack stability over long periods. This causes the output of a xenon lamp to fluctuate as a function of time, which affects measured fluorescence intensity of a given sample, all other conditions being equal. To perform accurate quantitative analyses, these fluctuations must be monitored and corrected to the measured fluorescence intensity. The LS-50B automatically makes this correction by determining the ratios of real-time lamp intensity to sample intensity. The lamp intensity is monitored continuously with a beam splitter to divert a portion of the exciting light to a reference photomultiplier tube (just after it exits the excitation monochromator and prior to entering the sample compartment). The output signal ratio is then scaled and multiplied by a rhodamine correction spectrum stored within the instrument. Comparison with the rhodamine spectrum corrects the wavelength-dependent response of the photomultiplier tubes and the transmission characteristics of the beam splitter. Determining source ratios permits sample fluorescence to be measured free of lamp-related artifacts.

## Signal Processing (LS-50B)

When operated in wavelength programming mode, the instrument automatically sets the excitation and emission wavelengths for each dye and dwell time for the specified integration time. The instrument then averages the appropriate number of lamp pulse cycles for the specified integration time. Longer integration time reduces the signal-to-noise ratio for the sample fluorescence intensity. When calculating the optimal sample integration, consider that 1) there are 60 lamp pulses per sec, and 2) the noise in a sample measurement is reduced by the square root of the number of lamp pulses used. Because of the square root relationship between noise reduction and pulse number, there is a point of diminishing return for long integration times. An integration time exceeding 2 sec is necessary only when fluorescence

intensities being measured are very small. **Note:** Long integration times (>5 sec) for multi-component samples can result in prohibitively long total analysis time.

## Slit Settings (LS-50B)

An important feature of the LS-50B is the availability of continuous variable slit adjustment (0.1-nm increments) on both the excitation and emission monochromators. This flexibility allows the user to fine-tune the instrument for both selectivity and sensitivity in dye discrimination and measurement. The slits can best be described as volume controls for the fluorescence intensity. For optimal instrumental performance, the excitation slit width automatically controls the sample photomultiplier tube voltage. This control provides an optimum signal-to-noise ratio as a function of sample intensity.

In general, a wider slit setting causes higher fluorescence signal measurements. However, because of the fluorescence ratioing system used in the LS-50B (see above), widening the excitation slit width will not increase the reported fluorescent signal ratio, but does increase sample fluorescence signal, resulting in an improved signal-to-noise ratio.

The spectral overlap of dyes used for blood flow analysis can be significant when all available dyes are employed in one experiment; wide slit settings should be avoided in these experiments as they prevent accurate separation of colors. For assays that require five or fewer dyes, the judicious selection of dyes that have minimal or no spectral overlap can be selected (see recommended color combinations in Section 4). As a result, slit settings up to 10-15 nm can be employed for maximum sensitivity. For assays using more than five dyes, care must be taken to insure that a wide slit setting will not result in significant cross-talk between adjacent dyes. With these types of assays there will always be a trade-off between sensitivity and selectivity of dye discrimination.

Solvent and tissue background fluorescent signals can become significant as slit widths are increased. High background signals in the Blue region are frequently seen when using the extraction method with lung tissues. We have no experience with other tissue, but recommend testing all tissue for background fluorescence (see Section 3).

## Preparation of Sample

Fluorescence is a very sensitive technique. This is the one criterion that makes it a viable replacement to many radioisotope-labeling procedures. However, it is extremely susceptible to interference by contamination of trace levels of organic chemicals. Potential sources of contamination are ubiquitous since any aromatic organic compound can be a possible source of fluorescence signal. For example, the researcher is a possible source of this type of contamination since oils secreted by the skin are fluorescent. Good laboratory procedure is essential in preventing solvents and chemicals from becoming contaminated with high background fluorescence that could hinder low-level measurements. Solvents should be of the highest level purity obtainable commercially. In addition, care must be taken to eliminate all forms of solid interference (suspended particulates such as dust and fibers). These will float in and out of the sampling area of the cuvette via convection currents, and cause false signals due to light scattering while they remain in the instrument's beam.

### Sample Temperature

All fluorophores are subject to intensity variations as a function of temperature. In general fluorescence intensity decreases with increasing temperature due to increased molecular collisions that occur more frequently at higher temperatures. These collisions bleed energy from the excited state that produces fluorescence. The degree of response of an individual compound to temperature variations is unique to each compound. While many commercially available dyes are selected for their temperature stability, care should be taken to eliminate exposure of samples to drastic temperature changes during measurement. If possible, the temperature of instrument's sample compartment should be regulated via a circulating water bath. At lower assay temperatures, higher fluorescence signal will be generated. We have found a 50% decrease in the fluorescence signal of yellow-green microspheres when exposed to 160°C for 15 minutes.

### Sample pH

Fluorescence variations due to pH changes are caused by the different ionizable chemical species formed by these changes. The results from these pH variations can be quite drastic since new ionization forms of the compound are produced. For blood flow analysis, the amount of pH variation is dependent on the tissue processing technique. A buffer step has been added to the final rinse for negative pressure filtration technique to minimize pH variations (see Section 5).

### Sample Exposure to Light

The fluorescent dyes within microspheres are very stable, losing less then 1% of their fluorescent signal in six months. Once the microspheres are dissolved in solvent, stability decreases. Exposure to sunlight has been shown to significantly degrade dye in less than one week. Therefore we recommend that the samples be stored in the dark both prior to and after extraction.

### Fluorimeter-to-Fluorimeter Variability

There is substantial machine-to-machine variability between fluorimeters, even from the same manufacturer. When the same sample is read on two different fluorimeters the fluorescence signals will not necessarily be equivalent. It may be possible to correct for this variability using the internal controls run prior to and during a fluorimeter session (see Section 3). All samples for a given experiment should be read on the same fluorimeter, using identical experimental conditions.

## Other Instruments

### Hitachi F-2000

The Hitachi F-2000 is another fluorescent spectrophotometer that has been used successfully to separate six different colors of microspheres (Chein et al., 1995). Although its spillover matrix is somewhat greater than the Perkin Elmer machine (Section 4), all colors can be easily separated if the spillover is corrected using a matrix inversion method (solving for a system of linear equations).

## ISA-Spex FluoroMax-2

The FluoroMax-2 is a commercially available spectrofluorometer that offers high sensitivity, fast-scanning capability, and selectivity for research and routine fluorescence measurements. The basic components include the source, slits, excitation monochromator, sampling compartment, reference detector, emission monochromator and detector.

### The Source

The xenon source that supplies UV performance, is mounted vertically, thereby eliminating sagging of the arc and increasing stability and useful life. The lamp lifetime extends to 1200 hours in the FluoroMax-2 system.

The xenon source is focused onto the entrance slit of the excitation monochromator with an elliptical mirror. Light collection is maximized throughout the system to provide high sensitivity. Besides insuring efficient collection, the reflective surface keeps all wavelengths focused on the slit, unlike lenses that have chromatic aberrations that make them most efficient only at one wavelength.

### The Slits

The slits themselves are bilaterally, continuously adjustable from the computer in units of bandpass (wavelength ) or millimeters. This preserves maximum resolution and instant reproducibility. The bandpass can range from 0-30 nm depending on the signal strength. For weakly fluorescing samples it is advantageous to increase the bandpass and collect more light. For highly fluorescent samples the narrow bandpass is recommended to avoid exposing the detector to too high signal levels.

### The Monochromators

The excitation monochromator is an aspheric design that insures that the image of the light diffracted by the grating fits through the slit. This is an important feature when wanting to measure fluorescence from extremely small sample volumes. The FluoroMax-2 measures high sensitivity regardless of sample volume. The gratings themselves are plane, ruled gratings that avoid the two major disadvantages of the more common concave holographic gratings: poor polarization performance and inadequate imaging during scans that throws away light. The unique wavelength drive scans the grating at speeds as high as 200 nm/s. The grating grooves are blazed to provide maximum light in the UV and visible region.

### The Reference Detector

Before the excitation light reaches the sample, a photodiode reference detector monitors the intensity as a function of time and wavelength to correct for any change in output due to age or wavelength.. The photodiode detector has a wider wavelength response range than the older, traditional rhodamine-B quantum counter, and requires no maintenance.

### The Sample Chamber

A spacious sample chamber is provided to allow the use of a long list of accessories for special samples, and encourage the user to utilize a variety of sample schemes.

### Detector

Emission detector electronics employ photon- counting for low-light-level detection. Photon counting concentrates on signals that originate from fluorescence photons, ignoring the smaller pulses originating in the pmt electronics. The more common method of analog detection adds noise and signal together hiding low signals in the noise.

The emission detector housing also contains and integral high voltage supply that is factory set to provide the maximum count rate, while eliminating most of the dark noise. An optional detector extends the useful range of the system further into the IR.

### The Emission Monochromator

All features of the excitation monochromator are also incorporated into the emission monochromator. Gratings are blazed to provide maximum efficiency in the visible.

### Computer Control

The FluoroMax-2 is controlled by a PC via a serial link. On start up, the system automatically calibrates and presents itself for either new experiments or stored routines.

### The Fluorescence Measurements

The type of scans automatically defined in the sophisticated DataMax software allow the following types of fluorescence measurements:

| | |
|---|---|
| Excitation | Constant Wavelength Analysis |
| Emission | Multiwavelength Scanning |
| Synchronous | Single Point Analysis |
| Time Base Scans | Recall Experiment |

## References

Chien, G. L., C. G. Anselone, R. F. Davis and D. M. Van-Winkle. Fluorescent vs. radioactive microsphere measurement of regional myocardial blood flow. *Cardiovasc Res*. 30:405-12, 1995.

Guilbault, G. G. Practical Fluorescence. Modern Monographs in Analytical Chemistry. 3: 1990.

# 3 Standard Curves, Fluorescent Controls, Background Fluorescence & Sources of Error

## Standard Curves

Fluorescence is linearly proportional to dye concentration in dilute samples (see Section 2). However, if the concentration is too great, quenching occurs and the relationship between fluorescence and concentration becomes curvilinear. Standard curves (shown in Figure 3-1) are constructed by analyzing serial dilutions of a single color of microsphere in solvent. They are used to evaluate a spectrophotometer's linearity as well as determine the number of microspheres per ml solvent added to each sample for a given microsphere lot. As shown in Figure 3-1 fluorescence is linear with respect to the number of microspheres in a sample at lower concentrations (generally 2,000 microspheres/ml of solvent) and becomes curvilinear at higher concentrations.

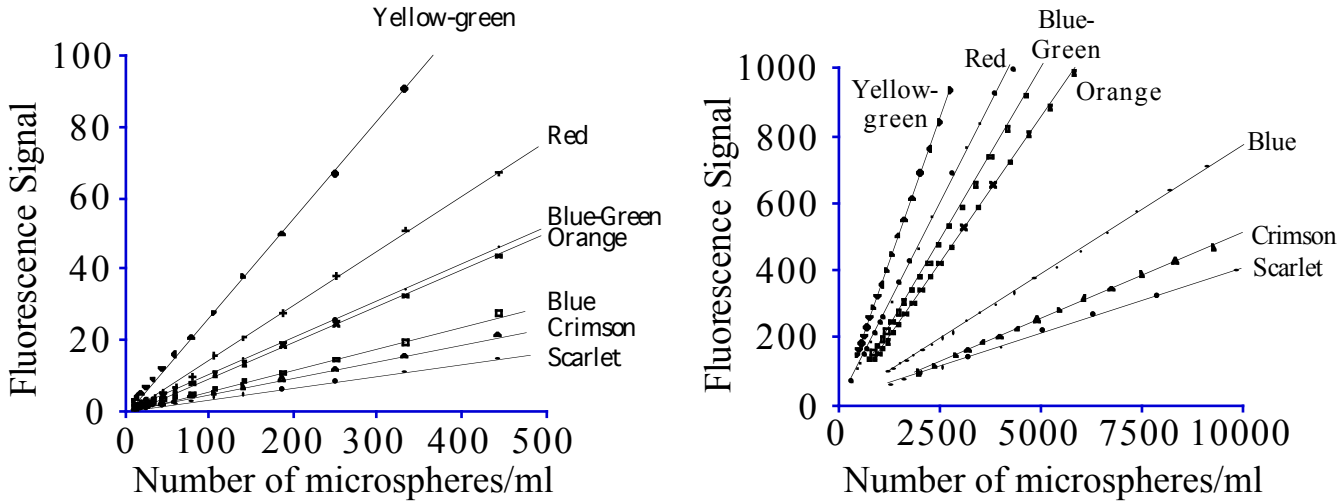


Figure 3-1 Relationship between the fluorescence intensity and the number of fluorescent microspheres per sample.

Each microsphere varies with respect to the quantum efficiency of the dye and the relative "dye load" for that lot of microspheres. These factors affect the fluorescence intensities per number of microspheres. A standard curve should be constructed for each new lot of microspheres to confirm the linearity and concentration range (see below).

## Construction of Standard Curves

1) Take 5 µl of 0.2% FluoSpheres® (5,000 fluorescent microspheres) and add it to 10 ml of solvent (we use 2-ethoxyethyl acetate). This yields the fluorescence intensities for ~500 fluorescent microspheres/ml.

2) Depending on the range of your fluorimeter (based on the manufacturer's recommended operating range), calculate the number of µl required to add to 10 ml solvent to yield a fluorescent microsphere concentration that will be just above the upper intensity limit for your fluorimeter.

3) Using this high-stock solution, make multiple serial dilutions of microspheres with very accurate pipetting. Calculate the number of microspheres per ml for each dilution.

4) The fluorescence intensities per number of microspheres per ml are plotted to yield a standard curve for that lot of microspheres.

# Fluorescence Controls

Samples of known fluorescence intensities should be measured in the fluorimeter prior to and during the running of a series of samples. Measuring these controls has three important purposes:

1) To make sure that all experimental parameters on the fluorimeter are appropriately set.
2) To check that the lamp and photomultiplier tube of the fluorimeter are functioning properly and the monochromators are appropriately set.
3) To monitor methodological noise.

A change in control intensities may be an early indication that the lamp is beginning to fail or your machine parameters are not properly set.

The best controls would be Lucite-embedded fluorescent dyes that could be used repeatedly. Unfortunately these are not currently available. We routinely make a set of control solutions of fluorescent microspheres dissolved in 2-ethoxyethyl acetate (see the following section on making a set of controls). We read these controls prior to every experimental run and after every 50 samples during a run. Using the internal control function found in the FAC or WINFAC programs (see FAC manual version 8 or higher), a control data file is generated to determine methodological noise. FAC has an automated control check that compares current control intensities to past control intensities stored in the control data file. If intensities differ by more than 5%, a message is sent to the operator that controls are out of range. Each technician should routinely evaluate controls to make sure they do not vary from day to day. Controls are also analyzed at the completion of an experiment to determine methodological noise (see components of methodological noise below). We plot the control intensities and calculate the coefficient of variation (standard deviation divided by the mean). Examples from two of our experiments, as well as "fluorimeter variability" are shown in Figures 3-2, 3-3 and 3-4. Our coefficient of variation (measurement of method noise) runs approximately 2-3% with good operator technique.

Methodological noise measured by the coefficient of variation consists of:

1) Fluorimeter (system) noise (i.e., the reproducibility of intensities without variables such as cuvette washing or cuvette orientation): The LS-50B used in our laboratory has a coefficient of variation of ~1% with the exception of scarlet, which varies up to 2% (Figure 3-2).

2) Other variability: cuvette cleaning, cuvette orientation and cuvette matching. Good technical methods are required to make sure the cuvettes remain clean. If a cuvette is not properly cleaned between samples, the method noise dramatically increases, directly decreasing the confidence in sample intensity. Other sources of operator variability include improper handling of the cuvettes (finger prints/ talcum powder) and particulate material in your sample. Poorly matched cuvettes will dramatically increase coefficient of variation. It is important to use the same set of cuvettes for all the samples from a single experiment.

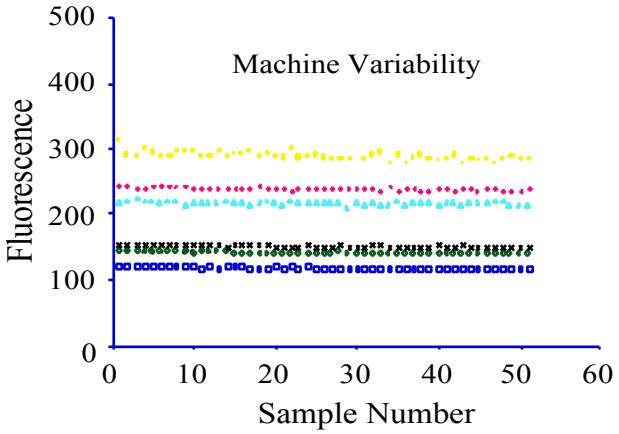


Figure 3-2
Example of machine variability from multiple reading of the control solution without moving the cuvette:

Coefficient of Variation
Blue 0.68%
Blue-Green 0.61%
Yellow-Green 0.63%
Orange 0.61%
Red 0.77%
Crimson 1.07%
Scarlet 2.11%

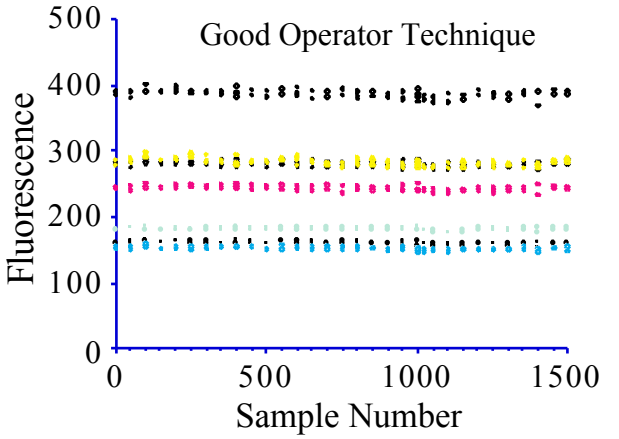


Figure 3-3
Example of a set of controls with good operator technique:

Coefficient of Variation
Blue 1.41%
Blue-Green 1.58%
Yellow-Green 1.57%
Orange 1.37%
Red 1.54%
Crimson 1.70%
Scarlet 1.93%

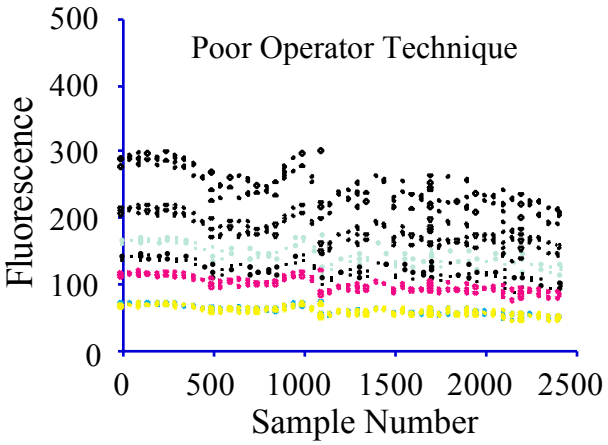


Figure 3-4
Example of a set of controls with poor operator technique

Coefficient of Variation
Blue 11.27%
Blue-Green 11.61%
Yellow-Green 11.99%
Orange 11.58%
Red 10.74%
Crimson 10.71%
Scarlet 10.39%

Figure 3-3 shows a set of controls from a "typical" data set with good operator technique. Figure 3-4 demonstrates a data set with a new technician who was not adequately cleaning the cuvettes between samples. Note the extremely high coefficient of variation.

## Making Control Solutions

When making an appropriate set of control solutions, it is important to consider the number of fluorescent microspheres per volume of solvent being used and their "typical" intensities.

1) Control solutions should have a fluorescent signal that is approximately the mean signal for each color in your sample, and be on the linear part of the standard curve, as described earlier.

2) Take 5 µl of 0.2% FluoSpheres® (5,000 fluorescent microspheres) and add it to 10 ml of solvent (we use 2-ethoxyethyl acetate). This yields fluorescence intensities of ~500 fluorescent microspheres/ml and gives a reference intensity for making your control solution.

3) Depending on the number of different colored microspheres being used ("n"), a stock solution is made by dissolving one color of microspheres in 2-ethoxyethyl acetate to yield an intensity that is the "n" times more concentrated than average intensities from an experimental sample.

4) Stock solutions are then combined to yield a control solution in the range of our "typical" sample intensities.

For example, if we use three fluorescent microsphere colors (blue-green, orange and crimson), and our "typical intensities" are 100 for blue-green, 200 for orange and 50 for crimson, we should make a stock solution 3 x 100, or 300 for blue-green, 3 x 200, or 600 for orange, and 3 x 50, or 150 for crimson. The three stock solutions are then combined to yield a 1:3 dilution to make a control solution that reads 100, 200 and 50, respectively, for blue-green, orange and crimson.

## Solvent Blanks

Solvent "blanks" are routinely read at the beginning, during, and at the end of each fluorimetry session. This allows for correction of "background" fluorescence to be subtracted from the fluorescence intensity. In our system, 2-ethoxyethyl acetate produces significant background intensities in the blue region only.

Reading solvent blanks also helps assure clean cuvettes. A high blank fluorescence intensity should flag the operator to a dirty cuvette or other problems.

# Organ Fluorescence

Tissue can fluoresce causing an increase in fluorescence intensities. With direct extraction of microspheres from air dried lung tissue soaked in 2-ethoxyethyl acetate, there is a significant contribution in fluorescence intensity in the blue region. This tissue fluorescence has an optimum peak excitation and emission pair of 320 and 405- nm, respectively. There is significant background tissue fluorescence only in the blue region. This background tissue intensity can be subtracted from the measured fluorescence intensities.

We have encountered no significant background signal caused by tissue fluorescence in microsphere extractions filtered to remove tissue particulate. Prior to beginning an experiment with new tissue types or recovery methods, we recommend the organ of interest be harvested from an animal that received no fluorescent microspheres, tissue digested, and fluorescence determined for each excitation and emission wavelength pair of interest.

**Particulate**: It is important that the sample solution be free of particulate, by careful pipetting or filtering prior to analysis. The presence of particulate in solution causes the exciting light to scatter, potentially increasing and/or decreasing sample fluorescence intensities.

# Potential Sources of Error

An insufficient number of microspheres per tissue sample will introduce error into the flow estimate. The generally accepted number of microspheres needed for accurate flow measurement is 400/piece (Buckberg, 1971). This problem is solved by increasing the number of injected microspheres.

Under low-flow situations (i.e., small pieces of tissue with very low perfusion having less than 400 microspheres in a given sample), one can determine the relative error of a measurement by the number of microspheres in the reference blood sample and the number of microspheres in the tissue sample (Nose *et al*., 1985).

Low fluorescence intensities will introduce error into the flow estimates. The lowest acceptable intensities will depend on the sensitivity of the fluorimeter being used. Using a Perkin Elmer LS-50B, the mean of the intensities should be greater than 10 (preferably greater then 50) above background tissue or background solvent intensities.

Microspheres can be lost during the filtering process and/or when transferring the filtered material into the vials in which solvent is added. Microsphere loss will be reduced if the sample can remain in a single vessel during the entire process. Correction for microsphere loss is now presented in Section 5.

If solvent volumes are not precisely reproducible, the measured concentration of fluorescence will not accurately reflect the amount of fluorescent dye per sample. An accurate repeating pipette must be used to add solvent to each sample.

Dilution errors will lead to incorrect estimates of sample fluorescence. Dilutions should be performed with an accurate pipetting technique or by weight.

Samples must be properly stored and handled once the 2-ethoxyethyl acetate has been added. All samples should be stored in the dark until ready to read as light can decay the fluorescence intensities with time. **Note:** Free dye is less stable when not bound in the microspheres; prompt processing of the samples once solvent is added is important.

Quenching of the fluorescence intensities at high concentrations will cause an underestimate of the true amount of microspheres within a sample. Samples with high fluorescence should be accurately diluted until the fluorescence intensities are within linear range of the fluorimeter. The true fluorescence intensities are then calculated from the diluted sample intensities.

Light scattering caused by particles either on the surface of the cuvette or in the solution will lead to incorrect fluorescence intensities. Cuvettes must be cleaned regularly and talc-free gloves worn when handling cuvettes. **Note:** Particulate becomes a greater problem when read at larger slit widths.

Although spillover of one color into an adjacent color is small, error can occur if adjacent color intensities are of disparate magnitudes. This can be avoided by choosing colors that do not overlap or can be corrected mathematically for spillover.

Dye degradation over time. A single dye solution should consist of solvent and the fluorescent color to be used. This solution should be read daily to determine if degradation occurs in specific color/solvent combinations. The solution intensity should be stable for as long as samples are stored in solvent prior to reading.

Fluorimeter variability will introduce error into an experiment if the characteristics of the fluorimeter change over the course of sample measurement from a given experiment. Sources of variability can be the excitation lamp, the photomultiplier tube, or the parameters set by the operator. Measuring the intensity of the known control solution (described earlier) on a routine basis provides the first indication of a fluorimeter change. It is good technique to read all samples from a given experiment within a short period of time (1-2 weeks).

Improper reference blood withdrawal methods will lead to a systematic error (multiplication factor) in calculated piece flows.

Poorly matched cuvettes will dramatically increase your coefficient of variation and decrease accuracy of your measurements. Approximately 40% of the cuvettes we receive are returned because they do not meet our variation requirement of less than 5%.

Cuvette breakage and replacement: If a different cuvette must be used while reading a series of samples from the same experiment, the differences in the cuvette intensities can be corrected by using the percent change in control intensities from initial cuvettes to new cuvettes. Figure 3-5 shows a data set corrected for a new cuvette. Figure 3-5a shows the uncorrected values and Figure 3-5b shows the corrected values.

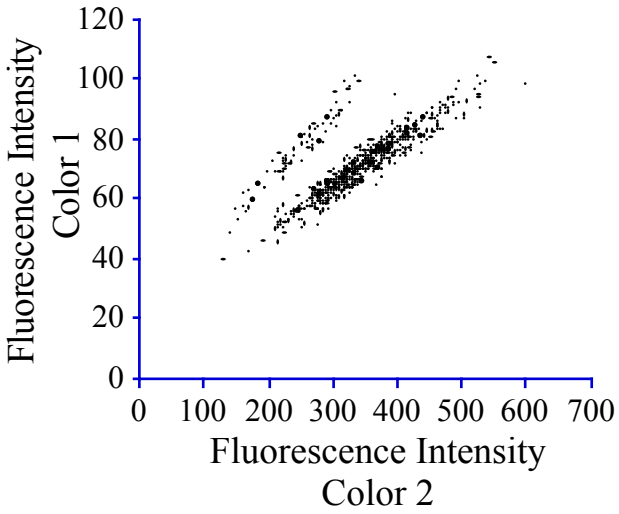


Figure 3-5a: Simultaneous injection of fluorescent microspheres. A cuvette broke during experimental readings and a new set was used to finish the experiment. The points that appear as outliers can be corrected by the percent change in control values.

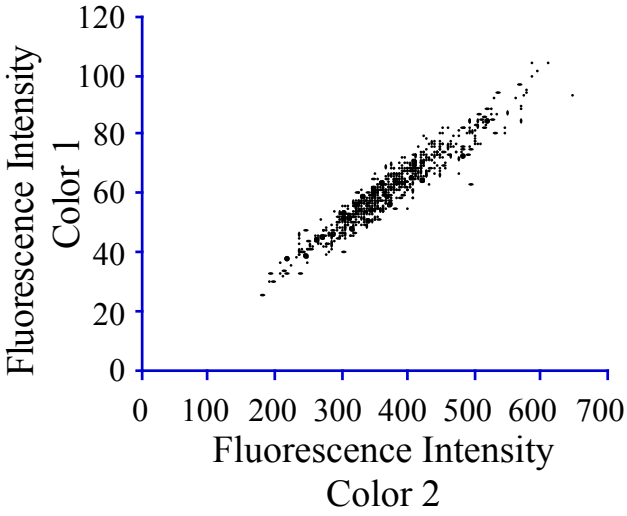


Figure 3-5b: These points have been corrected by the percent change in control values.

# 4 Fluorescent Microsphere Physical Characteristics

Fluorescent microspheres (FluoSpheres®) are available from Molecular Probes, Inc. and Triton Technologies (see Appendix A for addresses). Other Fluorescent microspheres are commercially available but have not been validated for measuring organ blood flow using the dye extraction method. The FluoSpheres® manufacturer provides the following information.

## Physical Properties

Uniform polystyrene microspheres used in regional blood flow measurements are 10 or 15 µm in diameter, with 0.2% (w/w) suspension in 10 ml (Molecular Probes) or 20 ml (Triton Tech) of saline, with 0.02% Tween-80® and 0.02% thimerosal added. Each microsphere reagent contains a single fluorescent dye that is spectrally distinct from the others. The different fluorescent dyes have the following approximate maximal excitation and emission wavelengths (nm) (Table 4-1). The exact excitation and emission spectra depend on the solvent used to extract the fluorescent dyes.

Table 4-1
Optimal Excitation and Emission Wavelengths of FluoSpheres® in 2-ethoxyethyl acetate

| Color | Excitation (nm) | Emission (nm) |
|---|---|---|
| Blue | 360 | 423 |
| Blue-Green | 420 | 467 |
| Green | 450 | 488 |
| Yellow-Green | 495 | 506 |
| Orange | 534 | 552 |
| Red | 566 | 598 |
| Crimson | 610 | 635 |
| Scarlet | 646 | 680 |

**Note:** The excitation and emission wavelengths at which the dyes are measured can be altered to provide better separation between colors.

## Storage

The microspheres are preserved from bacterial contamination by the addition of thimerosal. Microspheres can be stored at room temperature or refrigerated (DO NOT FREEZE). They should be protected from light when not in use. Sterile needles must be used to withdraw samples to avoid potential bacterial contamination. The microspheres are stable for at least one year when the recommended storage conditions are strictly observed. Do not use microspheres that show signs of deterioration.

# Indications of Deterioration

Presence of large clumps of solid matter that do not break up completely after vigorous shaking or sonication, black residue, "fuzzy" objects, or evidence of leakage may indicate that the reagents no longer meet appropriate standards for use. If there are any questions concerning the reagents, contact the vendor.

# Performance Characteristics

## Purity

The purity of the fluorescent dyes in FluoSpheres® blood flow reagents is determined by HPLC and spectrophotometric analytical techniques. Each lot of reagents has a purity of greater than 98%.

## Microsphere Uniformity

The size uniformity of FluoSpheres® is determined by flow cytometry analysis that identifies particle size distribution. Each lot has a coefficient of variation of ≤5%.

## Stability

The stability of fluorescent microspheres in aqueous suspension is evaluated for the following adverse conditions: 1) leaching of dyes into the aqueous medium during storage, and 2) reproducibility of the signal obtained from the microspheres after prolonged storage. Each lot complies with the following specifications:

1) < 1% loss of dye from microspheres after 6 months storage in dark.
2) < 10% change in fluorescent signal (3,000 microspheres/ml in xylenes) after 6 months storage in dark.
3) ~50% loss of the yellow-green signal when the microspheres are exposed to 160°C for 15 min.
4) Once the microspheres are dissolved in the solvent, a significant loss of fluorescent signal results when the dyes are stored in light.

The polystyrene beads, along with the encapsulated dye, are inert to alkaline hydrolysis when temperature is maintained below 60°C. Higher temperatures may cause softening of the beads and degradation of the fluorescence.

# Spillover of Fluorescence Into Adjacent Colors

Fluorescent dyes are designed to have narrow and well separated spectral emission bands. When excited at a specific wavelength, little spillover occurs from the emission of one color into the emission spectra of an adjacent color. For appropriately selected excitation and emission wavelength, up to seven color can be used without correction for spillover. When using more than 7 colors, the spillover of a fluorescent signal into the emission spectra of adjacent colors can be evaluated by measuring the fluorescence intensities of pure color solutions at each excitation/emission pair. These

values are used to construct a spillover matrix representing the quantity of the signal from a specific fluorescent color in each color band can be constructed (Table 4-2). Spillover can be minimized by appropriate selection of excitation and emission wavelengths, which can been seen by comparison of the following tables.

Table 4-2: Spillover Matrix of Fluorescent Colors
(Excitation and Emission Wavelengths Used to Maximize Fluorescent Signal)

| | Color Bands | | | | | | | | | |
|---|---|---|---|---|---|---|---|---|---|---|
| Color | Blue | Blue-Green | Green | Yellow-Green | Yellow | Orange | Orange-Red | Red | Crimson | Scarlet |
| Excitation | 360 | 420 | 450 | 490 | 512 | 534 | 553 | 566 | 610 | 646 |
| Emission | 420 | 467 | 488 | 506 | 522 | 552 | 569 | 598 | 635 | 680 |
| Blue | 100.0 | 0.0 | 0.0 | 0.0 | 0.0 | 0.0 | 0.0 | 0.0 | 0.0 | 0.0 |
| Blue-Green | 1.2 | 100.0 | 28.7 | 0.1 | 0.0 | 0.0 | 0.0 | 0.0 | 0.0 | 0.0 |
| Green | 0.0 | 10.6 | 100.0 | 14.6 | 0.0 | 0.0 | 0.0 | 0.0 | 0.0 | 0.0 |
| Yellow-Green | 0.0 | 0.0 | 4.2 | 100.0 | 20.0 | 0.0 | 0.0 | 0.0 | 0.0 | 0.0 |
| Yellow | 0.0 | 0.0 | 0.0 | 3.2 | 100.0 | 1.4 | 0.0 | 0.0 | 0.0 | 0.0 |
| Orange | 0.0 | 0.0 | 0.0 | 0.1 | 6.1 | 100.0 | 12.6 | 0.3 | 0.0 | 0.0 |
| Orange-Red | 0.0 | 0.0 | 0.0 | 0.0 | 0.0 | 13.9 | 100.0 | 10.7 | 0.0 | 0.0 |
| Red | 0.0 | 0.0 | 0.0 | 0.0 | 0.0 | 0.2 | 9.6 | 100.0 | 0.7 | 0.0 |
| Crimson | 0.0 | 0.0 | 0.0 | 0.0 | 0.0 | 0.0 | 0.8 | 2.6 | 100.0 | 1.1 |
| Scarlet | 0.0 | 0.0 | 0.0 | 0.0 | 0.0 | 0.0 | 0.0 | 0.0 | 2.0 | 100.0 |

* Spillover matrix was constructed on a Perkin-Elmer LS-50B with excitation and emission slit widths of 4 nm and a red-sensitive photo multiplier tube.

Table 4-3: Spillover Matrix of Fluorescent Colors
(Excitation and Emission Wavelengths Used to Minimize Fluorescent Spillover)

| | Color Bands | | | | | | | | | |
|---|---|---|---|---|---|---|---|---|---|---|
| Color | Blue | Blue-Green | Green | Yellow-Green | Yellow | Orange | Orange-Red | Red | Crimson | Scarlet |
| Excitation | 360 | 430 | 460 | 493 | 512 | 530 | 557 | 578 | 613 | 655 |
| Emission | 423 | 467 | 490 | 506 | 524 | 545 | 568 | 598 | 635 | 680 |
| Blue | 100.0 | 0.0 | 0.0 | 0.0 | 0.0 | 0.0 | 0.0 | 0.0 | 0.0 | 0.0 |
| Blue-Green | 1.2 | 100.0 | 7.0 | 0.0 | 0.0 | 0.0 | 0.0 | 0.0 | 0.0 | 0.0 |
| Green | 0.0 | 7.2 | 100.0 | 8.5 | 0.0 | 0.0 | 0.0 | 0.0 | 0.0 | 0.0 |
| Yellow-Green | 0.0 | 0.0 | 3.2 | 100.0 | 12.0 | 0.0 | 0.0 | 0.0 | 0.0 | 0.0 |
| Yellow | 0.0 | 0.0 | 0.0 | 2.7 | 100.0 | 1.4 | 0.0 | 0.0 | 0.0 | 0.0 |
| Orange | 0.0 | 0.0 | 0.0 | 0.1 | 4.1 | 100.0 | 2.9 | 0.3 | 0.0 | 0.0 |
| Orange-Red | 0.0 | 0.0 | 0.0 | 0.0 | 0.0 | 5.0 | 100.0 | 1.6 | 0.0 | 0.0 |
| Red | 0.0 | 0.0 | 0.0 | 0.0 | 0.0 | 0.1 | 11.4 | 100.0 | 0.3 | 0.0 |
| Crimson | 0.0 | 0.0 | 0.0 | 0.0 | 0.0 | 0.0 | 0.8 | 2.6 | 100.0 | 0.5 |
| Scarlet | 0.0 | 0.0 | 0.0 | 0.0 | 0.0 | 0.0 | 0.0 | 0.0 | 2.0 | 100.0 |

* Spillover matrix was constructed on a Perkin-Elmer LS-50B with excitation and emission slit widths of 4 nm and a red-sensitive photo multiplier tube.

The values in table 4-2 represent an amount of a given color signal in each color band and are relative to an arbitrary value of 100 for the color signal within its own color band. This spillover matrix was constructed with excitation and emission slit widths of 4 nm. As the slit widths are increased, the relative spillover of each color changes very little because the relative strength of the fluorescence signals increases markedly. This spillover matrix was constructed using a Perkin Elmer LS-50B equipped with a red-sensitive photomultiplier tube.

# Spillover Correction Methods

Currently, thirteen different colors of fluorescent microspheres are commercially available that have emission bands spaced such that spillover is low (generally less than ten percent of peak maxima) and only occurs for adjacent colors. Up to seven colors, can be used without correction for spillover. However when using more than 7 colors, spillover between some adjacent colors becomes significant and must be mathematically corrected to avoid over-estimation of some flows. Using spillover correction, up 13 colors can be used reliably to determine regional organ blood flow at 13 different points in time. Three different methods of spillover correction have been rigorously validated for blood flow measurement: 1) matrix inversion of fixed wavelength intensities 2) least squares fit of an over-determined system of linear equations for synchronous scan spectra and 3) least squares fit of combined Gaussian and Lorenzentian function for synchronous scan spectra. All three methods work well for spillover correction, and yield essentially identical results in most situations (Schimmel et al., 2001). A public domain program, FMSPILL, can be used to correct fluorescent spillover. FMSPILL enables correction for either fixed wavelength intensities, using a matrix inversion method, or for synchronous scans, using a least-squares over-determined method. Files produced from the WINFAC program can be directly read by FMSPILL. This program is available from the FMRC web site (http://fmrc.pulmcc.washington.edu/). The program currently requires a Windows® based operating system.

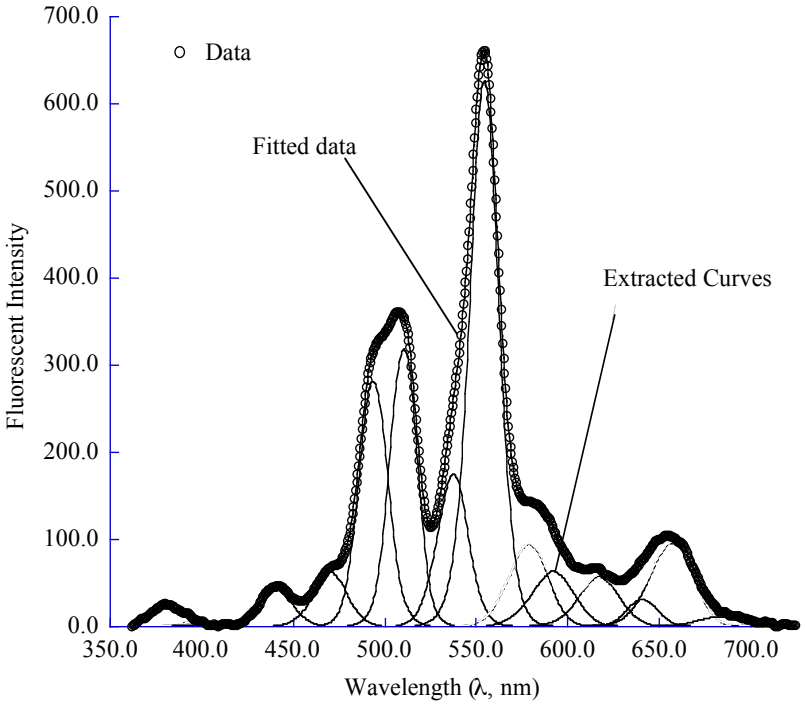


Figure 4-1 Curve extraction of 13 colors from a synchronous scan of a tissue sample with 13 different colored fluorescent microspheres.

# Choosing Appropriate Colors for an Experiment

A judicial choice of colors prior to performing an experiment will help insure optimal results. The first decision is to determine how many different measurements will be performed (separated by time and/or physiological interventions). Each measurement requires a different color. To minimize spillover and take advantage of some inherent characteristics of specific dyes, we suggest the following color combinations for a given number of colors (Table 4-4):

Any color can be used for an experiment using only one color. However, blue is the least favorable because of the high background due to tissue auto-fluorescence and solvent background in that region. Crimson and scarlet are less favorable because their quantum efficiency is relatively poor. Injecting more microspheres can compensate for this reduced efficiency. In our fluorimeter, scarlet signals are comparable to crimson even though the quantum efficiency of scarlet is less. We have found very low crimson and scarlet signals to be very linear and reliable. Spillover becomes a significant issue if colors other than those listed below are used. Hence spillover will occur if more than seven colors are used in a single experiment or if colors with excitation and emission wavelengths that fall between those listed below are used together.

Experiments using aerosols and intravenous fluorescent markers will produce fluorescent signals with significantly different intensities. Ventilation signals are usually an order of magnitude less than blood flow signals. If enough colors are used in an experiment to cause spillover problems, the colors used to mark ventilation and perfusion must be carefully selected. Colors that will have low fluorescent signals should be grouped together in the color spectrum and similarly, colors that will have high fluorescent signals should also be grouped together in the color spectrum. This will minimize the error introduced when spillover correction is used.

Table 4-4
Color Selection Guide in order of Preference. All colors except Scarlet, Blue and Blue-Green are equivalent when using a single color (see comments). The first four colors can be used without correction for spillover. Additional colors having increasing spillover in some adjacent colors.

| | Color Band | Ex WL | Em WL | Comments: |
|---|---|---|---|---|
| 1 | Yellow-Green | 493 | 506 | |
| 2 | Orange | 530 | 545 | |
| 3 | Red | 578 | 598 | when using Carmine FWL = 578/595 |
| 4 | Crimson | 610 | 635 | when using Carmine FWL = 618/636 |
| 5 | Green | 460 | 490 | spillover correction required, <5% |
| 6 | Yellow | 512 | 524 | spillover correction required, 2-8% |
| 7 | Orange-Red | 557 | 568 | spillover correction required, 2-11% |
| 8 | Scarlet | 654 | 680 | Correlation w/ RM are a few % lower than other FM |
| 9 | Blue-Green | 430 | 461 | 2-ethoxy may contain impurities which interact with BG in tissue |
| 10 | Blue | 360 | 418 | Tissue fluorescence may be significant |
| 11 | Dark Red | 639 | 650 | spillover correction required, 30% |
| 12 | Carmine | 585 | 617 | spillover correction required, 30-45% |

# References

Schimmel, C., D. Frazer and R.W. Glenny. 2001. Extending Flourescent Microsphere Methods for Regional Organ Blood Flow to 13 Simultaneous Colors. *Am. J. Physiol. Heart. Circ. Physiol.* 280: H2496-506.

# 5 Microsphere Measurement of Regional Organ Perfusion

Regional organ perfusion can be estimated with hematogenously delivered microspheres (Heyman et al., 1977). When appropriately sized microspheres are used, regional blood flow is proportional to the number of microspheres trapped in the region of interest (Bassingthwaighte et al., 1990). A number of excellent review articles describe and validate the use of microspheres for measurement of regional organ perfusion, but the classic review by Heyman *et al*. (1977) contains many details for radioactive microsphere use that apply to fluorescent microspheres.

Over the last twenty years, new and/or refined methods for measuring regional organ perfusion have been published. Many of these publications are listed in our reference section. A careful search of the literature should be done prior to starting a study to determine the most appropriate method for measuring regional organ perfusion for any given experimental protocol. It is not feasible for this manual to address the wide variety of methods currently accepted. We have outlined below, methods for measuring regional organ perfusion that we have utilized in our laboratory.

## Preparation of Fluorescent Microspheres for Injection

### Calculation of Microspheres for Injection

A minimum of 400 microspheres are needed per tissue piece to be 95% confident that the flow measurement is within 10% of the true value (Buckberg et al., 1971). If measurement of regional blood flow (ml/min) is the primary objective of a study, the number of microspheres injected must be calculated to assure a sufficient number reach the organ of interest.

The following equation estimates the minimum total number of microspheres needed per injection to accurately measure blood flow.

$$N_{min} = 400(n)/[Q_{organ}/Q_{total}] \quad (1)$$

where:

$N_{min}$ = minimum number of microspheres needed for injection

$n$ = total number of organ pieces

*Example: in a 200-gram heart, if you plan to evaluate ten, 1-gram pieces, the total number of pieces per organ should be 200 (even though you plan to evaluate only 5% of the organ).*

$[Q_{organ}/Q_{total}]$= fraction of total cardiac output supplying organ of interest

With this calculation, 400 microspheres are provided for each organ piece with an average blood flow. A piece with twice the average flow will have 800 microspheres and a piece with 0.5 times the average

flow will have 200 microspheres. We usually double the minimum number ($N_{min}$) to make sure that low-flow organ pieces also have an adequate number of microspheres (Buckberg et al., 1971; Nose et al., 1985). This 400 microsphere "rule" only applies to measurements of perfusion to a single region or organ piece. A recent paper by Polissar et al. (1999), reports that fewer microspheres are required for accurate measurements of heterogeneity and correlation. Polissar suggests a minimum of 15,000 microspheres, total, for all pieces combined for accurate measurements of heterogeneity and 25,000 microspheres, total, for accurate estimates of correlation coefficients.

## Estimating the Number of Microspheres per ml

The following equation (based on percent solids) estimates the number of microspheres per ml of microsphere suspension:

$$N(\text{microspheres/ml}) = (6.03\text{x}10^{10})(\%\text{solids})/(3.3144d^3) \quad (2)$$

where:

$d$ = diameter of microspheres in microns (μ)
% solids supplied by manufacturer (use %, 2% = 2, not 0.02)

## Calculation of Injectate Volume

$$\text{mls of suspension} = N_{\text{min}}/N(\text{microspheres/ml}) \quad (3)$$

## Preparation of FMS for Injection

**Note**: The dye "load" varies for each lot of fluorescent microspheres; therefore, signal intensities should be checked for each new lot (Section 4). Also, the number of microspheres per ml can be checked with a hemocytometer. Do not mix fluorescent microspheres from different lots.

Method:

1. Remove from refrigerator and check supernatant solution. It should be clear due to the addition of thimerosal, a bacteriostatic agent. Cloudy fluid may indicate contamination.

2. Vortex (vigorous agitation) thoroughly (5 - 15 secs).

3. Place in ultrasonic water bath for at least 2-10 min to disperses the microspheres. Do not cover water bath or sonicate too long because the heat generated can melt the microspheres. For microspheres 15 μm or smaller, sonication time is less (smaller particles are more susceptible to heat).

4. Just prior to injection, vortex the vial of microspheres again and withdraw the desired volume based on the calculated number (see Calculation of Microspheres for Injection, previous page). Do not permit the microspheres to settle once they are drawn into the syringe. If injection time is delayed, vortex them thoroughly again.

5. Injection time varies for each experimental design and must be determined prior to injection. Most left-heart injections are done over short periods of time (5-15 seconds) while the reference withdrawal pump is withdrawing the sample. A left-heart injection should not appreciably change the animal's stroke volume. Slow and steady injections allow for uniform mixing of microspheres, whereas bolus injections often result in streaming (not desirable).

   Following injection, a visible rim of microspheres will remain in the syringe if plastic syringes are used. This can be expected and is of little concern since the remaining microspheres represent only a small fraction of the total used.

6. After injection, flush the dead space of the catheter thoroughly (at least three times the volume of the catheter) and change the stopcock (microspheres get caught in the stopcocks; discard along with the used syringes after each injection to avoid contamination of subsequent injections).

# Reference Blood Flow Sampling

A reference blood flow sample allows calculation of regional flow in ml/min. It is essential that the reference blood withdrawal catheter be accurately positioned so that a representative sample of well-mixed microspheres and blood can be obtained. If pulmonary perfusion is being measured, the reference blood sample should be obtained from a pulmonary artery. If systemic organ flows are measured, reference blood samples can be obtained from the descending aorta. The blood samples should be obtained as close to the organ of interest as possible without interfering with blood flow.

The site of microsphere injection is very important. For systemic blood flow measurements, left atrial injection of microspheres are best. If a left atrial catheter is not possible, then a left ventricular catheter is adequate. Left atrial injections allow for two-chamber mixing and more uniform distribution of the microspheres in the blood. Left ventricular injections allow one chamber mixing, shown to be sufficient in most species.

The reference withdrawal pump must be accurately calibrated so that reference blood is withdrawn at a uniform rate. If problems exist in the rate of withdrawal, the reference sample is invalid. Whenever possible, two reference blood samples should be withdrawn simultaneously, in case one catheter clots or one sample is lost.

Withdrawal syringes must be large enough to hold the volume of blood in the reference sample, heparin, and dead space volume. Example: if withdrawal rate is 5 ml/min and withdrawal time is 2 min after completion of a 1-min injection, heparin volume is 1 ml and dead space is 3 ml, then the syringe volume should be 20-30 ml. Glass syringes and containers are preferred; they decrease microsphere loss caused by "static" attraction of the plastic microspheres with the plastic containers or syringes.

## Method for Reference Blood Flow Sampling

There are 2 different anticoagulants that we routinely use: Heparin (syringe coated) and Citrate Phosphate Dextrose (10 cc per 30 cc syringe).

1. Using whole blood, calibrate the reference withdrawal pump at the predetermined withdrawal rate, including the catheters, extension tubing and matched anticoagulated glass syringes that will be used for the reference withdrawal. Have new stopcocks and flush syringes available.

2. Connect the matched glass anticoagulated syringes in the withdrawal pump to the catheters and the extension tubing so that everything is set up for withdrawing the reference sample. Do not turn the stopcock on the catheters until you are ready for injection (the blood will flux into the catheter dead space and may clot).

3. Once the microspheres have been drawn into the injection syringes, start the withdrawal pump and make sure blood is flowing freely into the extension tubing.

4. Inject the microspheres over the designated time period (sec or min) followed by a flush of warmed saline three times the volume of the catheter dead space.

5. A timer is set for 2 min after completion of injection for the reference blood withdrawal. At the end of the withdrawal, the pump is turned off, the stopcocks are opened and the blood remaining in the extension tubing is drawn into the syringe.

6. Transfer blood into labeled vials for further processing (see Digestion of Blood and Tissue, next page). Rinse syringes and extension lines with 2% Tween-80® (using approximately twice the volume of the blood) and add this rinse to the blood samples.

7. Flush the catheters again and change the stopcocks.

# Calculation of Regional Perfusion

Regional perfusion to the target organ can be calculated by one of two methods.

## Flow to Each Piece Relative to the Mean

This is most easily accomplished using a computer spreadsheet, but can be processed by hand or with a computer program. If the fluorescence of each organ piece is denoted by $fl_i$, where $i$ is the sample number and $n$ is the number of pieces, then flow to piece $i$ relative to the mean, $Q_{mi}$, is given by the equation:

$$Q_{mi} = fl_i/(\Sigma fl_i/n) \qquad (5)$$

The denominator in equation 6 consists of the mean fluorescence for all of the pieces. $Q_{mi}$ is a dimensionless number.

## Flow to Each Piece in ml/min

This is most easily accomplished using a computer spreadsheet, but can be processed by hand or with a computer program. A reference blood flow sample must be obtained at the time of microsphere injection (see section on Reference Blood Flow Sampling). If the fluorescence of each organ piece is denoted by $fl_i$ where $i$ is the sample number, $fl_{ref}$ is the fluorescence of the reference blood flow sample, and $R$ is the withdrawal rate of the reference blood flow sample in ml/min, then flow to piece $i$ , $Q_i$, is given by the equation:

$$Q_i(\text{ml/min}) = (fl_i/fl_{ref})\cdot\text{R(ml/min)} \qquad (6)$$

# Recovering Microspheres from Samples for Quantification

With the exception of lung tissue, microspheres must be physically separated from the tissue or blood in order to quantify the number of microspheres in each sample. Because lung tissue is porous, direct extraction of the microspheres from air-dried tissue (dried at total lung capacity) is possible.

The most practical methods to recover the microspheres from digested tissues are:

1) Negative Pressure Filtration
2) Sedimentation
3) Perkin Elmer polyamide woven filtration devices

Blood samples anticoagulated with Citrate Phosphate Dextrose can be directly filtered with the Perkin Elmer polyamide woven filtration devices.

How samples are digested depends on the method used for microsphere recovery. As a rule, potassium hydroxide (KOH) digests kidney and heart, but does not completely digest fat (brain), fascia, cartilage, etc. Ethanolic KOH, a very powerful digestion solution, successfully digests most tissue, including brain and fascia.

**Note:** Both solutions recommended for tissue digestion are extremely caustic; adequate precaution should be used when handling these solutions.

## Blood and Tissue Digestion Followed by Negative Pressure Filtration

Tissue and **heparinized** blood samples containing microspheres must be digested to recover the microspheres. Use of glass vials with caps for tissue digestion decrease the likelihood of spillage or microsphere loss. If negative pressure filtration method is used, the volumes and concentrations of solutions are not critical. However, when using the sedimentation method, the concentration of solutions is very important (see note under sedimentation regarding specific gravity).

## Digestion of Heparinized Blood for Negative Pressure Filtration

1. Add 7 ml of 89.2% KOH (16 N, 89 g in final volume of 100 ml $H_2O$) to each 30 ml of diluted blood (see step 6 on previous page) (i.e., ~10 ml of blood plus 20 ml 2% Tween-80® rinse solution) and digest overnight.

2. Filter blood (filter pore size must be smaller than the microspheres; e.g., 10 µm for 15-µm microspheres).

   **Note**: Digested blood samples can be stored (tightly capped) at room temperature and filtered at a later date.

## Digestion of Solid Tissue for Negative Pressure Filtration

1. For each 1-2 g of solid tissue (heart, kidney, etc.), add 5-10 ml of 22.4% KOH (4 N, 22.4 g in final volume of 100 ml $H_2O$). Freshly made KOH solution, warm due to the exothermic reaction, aids in tissue digestion.

2. Digestion time varies depending on the tissue; usually 24 hours is sufficient.

Digested tissue samples should not stand unfiltered for long periods of time since fat in them may solidify.

After samples have been digested with KOH, the microspheres are physically separated by negative pressure filtration. This method is inexpensive and has been rigorously tested; however, it is labor-intensive and may cause microsphere loss when the tissue sample is transferred from one vessel to another or if the filter fails.

Assemble filtration system as shown in Figure 5-1. A new (or sometimes multiple) filter is used for each sample. We have had success with the Poretics filtration device using Poretics polycarbonate filters. Although the manufacturer states that these filters are not compatible with alkaline solutions (KOH), we have found that they work well when allowed to remain in contact with the KOH for no longer than 3 min.

1. Assemble filtration apparatus and connect to suction (make sure it does not exceed maximum value allowed for the membrane). Place filter between graduated cylinder and filter screen. Clamp graduated cylinder to filter holder.

2. Make buffer rinse solution as follows:

   - Dissolve 5.88 g potassium phosphate (monobasic) $KH_2PO_4$ in 200 ml $H_2O$ and 22.9 g.
   - Dissolve $K_2HPO_4$ potassium phosphate (dibasic) in 800 ml $H_2O$.
   - Combine the two solutions.

3. Pour digested sample into the graduated cylinder and allow suction to filter sample. Exposure time of the filter to KOH should be minimized to assure that filters remain competent. Rinse

sample tube into filtration device with 2% Tween-80® solution. Rinse graduated cylinder two to three times (approximately 20 ml).

4. Do a final rinse with the 5-10 ml of the buffer rinse solution made in step 2.

5. Let vacuum air-dry the filter.

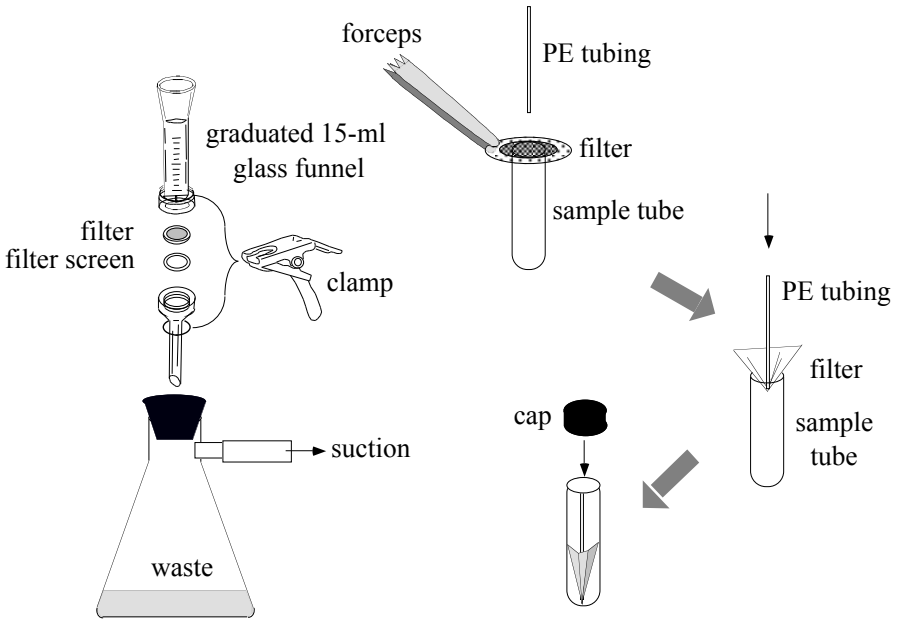


Figure 5-1

Schematic diagram for filtering apparatus using polycarbonate filters.

6. Remove filter with forceps. Handle only filter rims that are free of microspheres. Carefully place filter in sample tube with assistance from small plunger (we use PE 50 tubing [see Figure 5-1] cut into appropriate lengths). Leave the plunger in the polypropylene container, as it may contain microspheres (PE tubing will not affect the results).

   **Note:** If the filter becomes clogged with microspheres or tissue debris, the filtration process may slow or stop, due to filter failure caused by increased contact time with KOH. In this event, you should use smaller volumes of digested sample and multiple filters placed in one sample tube and the combined fluorescence measured.

## Polyamide Woven Filtration Devices

Perkin-Elmer offers filtering devices that have been specifically made to isolate fluorescent microspheres from CPD anti-coagulated blood or digested tissues. The major advantage of this system is that each tissue sample is digested, filtered, and the fluorescent dyes extracted in a single container, obviating the need to transfer materials from one vessel to another and theoretically decreasing microsphere loss. The devices are polypropylene and consist of three stages (Figure 5-2). The first stage has a polyamide membrane integrated into the bottom. Each tissue sample is placed in this first stage and digested with KOH. CPD anticoagulated blood can be directly filtered. The digested material is filtered by suction and dried by centrifugation. The filtered sample and container are then placed within the second stage and the third stage attached to the bottom of the second stage. The organic solvent is added to the first stage and then transferred to the last stage by centrifugation. The last stage then contains the organic solvent with the extracted dyes.

Figure 5-2

## Ethanolic KOH, Tissue and Blood Digestion, and Sedimentation

To use the sedimentation method for microsphere recovery, the sample must be digested in ethanolic KOH. Sedimentation of the microspheres is possible if the **specific gravity** of the solution is **less** than that of microspheres (van Oosterhout et al., 1994). Tissue digested with ethanolic KOH (as opposed to KOH in water), has a specific gravity that is much less than the microspheres. The following procedure has been successfully used for brain tissue (Powers et al., 1999).

### Solutions required:

A. 2.3 M ethanolic KOH with 0.5 % Tween 80.
B. Internal standard ( a non-study color)
C. 1% Triton X-100
D. Distilled Water Phosphate buffer
E. 0.25% Tween-80
F. 2-Ethoxyethyl acetate

### Recipes

A. 2.3 M ethanolic KOH with 0.5 % Tween 80.
   3 g KOH and 0.5 g Tween 80 are put into a glass beaker. 100 ml ethanol is added to the 100 ml line. The solution is stirred until a clear solution is obtained (approx. 20 min.).
B. Internal standard (a non-study color). **This is optional:**
   *Use a non study color*
   1. Vortex and sonicate microspheres (2% solids) in vial for 30 seconds.
   2. Vortex again and immediately withdraw 1 ml of solution with a sterile syringe.

3. Add microspheres to 100 ml of solution E (0.25% Tween-80)
4. Add stir bar and keep solution stirring with a stir bar while in use.

C 1% Triton X-100.
10 g Triton X-100 (Sigma no. X-100) is brought to 1 liter with distilled water and stirred until in solution.

D. Distilled Water Phosphate buffer (solution for rinsing)
5.88 g $KH_2PO_4$ in 200 ml distilled water (monobasic)
22.9 g $K_2HPO_4$ in 800 ml distilled water (dibasic)
Combine the two solutions.
Add 28.6 ml of the combined solution to 1000 ml distilled $H_2O$

E. 0.25% Tween-80
2.5 g Tween 80 is put into a beaker and the volume is brought up to 1 liter with distilled water. Stir with a stir bar until in solution.

F. 2-Ethoxyethyl acetate
Solvent used to dissolve microspheres and release dye (final solution for fluorimetry).

## Tubes

Polypropylene 15 ml centrifuge tubes with tightly fitting caps. Do not use polystyrene as this is what the microspheres are mode of and the 2-ethoxyethyl acetate will dissolve the tube. The tubes must be able to take 2000 x G for 20 min., 3 times. A tolerance of 6000 x G is therefore recommended.

## Taking Samples

1. Weigh 15 ml polypropylene tubes with caps.
2. Put tissue into tubes, pushing them to below the 7 ml line.
3. Store tissues for 2 weeks at room temp (in a fume hood) for autolysis to occur. If the samples have been stored cold, let them stand out for at least 2 days prior to processing.

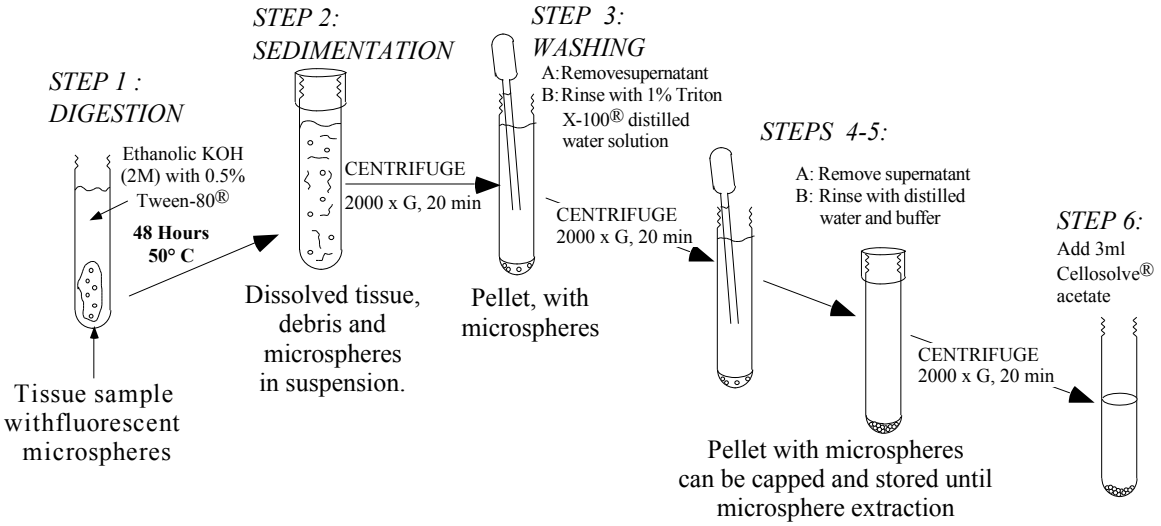


Figure 5-3:

Schematic diagram for sedimentation microsphere recovery.

## Tissue Processing

Day 1:

1. Weigh tubes and record tissue weight.
2. Add exactly 200 µl internal standard (if internal standards are being used)
3. Add approximately 8 ml ethanolic KOH. (Step 1)
4. Cap tightly and vortex for 20 sec.
5. Put tubes into 50 degree centigrade water bath with shaker.
6. Vortex at 24 hours for 20 sec per tube.

Day 3

1. Vortex at 48 hours or until particles are re-suspended (about 30 seconds). (Step 2). After vortexing, all samples, vortex again for 5 sec.
2. Centrifuge 20 min at 2000 x G.
3. Take off all but 1.5 ml supernatant using a Pasteur pipette attached to suction with a trap, and discard sup.
4. Add approximately 8 ml 1% Triton X-100 and vortex for 30 second. (Step 3)
5. Centrifuge 20 min., 2000 x G.
6. Take off all but 0.5-1 ml supernatant and discard. (Step 4)
7. Add 7 ml distilled water phosphate buffer to each tube. .(Step 5)
8. Vortex for 30 seconds until all particles are suspended.
9. Centrifuge 20', 2000 x G
10. Take off all but 1.0 ml sup and discard, using the suction with trap.
11. Remove all but 150 microliters of sup carefully by hand using a Pasteur pipette. (Step 6) More than 150 µl water when mixed with 2-Ethoxyethyl acetate creates two phases.
12. Add 3 ml 2-Ethoxyethyl acetate and vortex until particles are well suspended. Let samples sit in the dark and away from heat for 5 days.
13. Let samples sit in the dark and away from heat for 5 days.

Day 5

1. Vortex gently until pellet breaks up (approximately 20 sec).

Day 8

1. Vortex vigorously until pellet breaks up (approximately 30 seconds)
2. Centrifuge 20', 2000 x G
3. Supernatant is then used for fluorimetry-read all blood and tissue samples on the same day.

**WARNING**: Tissue digested with ethanolic KOH cannot be filtered through Poretics polycarbonate filters because the filters will not withstand the ethanolic KOH. The ethanol available in Europe contains additives to discourage human consumption. These additives turn the ethanol brown in the presence of KOH, which renders the ethanol unsuitable for use in this technique.

Additional notes:

1. do not mix caps up, it may render your weights in accurate.
2. Spilled ethanolic KOH or Cellosolve can remove writing on tubes
3. Accurate volumes of 2-Ethoxyethyl acetate are required for accurate flow measurements.

# Quantification of Fluorescent Microspheres

## Internal Standard Test for Complete Microsphere Recovery

The method introduced by Chien et al. (1995) is used to check and correct for any microsphere loss during the filtration or sedimentation process. A known amount of microspheres of a color not used in your experiment is added to each sample vial of tissue prior to digestion. This microsphere acts as an internal standard. After the filtration or sedimentation is complete, all samples should have comparable signals. If large discrepancies in the signal between samples exist, your technique should be evaluated to determine the source of loss. If discrepancies are small, the microsphere signals can be corrected by the proportion of loss to yield a corrected set of signals for each sample. The correction formula is:

$$I_{true} = I_{obs} \cdot \left( \frac{I_{st,true}}{I_{st,obs}} \right) \quad (4)$$

Where $I_{true}$ is the true fluorescence signal, $I_{obs}$ is the observed (measured) fluorescence signal, $I_{st,true}$ is the true florescence standard signal and $I_{st,obs}$ is the measured fluorescence standard signal. This method assumes that the relative number of lost microspheres is similar for the internal standard and all other colors.

## Fluorescent Dye Extraction

### Organic Solvent for Fluorescent Dye Extraction

The following organic solvent has been tested and used extensively to dissolve the microspheres and release the encapsulated dyes:

| Solvent | Boiling Point | Hazard |
|---|---|---|
| 2-ethoxyethyl acetate (Cellosolve® acetate) | 156º C | teratogen |

The Material Safety Data Sheets (MSDS) should be obtained for any solvent being considered to determine risks and proper precautions. Your chemical vendor will supply this data on request.

**Do not confuse the fluorescent microsphere solvent, 2-ethoxyethyl acetate (Cellosolve® acetate) with ethyl Cellosolve, which will not dissolve the microspheres.**

All potential solvents have not been tested, and other solvents may give satisfactory results. It is advantageous to use a solvent with low volatility to minimize evaporation and potential safety hazards from inhaling the vapors. Dimethyl sulfoxide and dimethyl formamide are not suitable solvents as they render the fluorescent dyes unstable.

**Note:** Fluorescence degrades if exposed to light for any length of time.

The maximum excitation and emission wavelengths for some fluorescent dyes are solvent-dependent (see Table 2-2). Therefore, the choice of solvent may depend on the fluorescent colors chosen for the study.

Different lots of solvent may contain impurities that can degrade some of the fluorescent colors over time. We suggest making a single test solution containing solvent and all the fluorescent colors to be used. This solution should be read daily for as long as you normally allow your samples to remain in the solvent before reading them in the fluorimeter (e.g., if samples are to remain in solvent for 72 hours, read the test solution every day for 3 days). Repeat this with each new solvent lot. If degradation occurs in specific colors, avoid these colors or use a new solvent lot. We have observed that the stability of fluorescent colors vary between different lots of Cellosolve® acetate.

### Direct Extraction of Air-Dried Lung Tissue

Microspheres can be directly extracted from air-dried lung tissue without prior tissue digestion by adding organic solvent directly to the tissue and allowing at least 2-7 days for complete extraction of dyes from the microspheres. The time for complete extraction varies with species and lung injury.

### Extraction of Microspheres Following Sedimentation or Filtration Recovery Techniques

Once the microspheres are separated from the samples by sedimentation or filtration, the fluorescent dye is extracted from the microspheres by adding an accurately measured volume of organic solvent to the microspheres. The solvent dissolves the microspheres and releases the fluorescent dye into the organic solvent. The fluorescent signal in this solution is proportional to the number microspheres present in the sample; therefore, the accuracy of the volume of solvent is critical.

We routinely add 2 ml of 2-ethoxyethyl acetate to each sample with an Eppendorf repeater pipette with an accuracy of ±0.3-2.5% and precision of <0.1-1.0%. Once the organic solvent has been added to the sample, it is then vortexed and allowed to sit for ~1 hour before the fluorescence is read. If the fluorescent signal is high, dilute the sample (see Section 3 on linearity).

## Fluorescence Measurement

Depending on the fluorimeter used, fluorescence can be measured using matched glass cuvettes, a 96-wellplate reader, or an automated flow cell. We routinely measure fluorescence with matched glass cuvettes. The excitation and emission wavelengths recommended in this manual (Table 2-1) are optimal in our Perkin-Elmer LS-50B using red-sensitive photomultiplier tubes.

### Machine Settings

The excitation and emission monochromators and slit widths are most important since they greatest effect on resolution and signal to noise. These settings can be specified for each color for a given analysis and should selected based on all the colors used and the expected intensity range. Count time or

scan speed is also important, since fluorescent intensity is actually an average emission over the specified time period. In general, count times of 1 second and scan speeds of 240 - 480 nm per minutes allow sufficient counts within a reasonable total analysis time. PMT gain is automatically adjusted according to the slit width. All samples from a given experiment must be processed with identical parameter settings.

Increasing the emission slit widths increases the measured fluorescent signal and therefore, improves signal to noise. Increasing the excitation slit width in the Perkin Elmer LS-50 improves resolution and signal to noise. Slit widths should be customized to the colors used in a given experiment. When using multiple colors, we recommend excitation and emission slit widths of 4–8 nm, for optimal resolution and signal to noise. For less than 3 or 4 colors, which are separated by 20–40 nm, slit widths can be increased to 10-15 nm to improve the signal-to-noise ratio.

Excitation wavelengths should be set to optimal wavelengths for fluorescent dyes used in a given experiment to achieve the best emission signals. Selecting excitation and emission wavelengths that are not at the respective peak wavelengths can optimize separation of adjacent colors. Protocols requiring dyes that spillover into adjacent colors need to be mathematically corrected for spillover (see Section 4).

## Sample Dilution

The concentration of dyes, from tissue samples, in the final solvent solution is important for two reasons. Intensity is linearly proportional to concentration only for sufficiently dilute solutions. At high dye concentration intensity is reduced or "quenched" relative to increasing concentration. This quenching effect is more pronounced with increasing numbers of colors used, although the true linear range remains essentially unchanged. We recommend standard curves be made for every color to be used and for the maximum colors to be used in a single experiment. Injecting only a sufficient number of p necessary for accurate counting statistics is the first means to minimize quenching. During the final sample processing, increasing the amount of solvent volume used per sample is the best way to minimize quenching. Additionally, intensity values are reported using an arbitrary scale with a maximum value of 1000, based on the count range of the PMT. If a broad range of intensities are expected the slit widths can be decreased to avoid maxing out the PMT. If you plan to markedly change blood flow to an organ of interest and blood flow increases dramatically, serial dilutions may be necessary to accurately measure fluorescence intensities. To prevent serial dilutions, the number of microspheres injected can be reduced to optimize the intensities under varying flow conditions.

Samples must be diluted accurately by careful pipetting or by weight to minimize introduced errors that will be amplified by serial dilution. Dilution of samples with solvent should continue until the fluorescence reaches an appropriate range. At each step, the dilution factor must be calculated. The true fluorescence signal is then calculated by multiplying the final fluorescence reading by the dilution factor. This must be done accurately because, when many dilutions are required, any error in measurement will be magnified by the multiplication factor. When a final dilution is reached and the fluorescence measured, a further dilution should be performed and the fluorescence measured to assure that quenching has not occurred.

## Cuvettes

Because of the solvent used to extract the fluorescent dyes from the microspheres, only glass or quartz cuvettes can be used. The additional expense of quartz cuvettes is not necessary, as the wavelengths of the fluorescent colors are in the 350 to 800 nm range.

If more than one cuvette is used to make multiple fluorescent measurements, it is imperative to use matched cuvettes. A statement by the cuvette manufacturer that two cuvettes are "matched" is not a guarantee that they are. Cuvettes should be tested prior to reading a series of samples by measuring a fluorescent solution in each cuvette to ascertain whether or not they produce similar fluorescence signals (within 5% variation). We routinely test our matched cuvettes when they are new, and also with our fluorescent controls prior to and during each run. This acts as a quality control and is recorded in a separate control program (see Section 3).

Meticulous cleanliness is mandatory when using optical instrumentation. Any scattering of light will alter the fluorescence signal. Use powder-free gloves whenever handling cuvettes. Cuvettes should be washed with methanol between each sample (we use a commercially available cuvette washer). We also read a Cellosolve blank every 50 samples to check for cleanliness and background noise.

**PLEASE NOTE THAT WE ACCEPT NO RESPONSIBILITY FOR THE USE OF OR THE SUCCESS OF THESE SUGGESTIONS. THE IMPLEMENTATION IS ENTIRELY AT THE DISCRETION OF THE USER.**

## Software/Data Management

Because only the peak emission value is required for quantification, it is not necessary to obtain full spectral curves, as shown in Figure 2-3. Some instruments (such as the Perkin-Elmer LS-50) can be programmed to output peak intensity readings at specified wavelengths, thus shortening the analysis time.

WINFAC, a public domain program, is available to drive the Perkin Elmer LS-50 and LS-50B to measure peak intensity readings at specified wavelengths. This program calculates either fluorescent intensities or number of microspheres per sample and produces text files that are easily imported into spreadsheet programs. WINFAC is available through the Fluorescent Microsphere Resource Center.

## Wellplate Reader

The Perkin Elmer LS-50B can accommodate a 96-wellplate reader. The wellplates used for this accessory must be opaque and resistant to the solvents used Dan Rurak's lab in Vancouver has successfully adapted a 96-well plate reader to measure regional blood flow in all organs (Tan, W. P., K, 1997).

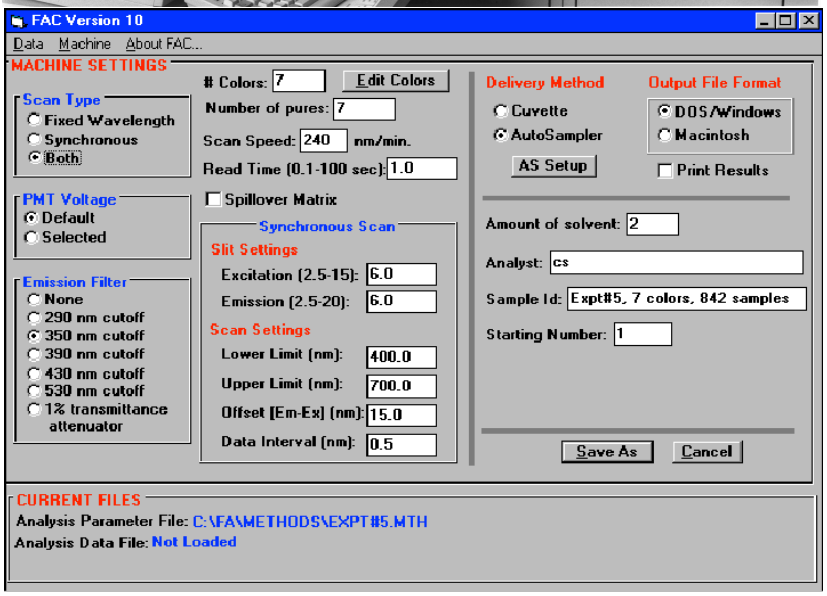


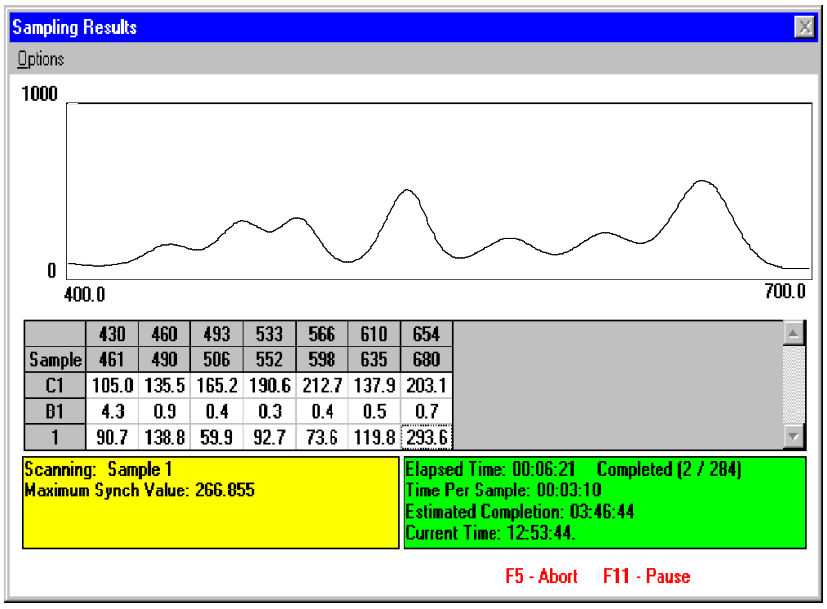


| | 430 | 460 | 493 | 533 | 566 | 610 | 654 |
|---|---|---|---|---|---|---|---|
| Sample | 461 | 490 | 506 | 552 | 598 | 635 | 680 |
| C1 | 105.0 | 135.5 | 165.2 | 190.6 | 212.7 | 137.9 | 203.1 |
| B1 | 4.3 | 0.9 | 0.4 | 0.3 | 0.4 | 0.5 | 0.7 |
| 1 | 90.7 | 138.8 | 59.9 | 92.7 | 73.6 | 119.8 | 293.6 |

Figure 5-4. Automated fluorescent sampler.
Top: Computer and hardware configurations integrate a Perkin-Elmer LS-50B, AS-91 autosampler, and a dilutor station through a computer running Windows 95.
Middle: User definable options for acquiring fluorescent data.
Bottom: Data window as samples are read showing synchronous scans and fixed wavelength intensities.

### Automated Flow Cell

Working in conjunction with Perkin Elmer, we have developed a fully automated system (Figure 5-4) that reads fluorescent samples (Schimmel, et al., 2000). Dave Frazer and Carmel Schimmel developed the software to drive the automated fluorescent sampler. They integrated a Perkin-Elmer LS-50B, AS-91 autosampler, and a dilutor station through a computer running Windows 95. The autosampler allows 270 samples to be read without technician intervention. This system has greatly reduced the analysis error and labor required for the fluorescent microsphere method (Schimmel, et al., 2000). The software package is available without charge via the Fluorescent Microsphere Resource Center web page (http://fmrc.pulmcc.washington.edu/).

## Other Methods for Quantitating Fluorescent Microspheres

Three additional methods for measuring regional organ perfusion using fluorescent microspheres without extracting the dye are currently being used.

### Direct Counting of Microspheres

Direct counting of serial dilutions in the digested sample is less accurate, labor-intensive, and requires a fluorescent microscope and a counting chamber (hemocytometer).

### Flow Cytometer

Flow cytometry has been used for counting fluorescent microspheres (Austin et al., 1989). A laser detects individual fluorescent particles and can differentiate particle size as well as different dye loads. Sample processing is available commercially by Interactive Medical Technologies (IMT), where both 10- and 15-µm microspheres (NuFlow™) can be purchased. Ten markers are available; three are used as internal controls, leaving seven colors to act as blood flow markers. The tissue processing requires digestion, sonication, centrifugation, filtration, and a second centrifugation. The samples are then read by a flow cytometer. IMT will process tissues and return the results in a formatted spreadsheet. The FMRC compared the NuFLOW™ Microspheres and Investigator Partner Service (IPS) for measuring regional organ blood flow and found it compares well with radioactive microspheres.

Methods: Seven different colored NuFLOW™ microspheres 15 µm in diameter were obtained from Triton Technologies (San Diego, CA) in a kit costing *$255.* The specific colors used were red-high, violet-high, blue-high, red-med, orange-high, violet-med, and red-low. Each 2.1 ml bottle contained 50 million spheres in a saline solution, 0.01% Tween 80 and 0.01% Thimerosal as a bacteriostat. 1.25 million microspheres of each color were mixed with 1.3 million Ruthenium labeled microspheres and simultaneously injected into the left ventricle of an anesthetized and mechanically ventilated pig (15 kg). Two simultaneous reference blood samples were obtained from right and left femoral arterial lines. The animal was killed by anesthetic overdose and the heart and kidneys removed, diced into approximately 1 gram pieces and the radioactivity determined in a scintillation counter. The radioactive count in each sample was corrected for background and decay. Blood flow to each piece (ml/min) was determined in duplicate from the two arterial reference blood samples. The organ and blood samples were frozen and stored until the radioactivity decayed to a safe level for shipment (3 months).

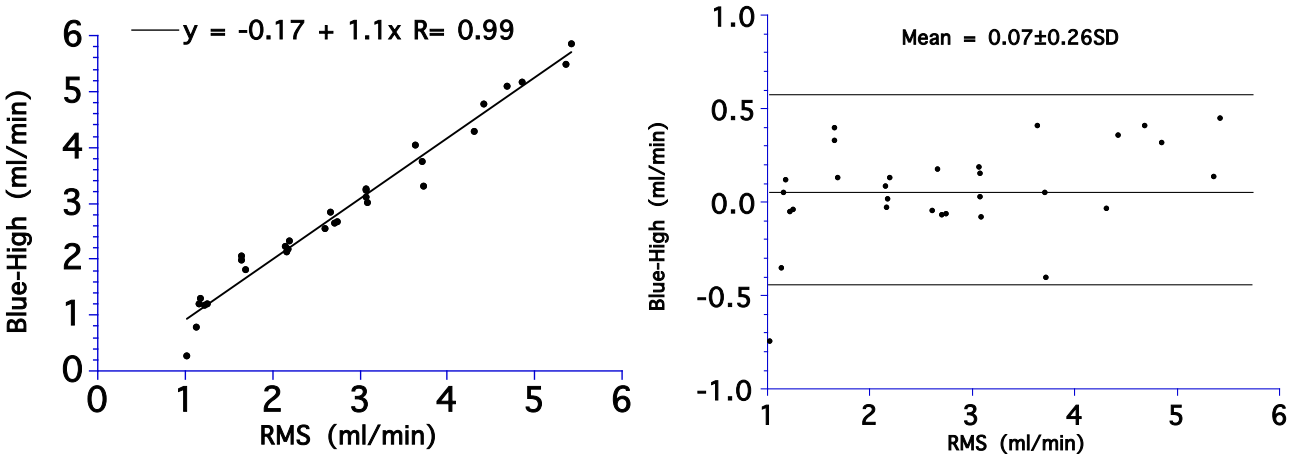


Thirty samples were selected on the basis of their initial radioactive counts to provide a wide range of flow values. Each sample was placed in an individual tube and sent to the IPS laboratory along with the reference blood samples ($12.50/sample). An electronic spreadsheet with the estimated blood flow for each sample (ml/min) was returned by email 2 weeks later for a fee of $60.

Results: Blood flows to each sample estimated from the NuFLOW™ Microspheres and Investigator Partner Service were compared to blood flows determined by the radioactive microsphere method. One correlation plot and its companion Bland-Altman plot are presented below. The table summarizes all plots for all colors tested. Left and right arterial samples produced similar results. Only the results from the left reference sample are presented.

Figure 5-4 correlation plots and its companion Bland-Altman plot comparing radioactive microspheres (RMS) and fluorescent microspheres counted by flow cytometry.

| | Correlation Plots | | | Bland-Altman Plots | |
|---|---|---|---|---|---|
| **Color** | **Slope** | **Intercept** | **R** | **mean** | **SD** |
| Red-High | 1.00 | -0.10 | 0.98 | -0.04 | 0.24 |
| Violet-High | .87? | 0.21 | 0.97 | -0.15 | 0.31 |
| Blue-High | 1.10 | -0.17 | 0.99 | 0.07 | 0.26 |
| Red-Med | .99 | -0.01 | 0.99 | -0.03 | 0.19 |
| Orange-High | 1.00 | -0.17 | 0.98 | -0.12 | 0.24 |
| Violet-Med | .96 | -0.04 | 0.98 | -0.14 | 0.29 |
| Red-Low | 1.00 | -0.06 | 0.99 | -0.07 | 0.19 |

Conclusions: The NuFLOW™ Microspheres and Investigator Partner™ Service provide an accurate determination of regional myocardial and renal blood flow. We cannot comment on other tissues because of potential problems with digesting lipid rich tissues such as brain and gut. The primary drawback is the cost ($390 for 30 samples, 2 reference blood samples, a report, and shipping). Although the entire process has not been validated in the peer review literature, validation studies are reportedly in progress [source: Triton Technologies].

## Cryomicrotome/Fluorescent Imaging System

The Regional Flow Imaging System (Barlow Scientific, Inc. Olympia WA) is a fluorescence cryomicrotome that determines the spatial distribution of organ blood flow at the microscopic level. Briefly, the system rapidly collects microcirculation data from organs containing up to four different colors of fluorescent microspheres. The instrument (Figure 5-4) consists of a charge-coupled device (CCD) video camera, a computer (Dell Computer Inc., Round Rock, Texas), metal halide lamp (HTI 403W/24, Osram, Sylvania), excitation filter-changer wheel, emission filter-changer wheel, and a cryostatic-microtome. Fluorescence images are acquired using a Kodak digital camera (2040 x 2040 pixel array) with a 200 mm zoom Nikkor lens (Nikon) with a macro-focusing baffle. Two motorized filter wheels containing excitation and emission filters are mounted in front of the light source and camera, respectively. The computer through photomicrosensors controls the filter positions. A custom designed microtome is outfitted with an asynchronous stepper motor to serial section frozen organs. Computer control of the microtome motor, emission filter wheel, and image capture and display is accomplished through a virtual instrument written in LabView 5.0.1 (National Instruments Inc.).

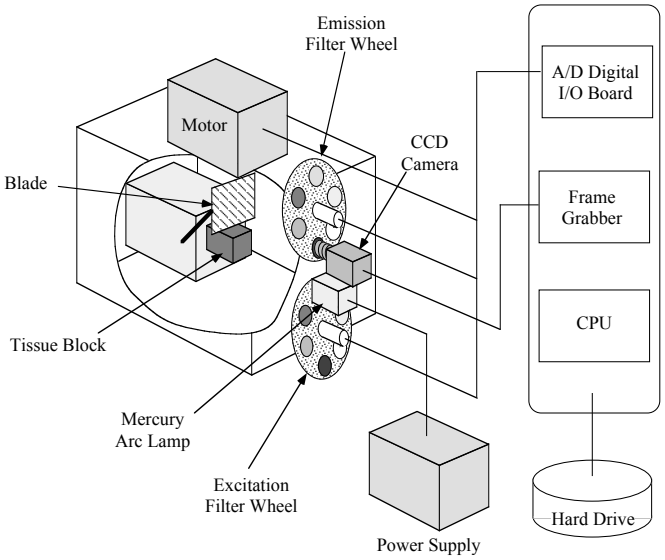


Figure 5-4

Schematic of imaging cryomicrotome.

The imaging cryomicrotome serially sections through the frozen organ at a selected slice thickness. Digital images of the tissue surface (en face) are acquired with appropriate excitation and emission filters to isolate each of four different fluorescent colors (Figure 5-5). Four 1-4 MB images at each of four fluorescence excitation/emission wavelengths are collected. Each image is processed so that X, Y, and Z (slice) locations of each microsphere are determined and saved in a text file. The spatial resolution of the system depends on the size of the organ being processed, but is typically 15 μm in the X and Y directions and 30 μm in the Z direction. Images of organ cross-sections produce a three-dimensional binary map defining the spatial location of organ parenchyma. This map determines the organ space locations to be sampled and the three-dimensional space for the statistical sampling (see below)

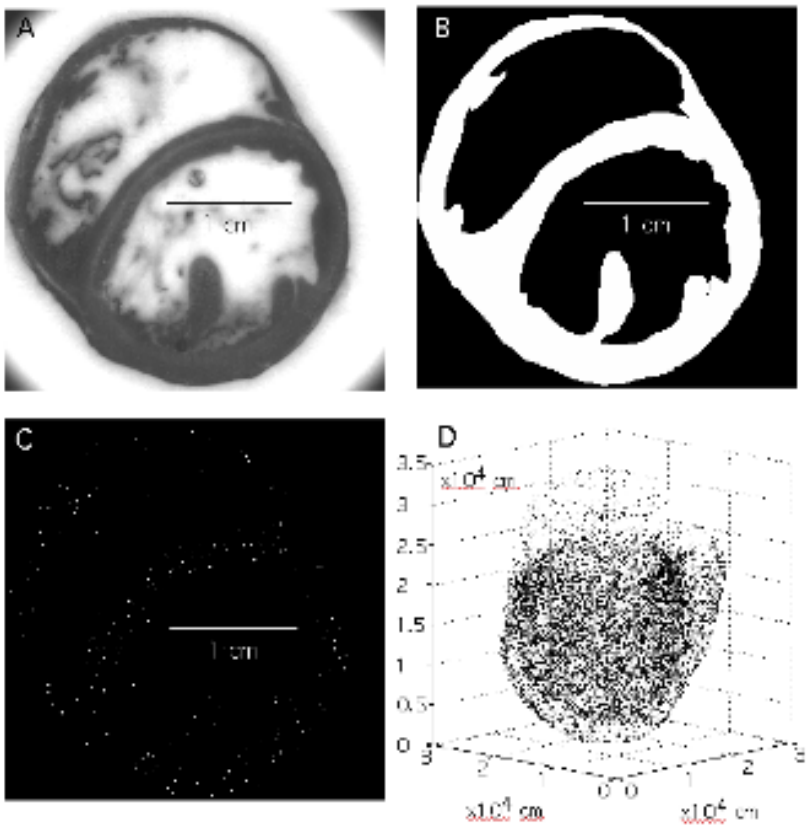


Figure 5-5. Processing of fluorescent images. A. 2000 x 2000 pixel outline image of rabbit heart en face. B. Bitmap image (black = 0 and white = 1) defining the spatial location of heart tissue. C. Fluorescent image obtained with a specific excitation/emission filter pair to determine individual microsphere location. Each point represents a microsphere located at x, y, and z (slice) location. D. Three-dimensional distribution of 26083 yellow microspheres.

Acquired images are analyzed with an analysis program also written in LabView, which applies an intensity threshold to convert areas of microsphere fluorescence into binary image blobs. The center of mass of each blob is calculated to fine the X and Y positions of each microsphere, with the Z coordinate being the slice number. The spatial coordinates and blob size is written to a text file.

Data reduction is automated through a final analysis program. A linked list of all microsphere locations (X, Y, and Z coordinates) is created. Any microsphere observed in the same X and Y coordinate across consecutive Z slices is reduced to a single observation occurring in the Z slice in which the microsphere is the largest. The number of consecutive slices in which a given microsphere is observed and the number of pixels representing each microsphere are also used to eliminate artifacts.

The imaging cryomicrotome provides the spatial location of every microsphere in an organ. It allows blood flow measurements to made be at a scale of resolution not previously possible. Microsphere locations are determined in a fully automated system. If all four colors are used, a rabbit heart can be completely processed in 20 hours without user input. The saved images are processed to produce a text file containing the spatial coordinates of every imaged microsphere. This approach obviates the need to physically dissect the organ and to separate the microspheres and tissue prior to eluting the fluorescent signals. Most importantly, it offers a method to study organ blood flow distribution at a very high resolution in small laboratory animals.

# References

Austin, R. E., Jr., W. W. Hauck, G. S. Aldea, A. E. Flynn, D. L. Coggins and J. I. Hoffman. Quantitating error in blood flow measurements with radioactive microspheres. *Am J Physiol*. 257:H280-8, 1989.

Bassingthwaighte, J. B., M. A. Malone, T. C. Moffett, R. B. King, I. S. Chan, J. M. Link and K. A. Krohn. Molecular and particulate depositions for regional myocardial flows in sheep. *Circ Res*. 66:1328-44, 1990.

Buckberg, G. D., J. C. Luck, D. B. Payne, J. I. E. Hoffman, J. P. Archie and D. E. Fixler. Some sources of error in measuring regional blood flow with radioactive microspheres. *J. Appl. Physiol.* 31:598-604, 1971.

Chien, G. L., C. G. Anselone, R. F. Davis and D. M. Van-Winkle. Fluorescent vs. radioactive microsphere measurement of regional myocardial blood flow. *Cardiovasc Res*. 30:405-12, 1995.

Heyman, M. A., B. D. Payne, J. I. Hoffman and A. M. Rudolf. Blood flow measurements with radionuclide-labeled particles. *Prog. Cardiovasc. Dis.* 20:55-79, 1977.

Polissar, N. L., D. Stanford and R. W. Glenny. The 400 microsphere per piece "rule" does not apply to all blood flow studies. Am. J. Physiol. in press.

Powers, K. M., C. Schimmel, R. W. Glenny and C. M. Bernards. Cerebral blood flow determinations using fluorescent microspheres: variations on the sedimentation method validated. *Journal of Neuroscience Methods*. 87:159-165, 1999.

Schimmel, C, D. Frazer, S.R. Huckins and R.W. Glenny. Validation of Automated Spectrofluorimetry for Measurement of Regional Organ Perfusion Using Fluorescent Microspheres. *Comput. Methods Programs Biomed.* 62:115-25, 2000.

Tan, W. P., K. W. Riggs, R. L. Thies and D. W. Rurak. Use of an automated fluorescent microsphere method to measure regional blood flow in the fetal lamb. *Canadian Journal Of Physiology And Pharmacology*. 75:959-968, 1997.

van Oosterhout, M. F. M. and F. W. Prinzen. The fluorescent microsphere method for determination of organ blood flow. *FASEB J.* 8:A854, 1994.

# 6 Microscopic Use of Fluorescent Microspheres

Histological studies of tissues and organs perfused with fluorescent microspheres require modification of most routine tissue processing methods in order to preserve fluorescent microspheres for microscopic visualization. For example, formalin fixation followed by routine embedding in paraffin is not feasible as the standard organic solvents used during tissue processing dissolve polystyrene microspheres. Several different ways of processing tissue were studied and the advantages and disadvantages of each are evaluated. These included: 1) formalin fixation followed by embedding in paraffin; 2) formalin fixation followed by embedding in glycol methacrylate; 3) air-dried lung followed by Vibratome sectioning; 4) formalin fixation followed by Vibratome sectioning; 5) rapid freezing followed by cryomicrotome sectioning. Methods for staining sections and the types of mounting media that can be used to apply coverglasses to slides are also evaluated.

## Methods

Aldehyde fixation followed by embedment in paraffin or methacrylate produced sections of well-preserved tissue for microscopic examination. Paraffin blocks were sectioned at 7-10 µm with Sturkey disposable knives on a JB-4 microtome. Methacrylate blocks were sectioned with 12 mm wide triangular glass knives on a Sorvall (now Research & Manufacturing Co.) MT-2 microtome. The knives were made on a Sorvall Glass Knife Maker.

Unembedded tissue was sectioned with a Vibratome 1000 modified with a 1000 Ω rheostat in the cutting blade advance. This allowed a slow forward motion of the oscillating blade through the specimen. This rheostat modification was especially useful for specimens such as airways, which are tough and difficult to cut. A faster forward blade movement for these specimens resulted in deformation of the block and uneven section thickness. Without the rheostat modification, the forward motion of the razor blade carriage had to be stopped for short time periods with the speed control knob while the vibration of the blade continued. A blade clearance angle of 15-17° worked best for dry and ethanol-dehydrated specimens while 17-20° seemed better for gelatin-embedded specimens.

Sections were examined on a Leitz Diaplan compound microscope fitted with an incident mercury arc lamp. Three filter sets were used: 1) blue excitation light (450-490 nm) with a suppression filter for all wavelengths below 520 nm in the observation light path (commonly used for the fluorescein isothiocyanate (FITC) fluorophores); 2) green excitation light (530-560 nm) with a suppression filter for all wavelengths below 580 nm (commonly used for the rhodamine fluorophores); and 3) UV excitation (340-380 nm) with emission suppressed below 430 nm. The blue and UV excitation light caused microspheres of blue, green, yellow-green, and red emission colors to glow brightly (although most of our perfusion protocols used yellow-green and red microspheres only). The green excitation light was useful only for the red microspheres. With blue epi-illumination, microspheres photographed well against the green autofluorescence of tissue with Ektachrome 160T (tungsten) film. The UV illumination was used in combination with bright field transmitted illumination to provide better histological visualization.

# A. Paraffin (Paraplast Plus) Embedding

Paraffin sections can be cut serially and 7-10 µm-thick sections provide good histological detail. An antimedium (or transition fluid)—a fluid miscible with both alcohol (used to dehydrate the tissue) and paraffin—has to be used to allow infiltration of the tissue with paraffin since alcohol is not miscible with paraffin. Hydrocarbons such as toluene and xylene have routinely been used for this purpose (Humason, 1979). Such hydrocarbons are now regarded as hazardous chemicals and as fire hazards due to their high vapor pressures (Lyon, et al., 1995). More pertinent to the present study, toluene and xylene also have the undesirable property of dissolving microspheres or removing the fluorophore from microspheres.

Several companies now sell proprietary mixtures as substitutes for hydrocarbons. Several of the proprietary mixtures were evaluated—Histoclear, Histoclear II, Americlear, and Hemo-De. Of these, only Histoclear II retained the fluorescent of the microspheres in paraffin sections. The reasons for the differences in the properties of these four substitutes are not known since they are proprietary mixtures. A schedule for processing with Histoclear II is given in Table 1. Based on the manufacturer instructions, infiltration times were increased approximately 50% compared to the usual processing times used with toluene.

Lyon, et al. (1995) recommended butyldecanoate ($CH_3$-$(CH_2)_3$-O-O=C-$(CH_2)_8$-$CH_3$, sold as "Estisol 220") as a substitute for toluene. They recommended clearing and infiltrating times about 4-6 times longer (up to 12 hours per change) than the typical toluene schedule. Paraffin is less soluble in butyldecanoate than in toluene; at 45° C, a saturated solution of Paraplast Plus in butyldecanoate is less than 40% paraffin. A schedule for processing with butyldecanoate is given in Table 2. The fluorescence of microspheres is not as intense as after processing in Histoclear II, particularly for the red

**Table 1. Tissue Processing with Histoclear II Antimedium**

Tissue blocks up to approximately 10 $mm^3$. Formaldehyde or glutaraldehyde fixation (not evaluated with other fixatives).

1. Wash in tap water, 3-4 changes of 30 minutes
2. To 35% ethanol – 2 changes of 15 minutes
3. To 70% ethanol – 2 changes of 15 minutes
4. To 70% ethanol – 30 minutes
5. To 95% ethanol – 2 changes of 15 minutes (or overnight)
6. To 100% ethanol – 6 changes of 15 minutes
7. To 100% ethanol + Histoclear II, 1:1 – 20 minutes
8. To Histoclear II – 2 changes of 30 minutes
9. To Histoclear II – 60 minutes (probably a minimum for this medium)
10. To 50% Paraplast Plus dissolved in Histoclear II at 45° C – 60 minutes
11. To pure Paraplast Plus at 60°C – 2 changes of 60 minutes
12. Transfer tissue to embedding mold under an infrared lamp

**Table 2. Tissue Processing with Butyldecanoate Antimedium**

Tissue blocks up to approximately 10 $mm^3$. Formaldehyde or glutaraldehyde fixation (not evaluated with other fixatives).

1. Wash in tap water, 3-4 changes of 30 minutes
2. To 35% ethanol – 2 changes of 15 minutes
3. To 70% ethanol – 2 changes of 15 minutes
4. To 70% ethanol – 30 minutes
5. To 95% ethanol – 2 changes of 15 minutes (or overnight)
6. To 100% ethanol – 6 changes of 15 minutes
7. To 100% ethanol + butyldecanoate, 1:1 – 30 minutes
8. To butyldecanoate – 2 changes of 60 minutes
9. To butyldecanoate – overnight
   (alternative steps 8 & 9 – 2 changes of 12+ hours, agitating occasionally)
10. To 35-40% Paraplast Plus dissolved in butyldecanoate at 45° C – 60 minutes
11. To pure Paraplast Plus at 60° C – 2 changes of 60 minutes
12. Transfer tissue to embedding molds under an infrared lamp

microspheres. Yellow-green microspheres are still bright under blue excitation but red microspheres show fluorescence with green excitation only.

Biobond tissue adhesive was used to improve adhesion of paraffin sections to glass slides. Overnight drying after the sections are mounted on Biobond-coated slides is recommended for good adhesion. The Biobond coat is quite clear and does not stain as a gelatin-coated slide does.

## B. 2-Hydroxyethylmethacrylate (Historesin) Embedding

This class of methacrylate resin is also known as glycol methacrylate. The embedding procedure we used was adapted from that developed by Chappard (1985) and it has proven very useful for uniform embedment of lung tissue that contains cartilage-reinforced airways and heavily muscled arteries. Chappard (1985) suggested infiltrating dense tissue with the fully catalyzed hydroxyethylmethacrylate (GMA) monomer at -20° C so that the catalyst can diffuse fully into tissue blocks. At room temperature, the fully catalyzed mixture will polymerize in minutes but polymerization is often incomplete in the center of dense tissue blocks larger than approximately 6-8 $mm^3$ as the catalyst cannot diffuse to the center of tissue blocks in such a short time. Tissue in catalyzed Historesin can be kept at -20° C for several weeks without polymerization if the monomer is changed every 24 to 48 hours. Even slightly higher temperatures (e.g., -16° C) allow polymerization in less than 24 hours. Blocks with cartilage or thick-walled arteries require 14 or more days in the catalyzed monomer. A schedule for processing with Historesin is given in Table 3.

Blocks, 4 x 6 mm in size, of fixed lung, heart muscle and kidney section well at 3-5 µm after 14 days infiltration at -20° C. Air dried lung may also be embedded in GMA with this procedure. Both yellow-green and red microspheres retain their fluorescence throughout the embedding process.

**Table 3. Tissue Processing for Historesin Embedding**

Tissue blocks 5 x 5 x 8 mm. Glutaraldehyde fixation (not evaluated with other fixatives).

1. Rinse in buffer used for the glutaraldehyde – 3 changes of 15 minutes
2. To 35% ethanol – 2 changes of 15 minutes
3. To 70% ethanol – 4 changes of 15 minutes
4. To 95% ethanol – 2 changes of 15 minutes
5. To 100% ethanol – 4 changes of 15 minutes
6. To 100% ethanol + Historesin Infiltrating Solution, 1:1 – 20 min (optional)
7. To Historesin Infiltrating Solution at 4° C – overnight (vacuum degas enough of the Infiltrating Solution for step 7 and to make up the required Embedding Solution as well; lung tissue may benefit by being kept under vacuum overnight instead of in a refrigerator)
8. To Historesin Embedding Solution at –20° C – 24 hours (always handle the Embedding Solution on ice and return to freezer as quickly as possible)
9. To Historesin Embedding Solution at –20° C – 6-13 days, changing to freshly made Solution every 24 to 48 hours (usually safe to leave tissue in the same solution over a week-end after the third day)
10. Transfer tissue to embedding molds on ice, fill the lower half of the mold with fresh Embedding Solution, and cover the tissue and solution with a piece of Parafilm; polymerize overnight in a refrigerator at 4° C or keep larger molds on a bed of crushed ice
11. Attach to specimen mounts with the last of the Embedding Solution

## C. Vibratome Sectioning of Air-Dried Lung

Unfixed lungs can be dried over a period of several days by inflating with air at a known pressure. Dry lungs are sufficiently rigid to be sliced, and cubes of tissue, 10-15 mm on a side, can be cut out of the slices and fastened with a gel cyanoacrylate glue to 15x19 mm hardwood specimen mounts which fit in the chuck of the Vibratome. Of a number of glues tried, Quick Tite Super Glue Gel was the only really satisfactory product. "Non-gel" glues wick into much of the dry lung and render it too hard to section.

Sections were cut dry with the slowest advance of the cutting blade at a thickness of 100-150 µm and positioned without mounting medium under coverglasses on microscope slides. The coverglasses were then attached to the slides with narrow strips of Scotch Magic Tape.

## D. Vibratome Sectioning of Unembedded Fixed Tissue

Tissue (lung, heart, kidney) was formalin fixed and then hardened in absolute ethanol for one week to two months. Cubes of unembedded tissue were glued to reusable, rectangular aluminum specimen mounts with Quick Tite Super Glue Gel. As absolute ethanol does not have the water to catalyze the cyanoacrylate glue, pieces were briefly wet in 95% ethanol before being glued to the aluminum specimen mounts. The glue deteriorates in absolute ethanol so that mounted blocks cannot be stored long term. Tissue blocks were kept wet during sectioning by periodic application of drops of ethanol with a Pasteur pipette.

A slow blade advance is required, especially through airways. Bronchi reinforced with cartilage and heavily muscled arteries will section down to 50-100 µm. For bronchi, it is necessary to section through the same cartilage ring that is glued to the aluminum specimen mount to keep the specimen from bending in front of the knife blade. The histology of fixed lung sections is better than that of unfixed, air dried tissue.

## E. Vibratome Sectioning of Gelatin-Embedded (Bacto Gelatin) Fixed Tissue

Embedding irregularly shaped or subdivided specimens in a supporting medium allows the production of cohesive sections. Also, none of the specimen is rendered unsectionable by infiltrated hardened glue as happens with the unembedded material described above. Gelatin embedding does not degrade tissue histology or the fluorescence of the microspheres, but the processing time is lengthy. Gelatin-embedded specimens are usually frozen before sectioning, but Igarashi, et al. (1994) recently described a method for serially sectioning whole rat embryos using a rotating blade machine. We adapted their procedure for use with the oscillating-blade Vibratome.

Tissue pieces were fixed in buffered formalin. To prevent crosslinking (fixing) the gelatin in the infiltrating solutions, tissue was washed in water for at least one day with a minimum of 10-15 changes of water. Purified gelatin solutions of 15% and 30% (15 and 30 g in 100 ml distilled water) were prepared at 55° C. Thymol (0.1%) was added as a bacteriostatic agent. A processing schedule for gelatin embedding is given in Table 4.

Blocks of gelatin with tissue were cast in 22x40 mm Peel-A-Way disposable plastic embedding molds. Although disposable, they are durable enough to be used several times if desired. A 2-3 mm thick gelatin platform was cast in the bottom of the molds. This and the larger size of the mold allow for accurate orientation of the tissue on the specimen mount. The specimens and bottles of gelatin are handled under a red-coated infra-red lamp to prevent unwanted cooling while orienting the tissue in the molds. The warm tissue will sink into the platforms, however, if the latter are not thoroughly chilled beforehand in a refrigerator. Also, to prevent remelting the platform when the tissue is embedded, the molds are filled with the warm gelatin in two or more layers (allowing the first layer to gel at room temperature before adding the next layer).

**Table 4. Tissue Processing for Gelatin Embedding**

Tissue blocks up to approximately 10 $mm^3$. Formaldehyde or glutaraldehyde fixation (not evaluated with other fixatives).

1. Wash in tap water – 10-15 changes over 24 or more hours
2. To 15% gelatin (aqueous) at 37° C – 2 changes of 24 hours
3. To 30% gelatin (aqueous) at 37-40° C – 2 changes of 24 hours (more for dense tissue)
4. Transfer tissue to embedding molds (Peel-A-Way molds are particularly useful) under an infrared lamp
5. Chill gelatin and remove from molds
6. Fix tissue + gelatin block in 4% buffered formaldehyde – 24 hours
7. Warm gelatin block and wooden specimen mount; glue mount to block with molten 30% gelatin
8. Fix tissue + gelatin + mount in 4% formaldehyde – 24-48 hours

The filled molds are then chilled and the gelatin blocks removed from the molds. A thin spatula kept wet with water is inserted between the gelatin and mold wall freeing the sides of the block. Twisting the mold frees most of the bottom of the block and it can gently be pried out of the mold with the spatula. If the gelatin blocks are fixed in formaldehyde while still in the molds, they are somewhat prone to fracture during removal. In any case, the Peel-A-Way molds may simply be peeled apart freeing the gelatin block.

Tissue embedded in gelatin does not need much surrounding gelatin for sectioning. The travel of the specimen stage of the Vibratome limits the height of a piece of tissue to 10 mm. A block this tall needs a minimum length and width of about 10x10 mm for structural strength. After a gelatin block is released from its mold, its orientation to the cutting blade is determined and the larger excess dimensions cut away with a razor blade.

The gelatin blocks are then hardened in buffered 4% formaldehyde for 24 hours at room temperature (longer term storage is possible). Gelatin blocks and water-soaked, wooden mounts are then warmed in a 40° C oven and a bottle of 30% gelatin is warmed to about 55° C. The 30% gelatin is used as a glue to fasten gelatin blocks to the mounts. Mounted specimens are returned to formaldehyde for another 24 hours. Igarashi, et al. (1994) recommend 3 days or more.

The blocks, now fixed for a minimum of 48 hours, are given a final trimming with a razor blade. A rectangular cutting face works well, but the geometry of the face does not appear to be critical. The longer side of the block's cutting face should be parallel to the blade to better resist the lateral motion of the cutting stoke as the knife moves forward. The block and the razor blade holder are kept wet with distilled water.

Sections are cut using a slow blade advance. Cutting faces of 11x14 mm have been sectioned at 50 µm and smaller ones at 30 µm. With the larger faces, reliable serial sets have been cut at 100 µm, although it is difficult to avoid thick and thin zones in a small percentage of the sections.

## F. Frozen Sections

Historically, this was the first technique we tried in our laboratory to preserve fluorescent microspheres in histological sections. In terms of tissue preparation, the technique is straightforward—fresh unfixed tissue is frozen and sectioned at 20-60 µm. It has the obvious advantage of avoiding organic reagents but the disadvantage that it requires the specialized technique of cutting frozen sections on a cryostat. We have largely abandoned this approach because of several additional problems which include poor histological detail due to freezing damage (which becomes greatly accentuated the larger the tissue size), the sections are unfixed and deteriorate rapidly, and the practical difficulty or impossibility of obtaining serial sections. A variation that we have not tried that would result in better tissue structure and more permanent sections is to chemically fix tissue before freezing.

## G. Staining of Sections

Sections can be stained although the tissue autofluorescence with epi-fluorescence optics may be sufficient to allow sections to be viewed and analyzed without staining. This is particularly true for the thicker Vibratome sections and for sections of lung, which have more intense autofluorescent properties than sections of heart or kidney.

**Paraffin sections.** Sections can be stained with hematoxylin and eosin (Delafield's hematoxylin worked well) or with 0.5% aqueous methyl green (only lung tissue stained satisfactorily with methyl green). The methyl green staining procedure is followed with a rapid wash in absolute alcohol if immersion oil is used as a mounting medium. See the comments below about how mounting media cause fading of the stains.

**Methacrylate sections.** Tissue embedded in Historesin is not fluorescent so unstained sections are not easy to view with epifluorescence optics. But methacrylate sections can be stained routinely with Lee's stain and viewed with epifluorescence since basic fuchsin, a dye in Lee's stain, is fluorescent.

**Vibratome sections of air-dried lung.** Staining was not attempted.

**Vibratome sections of unembedded fixed tissue.** Staining was not attempted.

**Vibratome sections of gelatin–embedded fixed tissue.** Staining was not attempted.

## H. Coverglass Mounting Media

A mounting medium is spread on sections mounted on glass slides before covering them with a coverglass (or cover slip). For routine paraffin and methacrylate sections, mounting media contain organic solvents, usually toluene. Such mounting media can be expected to degrade the fluoresence of microspheres as toluene-based antimedia do. We tested three organic solvent-based mounting media—Clarion, Cytoseal, and Histolyte 60—and ten water-based mounting media—Advantage, Aquamount, Aqua-Poly/Mount, Crystal/Mount, Fluoromount-G, Gel/Mount, H&E Mount, Hydromount, Omnimount, and Mount Quick. Since the most extensive testing of mounting media was done on Vibratome sections of unembedded fixed tissue, see that section below for the most detailed description of the mounting media.

**Paraffin sections.** Cytoseal preserved hematoxylin and eosin (H&E) staining but largely extinguished the fluorescence of red microspheres. Aquamount, Aqua-Poly/Mount, Gel/Mount, Hydromount, and Omnimount were used on unstained sections and sections stained with H&E and aqueous methyl green. They are satisfactory with unstained sections, but eosin and methyl green are leached from tissue within a few hours, eosin yielding a uniformly fluorescent area under the coverglass. H&E Mount preserved both hematoxylin and eosin stains but was strongly fluorescent under blue excitation. The standard H&E procedure can be modified by substituting Histoclear II for toluene to preserve the fluorescence of the microspheres in stained sections. High viscosity immersion oil can then be used as a mounting medium as it does not affect fluorescence of the microspheres.

**Methacrylate sections.** Aquamount and Mount Quick aqueous coverglass mountants rapidly decolorize Lee's stain. Yellow-green and red microspheres remain fluorescent, although the medium shrinks badly.

Yellow-green microspheres remain fluorescent in Cytoseal mountant, but the fluorescence of red microspheres in the blue exciting light (450-490 nm) is extinguished within half an hour. Immersion oil works well as a coverglass mountant since it does not affect the stain or the fluorescence of yellow-green and red microspheres.

**Vibratome sections of air-dried lung.** Mounting media distort dry sections and were not used.

**Vibratome sections of unembedded fixed tissue.** Sections can be mounted under a coverglass in absolute ethanol and the preparation allowed to dry. Although lung tissue, for example, shows some damage, the section quality is better than that from air dried (unfixed) lung. The tissue shows good autofluorescence under blue excitation and the microspheres show up well. With the coverglasses secured after drying with narrow strips of Scotch Magic Mending Tape, this method provides a durable preparation with a minimum of labor.

Two of the organic solvent-based mounting media—Cytoseal, Clarion—were tried. Both diminish the fluorescence of yellow-green microspheres to some degree, extinguish the fluorescence of red microspheres under blue excitation, and leave only a faint remnant of the red microsphere's fluorescence under green excitation.

The water-based mounting media produced the following results.

*Aquamount:* This mountant shrinks considerably as it dries, and 100 µm sections need several applications of Aquamount in order to produce a durable, Aquamount-filled space under the coverglass. Sections are cut in 100% ethanol and usually require partial rehydration to facilitate the spreading of an aqueous mountant over sections placed on slides. Rehydration can be done by placing sections in a 100 mm glass Petri dish filled with 70% ethanol. A slide is placed in the dish with the label end resting on the side of the dish. A section is maneuvered onto the largely submerged slide with a good quality sable hair artist's brush (which work better than a camel hair brush). The slide is removed from the Petri dish and drained. The section is immediately covered with several drops of mountant, and allowed to dry for several hours to overnight. Repeated cycles of adding mountant and drying can be done before a coverglass is applied.

Sometimes, sections curl in Aquamount and need to be covered with a coverglass with the first application of the mountant. Aquamount will often shrink completely away overnight from a 22 $mm^2$ coverglass, essentially freeing the coverglass from the mountant-infiltrated section below. The coverglass can then be lifted or 'popped' off and more mountant added to evenly refill the space under a new coverglass. The initial drying or shrinkage step takes longer, about 1-2 weeks, with sections mounted under 22x40 mm coverglasses. Small bubbles sometimes form within the layer of Aquamount which do not refill with a new application of mountant; in such cases, briefly soaking the dried layer in distilled water may help to refill bubbles when more Aquamount is added. In our hands, Aquamount was the only aqueous mountant that allowed clean removal of coverglasses. With toluene-base mountants, additional mountant can be added by 'wicking' it under the coverglass which may or may not allow complete refilling of spaces that form due to shrinkage of the mounting medium. This is not a feasible method for aqueous mountants because of the pattern of shrinkage, i.e., the mountants do not shrink back evenly from the edges of the coverglasses.

Ringing coverglasses with nail polish prevented shrinkage and air bubble formation for up to a few weeks. Vacuum degassing Aquamount before use also helped. But even with a substantial amount of initial work, Aquamount is not a permanent mounting medium. The same problems with shrinkage and bubble formation also occur with 7-10 μm paraffin sections, although the initial bubbles are small and the process takes longer.

*Aqua-Poly/Mount, Gel/mount, Hydromount, and Omnimount:* These mounting media behave much like Aquamount. They preserve the fluorescence of both yellow-green and red microspheres and of the tissue. As with Aquamount, thicker mounts last much longer if drops of medium are put on sections several times before applying the coverglass. These media become firm in about an hour and, except Hydromount, last somewhat longer than Aquamount before air bubbles form under the coverglass. But they do not allow coverglasses to be lifted off the sections when they dry out. Overall, these four media behave much alike.

*Mount Quick:* When sections were infiltrated without a coverglass, Mount Quick formed many cracks upon drying. It is also not satisfactory for fluorescence imaging as it contains many small fluorescent particles not readily visible under brightfield illumination.

*Advantage*: This mounting medium showed substantial autofluorescence.

*Fluoromount-G:* Of all the aqueous mounting media tried with 100 μm-thick sections (five-week trials), this medium shows the least shrinkage from the edges of the coverglasses. The fluorescence of tissue and yellow-green and red microspheres was well preserved.

*Crystal/Mount:* This mounting medium is supposed to be used directly on sections and dried without coverglasses. For lung tissue, even with a generous amount of Crystal/Mount, the dried medium can form air pockets in alveoli which become bubbles when a second application is made. The dried preparations preserve the fluorescence of yellow-green and red microspheres, and the tissue shows bright autofluorescence. Instructions supplied with Crystal/Mount state that toluene-based media can be used to mount a coverglass over a dried layer of Crystal/Mount without affecting the section. A trial of 45 days with Cytoseal (60% toluene) over a thick layer of Crystal/Mount confirms that both yellow-green and red microspheres retain their fluorescence. Fluorophores diffuse out of microspheres in half an hour to overnight when coverglasses were mounted with Cytoseal over sections covered with a dried layer of Aquamount or Aqua-Poly/Mount.

Tissue autofluorescence and fluorescence of yellow-green and red microspheres under blue excitation appear the same with all of the above aqueous mounting media except Advantage. Kidney sections have somewhat less autofluorescence than lung or heart. Tissue autofluorescence may vary with the fixation procedure.

*Immersion Oil:* Several drops can be applied to the middle of a section in absolute ethanol and a coverglass added to prevent rapid drying. Immersion oil is slowly miscible with absolute ethanol but doesn't mix well with 95% alcohol. The coverglass may be removed after some hours to allow the ethanol to evaporate. This is risky, however, since sections are not bonded to the slide and section shrinkage and wrinkling may occur. Under a coverglass the small droplets of ethanol in the oil disappear after several weeks, but the preparation may require months to clear completely. No significant shrinkage of oil volume or gas bubble formation were evident for up to eight months.

Immersion oil does not seem to diminish the fluorescence of either the yellow-green or red microspheres. Tissue autofluorescence is about equal to that using the aqueous mounting media.

**Vibratome sections of gelatin–embedded fixed tissue**. Gelatin sections require an aqueous mounting medium because they shrink and distort if dried under a coverglass without a mounting medium. This also happens if drops of an aqueous medium, including Crystal/Mount, are dried on the sections without a coverglass. Aquamount dries under a coverglass in a few days and retracts forming air spaces around and over the sections although the coverglasses are not removable for several more days. By this time the sections adhere to the slides (although they are probably not infiltrated with the mounting medium) and more Aquamount can be added after the coverglass is removed.

## I. Visualization and photographic recording

**Paraffin sections.** Photography of 7-10 µm paraffin sections with simultaneous (single exposure) UV excitation and bright-field transmitted light is an effective photographic recording method if the intensity of the transmitted light is reduced. Dewaxed, coverglassed sections do not photograph well with simultaneous Nomarski interference contrast and UV. Since paraffin sections have considerable tissue autofluorescence under blue excitation, they can be photographed with blue epi-illumination alone (Fig. 1). With experimentation, an exposure index can usually be found so that both the tissue and fluorescent microspheres could be recorded in a single exposure on Ektachrome color film. Fluorescence is also present in sections that have not been dewaxed; with blue epi-illumination, un-dewaxed, uncovered sections look surprisingly good. Microsphere counts can easily be made on such sections.

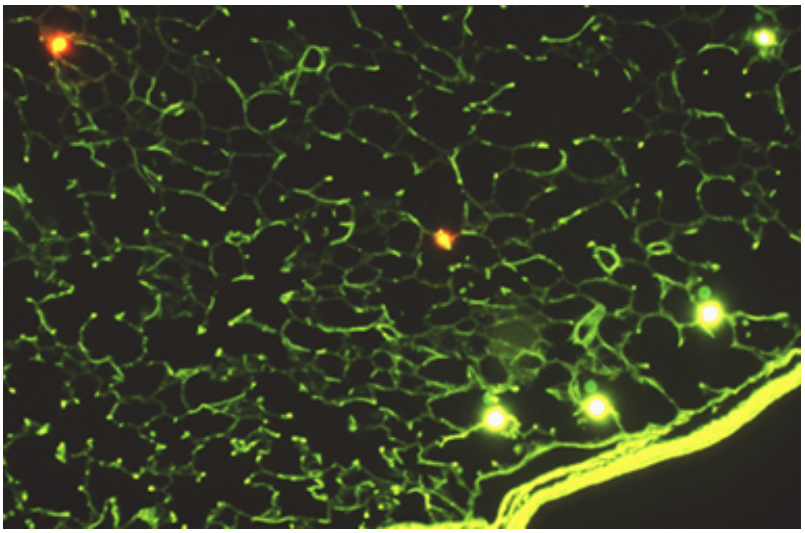

*Figure 1*. Paraffin section of lung showing several yellow-green and red microspheres in the parenchyma. This 7 µm-thick section was cut from a block after Histoclear II was used as the antimedium and the coverglass was mounted with Histoclear II as the coverglass mountant. This protocol preserves the fluorescence of the microspheres and the autofluorescence of the lung.

**Methacrylate sections**. Stained sections can be photographed with bright field illumination plus UV epi-illumination if the transmitted light is reduced. Unstained sections cannot be photographed using tissue autofluorescence since it is nonexistent. Unstained, uncovered sections can be photographed with simultaneous Nomarski interference contrast (using a sky blue background) and UV. Covering the sections markedly reduces the amount of interference contrast, depending on the refractive index of the mounting medium. Since we did not have a way of measuring the relative brightness of microspheres and tissue, bracketing exposures was necessary to obtain proper exposures.

**Vibratome sections of air-dried lung**. Sections under blue epi-illumination show considerable green autofluorescence. An alternative with sections up to 50 µm was a double exposure of blue epi-illumination only and bright field or Nomarski interference contrast transmitted light only. The exposure index used for the epi-illuminated exposure was about ten times that of the transmitted light exposure. This was the case even when a dark field correction was used with the epi-illuminated exposure. Experimentation was necessary to produce good photographs.

**Vibratome sections of unembedded fixed tissue.** The green autofluorescence of thick sections photographed much better than 10 µm paraffin sections although thicker sections show apparent loss of resolution. Simultaneous Nomarski transmitted illumination and UV epi-illumination or a double exposure of Nomarski illumination and blue epi-illumination produced colorful images with 35-50 µm sections (Fig. 2).

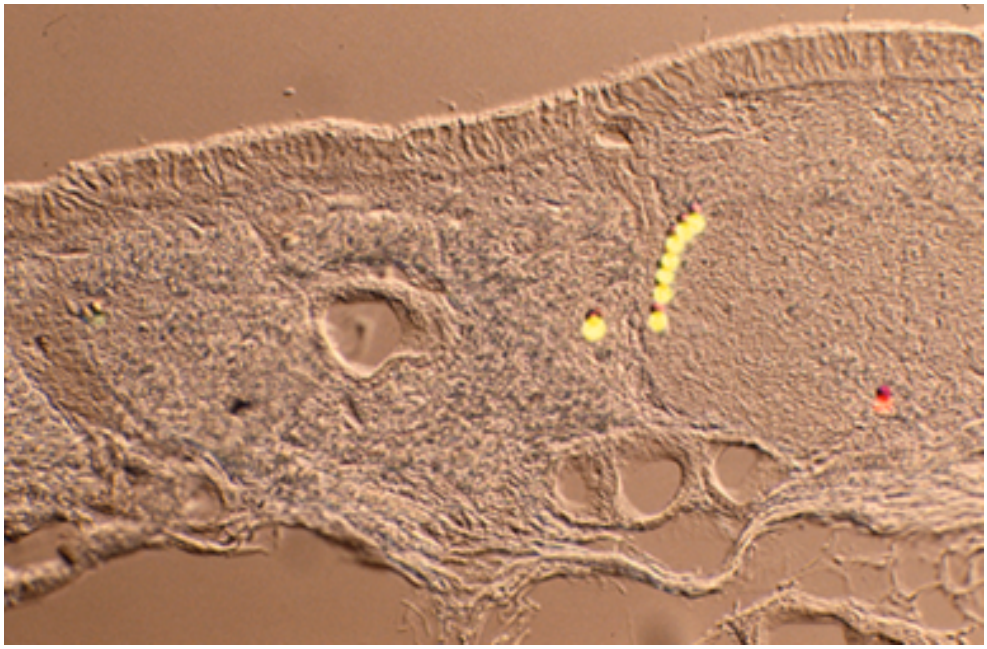

*Figure 2*. Section of a unembedded, formalin-fixed tracheal wall that was cut with a Vibratome. This 35 µm-thick section was photographed as a double exposure with epifluorescence and with Nomarski differential interference contrast optics. The tissue is visualized at moderate to good and the microspheres fluoresce brightly.

**Vibratome sections of gelatin–embedded fixed tissue**. Although gelatin has a faint fluorescence, sections show good autofluorescence under blue excitation, and yellow-green and red microspheres fluoresce brightly. The fluorescence is equal to that of unembedded, fixed tissue. Good color photographs may be made with blue epi-illumination although 100 µm sections are too thick to use a double exposure of Nomarski interference contrast and blue epi-illumination.

# REFERENCES

Chappard D. 1985. Uniform polymerization of large blocks in glycol methacrylate at low temperature with special reference to enzyme histochemistry. Mikroskopie 42: 148-150.

Humason GL. 1979. 4th ed. Animal tissue techniques. W.H. Freeman & Co., San Francisco, CA.

Igarashi E, Kawamura N, Takeshita S. 1994. A method for detecting visceral malformations in gelatin-embedded rat fetuses using an automatic slicing apparatus. Biotech. Histochem. 69: 305-310.

Lyon H, Holm I, Prento P, Balslev E. 1995. Non-hazardous organic solvents in the paraffin-embedding technique: a rational approach. Aliphatic monoesters for clearing and dewaxing: butyldecanoate. Histochemistry 103: 263-269.

# 7 Measurement of Regional Alveolar Ventilation With FMS Aerosols

Alveolar deposition of appropriately sized polystyrene FMS labels shows promise as a means to obtain high-resolution maps of regional ventilation. While larger particles deposit on the conducting airways, an aerosol of ≥ 1.0 micrometer particles will deposit primarily in the alveoli rather than on conducting airways, and the intensity of the fluorescence deposited is proportional to the regional alveolar ventilation.

While the smallest possible particle size would best reflect the movement of gas within the lung, the size of the fluorescent signal for a given microsphere is proportional to the cube of the particle diameter, and a balance between these two constraints must be sought. We have found that we can obtain a satisfactory fluorescence signal from lung regions of 1.0 $cm^3$ volume with 1.0 micron FMS. Gas movement to lung regions of 1.0 $cm^3$ volume comes primarily by convection, and hence the FMS aerosol method is appropriate at that scale. However it would be inappropriate to do microscopic counts of 1.0 micron FMS deposition and conclude that differences in particle deposition between adjacent alveolar clusters represented differences in regional ventilation. Gas molecules equilibrate within alveolar spaces by diffusion, whereas aerosol particles of the 1.0 micron size deposit by gravitational settling. Microscopic examination of lungs given 1.0 micron FMS aerosol exposure reveal a heterogeneous deposition pattern in alveolar spaces, and a suggestion that most particles are deposited on the same side of the airway walls, as would be expected for gravitational settling. Microscopic examination of these samples does reveal that there is only rare FMS deposition on surfaces of the conducting airways, mostly at airway bifurcations. More recently, we have found that adequate fluorescent signal may be obtained using a 0.04 micron FMS administered over a 10-min period. The deposition of a 0.04 micron particle will be substantially greater than that of a 1 micron particle thereby partially compensating for the decreased amount of dye loaded into each microsphere.

## Aerosol Administration System

The generation system should supply a stable monodisperse aerosol at a constant concentration throughout the administration period. It is desirable to be able to switch readily to different color labels. While the system described below attains these goals, it is possible that far simpler systems could work equally well if their aerosol composition were validated.

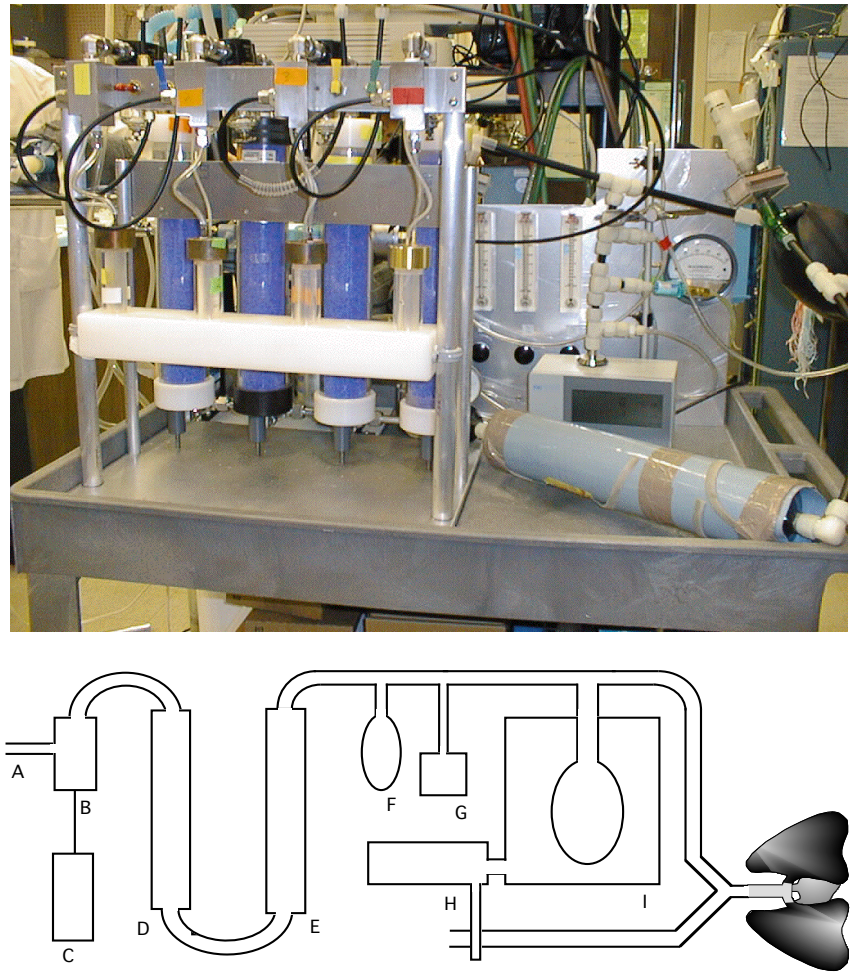


Figure 1. Current aerosol administration system with a schematic diagram.

1 The aerosol generator (B) draws the FMS suspension from the aerosol reservoir (C). We use a 3% suspension of FMS in distilled water with 0.02% Tween-80 and 0.01% thimerosal that is first vortexed and then sonicated for 30 seconds before pouring the mixture into the atomizer reservoir (C).

2. The aerosol is passed through a silica gel diffusion drier (D) to absorb the water, and through a Krypton-85 source charge neutralizer (E) to minimize deposition of charged aerosol on the walls of the administration system.

3. The aerosol has additional gas added to the reservoir bag (F) to satisfy the minute ventilation requirements of the animal, and the administered particle concentration is monitored with a laser particle counter (G).

4. The gas-aerosol mixture is administered to the lungs by a piston-pump ventilator (H) that drives a bag-in-box ventilation system (I). The aerosol only contacts conductive tubing and anesthesia bags with this ventilator, minimizing the loss due to electrostatic attraction.

# Approaches to Maximizing the FMS Signal

Several different approaches to maximizing the FMS aerosol signal delivered to the lung may be used, depending on the constraints of the experimental protocol. The first is to minimize the loss of aerosol within the administration apparatus itself. We found that feeding the aerosol into a standard piston-pump ventilator consumed 2/3 of the generated aerosol. The bag-in-box system described above consumes very little of the administered dose. Higher signals are obtained when the manufacturer maximizes the amount of fluorescence loaded on the microspheres. The concentration of fluorescence added to microspheres for cell biology applications is substantially lower than can be attained. The choice of fluorescent marker is important if signals are low-several dyes have very high specific fluorescence relative to other colors. Larger microspheres contain more dye, and hence have a greater signal, but particles larger than 2.0 microns will have significant deposition on the conducting airways. A higher density of FMS can be added to the aerosol apparatus, provided the aerosol generated remains monodisperse. Finally, if the experimental protocol permits, increasing the FMS administration time or altering the ventilatory parameters to increase settling time (larger tidal volumes or adding an inspiratory hold) will increase deposition.

# Potential Problems with the Aerosol Administration

Bacterial contamination of the FMS solution can occur, particularly if FMS suspensions are recycled from previous experiments. Aerosolized bacteria from such suspensions produce pulmonary hypertension, systemic hypotension, and hypoxemia in experimental animals. Cleaning and drying the generating system after each use and using thimerosal in the FMS suspension appears adequate to prevent this problem.

Deposition of particulates in the lung is not the same as retention, as particles deposited on ciliated airways will eventually be cleared over a period of hours. Particles deposited in alveolar spaces must be cleared by pulmonary macrophages, which then migrate to the airways. The latter process requires days. All of our studies have lasted less than 90 minutes before the lungs were removed and air-dried. We have not demonstrated any difference between particle distributions administered 90 minutes apart (see below), and would not expect a difference for particles deposited primarily in alveolar spaces.

The FMS mixture is supplied in distilled water with 0.01% thimerosal and 0.02% Tween-80. The distilled water is required to permit the microspheres to dry without a saline coating as they are administered. Adsorbed saline will cause the microspheres to pick up water and grow in size once they are in the fully humidified environment of the pulmonary airways.

# Potential Problems with Analysis of FMS Aerosol Signals

The small FMS have a far greater surface to volume ratio in comparison to the standard 15 micron FMS used for blood flow studies, and are prone to decolorization artifacts that cannot be detected with the larger microspheres. We have demonstrated that if a TLC-dried lung labeled with a 1.0 FMS aerosol is foamed with the quick setting isocyanate foam used with our previous studies, fluorescent activity is lost at the lung periphery, particularly for the yellow-green and blue-green fluorescent labels. The simple solution to this problem is to first coat the lung with a 1 to 2 cm layer of a slow setting polyurethane foam (Kwik Foam, DAP Inc., Dayton OH).

Because of the smaller fluorescence signal, two potential problems are background fluorescence from the lung and spillover from dyes adjacent to the ventilation marker in the fluorescent spectrum. Background fluorescence is most marked on the blue end of the spectrum, so that the colors blue, blue-green, and yellow-green are most influenced. A second important factor for lung samples is the amount of light scattering produced by a high particulate concentration in the soaked lung sample. A deliberately macerated piece of lung without fluorescence added can produce a background signal that can be eight times above the background signal for an intact, cleanly cut piece of lung. This artifact will resolve if the particles are allowed to settle in the cuvette, but adequate settling may require several minutes. Signals may be corrected for spillover from adjacent fluorescent colors using a matrix inversion technique (see Section4). Since signals from intravenously delivered 15 micron microspheres tend to be much larger than ventilation signals, we choose fluorescent colors that are adjacent on the fluorescent spectrum for our ventilation markers.

Simultaneous administration of different FMS markers has revealed that a small fraction (less than 1%) of the ventilation measurements show marked discrepancies, with one measurement being several standard deviations higher than its companion. Similar high ventilation signals in those particular pieces are never observed with any measurements preceding or following that measurement. We presume that these high signals are artifacts. While this artifact has been observed with all FMS colors, it occurs most frequently with orange. The two explanations which seem most likely are either there are very rare large "chunks" of color which do not deposit out either in the administration system or the conducting airways, or there are some naturally inhaled substances which give fluorescence. Favoring the former explanation, microscopic examination of FMS suspensions at low power will rarely reveal large irregular chunks of color among the uniformly sized microspheres.

# 8 Miscellaneous Tips

## Miscellaneous Tips Worth Repeating

- Always use the same fluorimeter with the same machine settings and the same set of cuvettes for all samples from a single experiment.

- The fluorescence intensity of a sample can be increased by three means:

  1) injecting more microspheres,
  2) increasing the excitation and/or emission slit widths, or
  3) using less solvent will increase the fluorescent dye concentration.

  Each of these approaches has advantages and disadvantages.

- If the solution to be measured is visibly colored, the fluorescence from that sample will most likely be too high.

- Meticulous cleanliness is mandatory when using optical instrumentation. Use talc-free gloves whenever handling cuvettes. Cuvettes should be washed on a regular basis. Cleaning methods suggested by a cuvette manufacturer (Starna, CA) are as follows:

  Cuvette Cleaning Methods

  Most laboratory detergents may be used at recommended concentrations; however, if the pH is greater than 8.5, etching may occur with repeated use. In general, neutral detergents such as 'Neutracon' are safe. We use ES™ 7X® Cleaning Solution from ICN Biomedicals, Inc., diluted 1:100 in distilled water.

  Rinse with distilled water followed by analytical grade methanol and/or acetone.

  These cleaning methods should never be used on cells that are not of fully-fused construction, as most of these reagents will attack the adhesives at the interface between the optical surfaces and the cell body.

- Tween-80® can cause transient hypotension in certain animals, depending on the concentration of Tween-80® and the rate of injection. If this is a problem, the microspheres can be centrifuged, the supernatant poured off, and the microspheres resuspended in saline. A small amount of Tween-80® should be used to prevent aggregation of the spheres.

- Suitable membrane filters are available from several manufacturers, including Millipore Corp., Bedford, MA and Poretics, Inc., Livermore, CA. In some cases, the filters have precisely sized holes that are made by charged particles from a nuclear reactor. Filters are available in several sizes and the filtration apparatus, which includes a glass support, a clamping device and a vacuum funnel, can be purchased from the filter suppliers. The filters should be stable to 4N KOH for a brief period of time (see Section 5).

- Do not use other tissue dyes in samples, as they may absorb the excitation and or emission light when measuring fluorescence (see Section 2 regarding vital dyes).

- If fluorescent dye solutions are too concentrated, quenching (reduction) of the fluorescent signal can occur, leading to incorrect results. Usually, solutions will be dilute enough to prevent this, but suspected quenching can be confirmed by diluting the sample 1:1 in the extraction solvent. The fluorescence reading should be 50% of the original solution if quenching is not present. If quenching is present, the diluted solution will have greater than 50% of the original solution (see Section 3).

- At equal concentrations, some fluorescent microspheres emit a greater signal intensity than others when the recommended wavelength pairs from Table 1 are used (see Figure 1). It is possible to decrease one or more of the individual peak emission intensities so that all peaks are at about the same intensity by reducing the microsphere concentration, moving the excitation to a shorter, less-optimal wavelength, or narrowing the slit width.

- Different lots of solvent may contain impurities that can degrade some of the fluorescent colors over time. We suggest making a single test solution containing solvent and all the fluorescent colors to be used. This solution should be read daily for as long as you normally allow your samples to remain in the solvent before reading them in the fluorimeter (e.g., if samples are to remain in solvent for 72 hours, read the test solution every day for 3 days). Repeat this with each new solvent lot. If degradation occurs in specific colors, avoid these colors or use a new solvent lot. We have observed that the stability of fluorescent colors vary between different lots of Cellosolve® acetate.

- Whenever possible, tissue and blood samples should be digested in glass containers. This decreases microsphere loss due to electrostatic attractions between the microspheres and plastic vials.

# 9 Non-radioactive Microsphere Bibliography


Abe, Y., Y. Kitada and A. Narimatsu. Effect of a calcium-sensitizing positive inotropic agent MCI-154 and its combined use with enalapril on postischemic contractile dysfunction of dog hearts. *J Cardiovasc Pharmacol*. 26:653-9., 1995.

Abel, F. L., R. R. Beck and R. H. Cooper. Fluorescent microspheres [letter]. *J Appl Physiol*. 76:986, 1994.

Abel, F. L., R. H. Cooper and R. R. Beck. Use of fluorescent latex microspheres to measure coronary blood flow distribution. *Circ Shock*. 41:156-61, 1993.

Abraham, S. A., F. N. Mirecki, D. Levine, A. D. Nunn, H. W. Strauss and H. Gewirtz. Myocardial technetium-99m-teboroxime activity in acute coronary artery occlusion and reperfusion: relation to myocardial blood flow and viability. *J Nucl Med*. 36:1062-8., 1995.

Altemeier, W. A., H. T. Robertson and R. W. Glenny. Pulmonary gas-exchange analysis by using simultaneous deposition of aerosolized and injected microspheres. *Journal of Applied Physiology*. 85:2344-2351, 1998.

Altemeier, W. A., H. T. Robertson, S. McKinney and R. W. Glenny. Pulmonary embolization causes hypoxemia by redistributing regional blood flow without changing ventilation. *Journal of Applied Physiology*. 85:2337-2343, 1998.

Angelborg, C., N. Slepecky, H. C. Larsen and L. Soederberg. Colored microspheres for blood flow determinations twice in the same animal. *Heart Res*. 27:265-9, 1987.

Ardehali, A., R. N. Gates, H. Laks, D. C. Drinkwater, Jr., E. Rudis, T. J. Sorensen, P. Chang and A. Aharon. The regional capillary distribution of retrograde blood cardioplegia in explanted human hearts. *J Thorac Cardiovasc Surg*. 109:935-9; discussion 939-40., 1995.

Ardevol, A., C. Adan, X. Remesar, M. Alemany and J. A. Fernandezlopez. Muscle blood flow during intense exercise in the obese rat. *Archives of Physiology & Biochemistry*. 104:337-343, 1996.

Ardevol, A., C. Adan, X. Remesar, J.-A. FernandezLopez and M. Alemany. Hind leg heat balance in obese Zucker rats during exercise. *PFLUGERS ARCHIV-EUROPEAN JOURNAL OF PHYSIOLOGY*. 435:454-464, 1998.

Ardevol, A., C. A. X. Remesar, J. A. FernandezLopez and M. Alemany. Lactate-bicarbonate interrelationship during exercise and recovery in lean and obese Zucker rats. *International Journal Of Obesity*. 21:333-339, 1997.

Arshady, R. Microspheres for biomedical applications: preparation of reactive and labelled microspheres. *Biomaterials*. 14:5-15, 1993.

Atef, N., A. Ktorza, L. Picon and L. P'Enicaud. Increased islet blood flow in obese rats: role of the autonomic nervous system. *Am J Physiol*. 262:E736-40., 1992.

Atef, N., M. C. Laury, J. M. Nguyen, N. Mokhtar, A. Ktorza and L. Penicaud. Increased pancreatic islet blood flow in 48-hour glucose-infused rats: Involvement of central and autonomic nervous systems. *Endocrinology*. 138:1836-1840, 1997.

Atef, N., B. Portha and L. P'Enicaud. Changes in islet blood flow in rats with NIDDM. *Diabetologia*. 37:677-80., 1994.

Audet, D. M. and W. L. Olbricht. The motion of model cells at capillary bifurcations. *Microvasc Res*. 33:377-96, 1987.

Austin, G. E., M. B. Tuvlin, D. Martino-Salzman, R. L. Hunter, A. G. Justicz, N. K. Thompson and A. C. Brooks. Determination of regional myocardial blood flow using fluorescent microspheres. *Am J Cardiovasc Pathol*. 4:352-7, 1993.

Austin, R. E., Jr., W. W. Hauck, G. S. Aldea, A. E. Flynn, D. L. Coggins and J. I. Hoffman. Quantitating error in blood flow measurements with radioactive microspheres. *Am J Physiol*. 257:H280-8, 1989.

Baer, R. W., B. D. Payne, E. D. Verrier, G. J. Vlahakes, D. Molodowitch, P. N. Uhlig and J. I. E. Hoffman. Increased number of myocardial blood flow measurements with radionuclide-labeled microspheres. *Am. J. Physiol.* 246:H418-H434, 1994.

Baile, E. M., J. M. Nelems, M. Schulzer and P. D. Par'e. Measurement of regional bronchial arterial blood flow and bronchovascular resistance in dogs. *J Appl Physiol*. 53:1044-9, 1982.

Bailey, W. F., Jr., M. G. Magno, P. D. Buckman, F. DiMeo, T. Langan, V. T. Armenti and J. D. Mannion. Chronic stimulation enhances extramyocardial collateral blood flow after a cardiomyoplasty. *Ann Thorac Surg*. 56:1045-52; discussion 1052-3., 1993.

Barnes, M. D., N. Lermer, W. B. Whitten and J. M. Ramsey. CCD based approach to high-precision size and refractive index determination of levitated microdroplets using Fraunhofer diffraction. *Review Of Scientific Instruments*. 68:2287-2291, 1997.

Bassingthwaighte, J. B., M. A. Malone, T. C. Moffett, R. B. King, I. S. Chan, J. M. Link and K. A. Krohn. Molecular and particulate depositions for regional myocardial flows in sheep. *Circ Res*. 66:1328-44, 1990.

Bassingthwaighte, J. B., M. A. Malone, T. C. Moffett, R. B. King, S. E. Little, J. M. Link and K. A. Krohn. Validity of microsphere deposition for regional myocardial flows. *Am. J. Physiol.* 253:H184-H193, 1987.

Bauer, R., R. Bergmann, B. Walter, P. Brust, U. Zwiener and B. Johannsen. Regional distribution of cerebral blood volume and cerebral blood flow in newborn piglets - effect of hypoxia/hypercapnia. *Developmental Brain Research*. 112:89-98, 1999.

Bauer, R., D. Hoyer, B. Walter, E. Gaser, H. Kluge and U. Zwiener. Changed systemic and cerebral hemodynamics and oxygen supply due to gradual hemorrhagic hypotension induced by an external PID-controller in newborn swine. *EXPERIMENTAL AND TOXICOLOGIC PATHOLOGY*. 49:469-476, 1997.

Bauer, R., B. Walter, A. Torossian, H. Fritz, O. Schlonski, T. Jochum, D. Hoyer, K. Reinhart and U. Zwiener. A piglet model for evaluation of cerebral blood flow and brain oxidative metabolism during gradual cerebral perfusion pressure decrease. *Pediatric Neurosurgery*. 30:62-69, 1999.

Bauer, R., B. Walter, E. Wurker, H. Kluge and U. Zwiener. Colored microsphere technique as a new method for quantitative-multiple estimation of regional hepatic and portal blood flow. *Experimental & Toxicologic Pathology*. 48:415-420, 1996.

Baumgart, D., T. Ehring and G. Heusch. A proischaemic action of nisoldipine: relationship to a decrease in perfusion pressure and comparison to dipyridamole. *Cardiovasc Res*. 27:1254-9, 1993.

Baumgart, D., T. Ehring, P. Kowallik, B. D. Guth, M. Krajcar and G. Heusch. Impact of alpha-adrenergic coronary vasoconstriction on the transmural myocardial blood flow distribution during humoral and neuronal adrenergic activation. *Circ Res*. 73:869-86., 1993.

Beck, K. C. Regional trapping of microspheres in the lung compares well with regional blood flow. *J Appl Physiol*. 63:883-9, 1987.

Beezhold, D. H., G. L. Sussman, G. M. Liss and N. S. Chang. Latex Allergy Can Induce Clinical Reactions to Specific Foods. *Clinical & Experimental Allergy*. 26:416-422, 1996.

Bernard, S. L., R. W. Glenny, H. H. Erickson, M. R. Fedde, N. Polissar, R. J. Basaraba and M. P. Hlastala. Minimal redistribution of pulmonary blood flow with exercise in racehorses. *Journal Of Applied Physiology*. 81:1062-1070, 1996.

Bernard, S. L., R. W. Glenny, N. L. Polissar, D. L. Luchtel and S. Lakshminarayan. Distribution of pulmonary and bronchial blood supply to airways measured by fluorescent microspheres. *Journal of Applied Physiology*. 80:430-436, 1996.

Bernard, S. L., D. L. Luchtel, R. W. Glenny and S. Lakshminarayan. Bronchial circulation in the marsupial opossum, Didelphis marsupialis. *Respiration Physiology*. 105:1-2, 1996.

Black, S. C. and I. W. Rodger. Methods for studying experimental myocardial ischemic and reperfusion injury. *Journal Of Pharmacological And Toxicological Methods*. 35:179-190, 1996.

Bland, J. M. and D. G. Altman. Statistical methods for assessing agreement between two methods of clinical measurement. *Lancet*. 1:307-10, 1986.

Bock, J. C., A. H. G. Goetze and R. Felix. Confirmation by animal experiment of a semiquantitative single-layer tomography for MR imaging of regional cerebral perfusion. *Rofo Fortschritte Auf Dem Gebiet Der Rontgenstrahlen Und Der Bildgebenden Verfahren*. 166:335-341, 1997.

Boeckxstaens, C. J. and W. J. Flameng. Retrograde cerebral perfusion does not perfuse the brain in nonhuman primates [see comments]. *Ann Thorac Surg*. 60:319-27; discussion 327-8., 1995.

Bolender, R. P., D. M. Hyde and R. T. Dehoff. Lung morphometry: a new generation of tools and experiments for organ, tissue, cell, and molecular biology. *Am J Physiol*. 265:L521-48, 1993.

Bone, H. G., P. J. Schenarts, S. R. Fischer, R. McGuire, L. D. Traber and D. L. Traber. Pyridoxalated hemoglobin polyoxyethylene conjugate reverses hyperdynamic circulation in septic sheep. *JOURNAL OF APPLIED PHYSIOLOGY*. 84:1991-1999, 1998.

Booke, M., F. Hinder, R. McGuire, L. D. Traber and D. L. Traber. Selective inhibition of inducible nitric oxide synthase: Effects on hemodynamics and regional blood flow in healthy and septic sheep. *Critical Care Medicine*. 27:162-167, 1999.

Bouaziz, H., N. Okubo, J. M. Malinovsky, D. Benhamou, K. Samii and J. X. Mazoit. The age-related effects of epidural lidocaine, with and without epinephrine, on spinal cord blood flow in anesthetized rabbits. *Anesthesia and Analgesia*. 88:1302-1307, 1999.

Boyde, A., L. A. Wolfe, M. Maly and S. J. Jones. Vital confocal microscopy in bone. *Scanning*. 17:72-85, 1995.

Bray, R., K. Forrester, J. J. McDougall, A. Damji and W. R. Ferrell. Evaluation of laser Doppler imaging to measure blood flow in knee ligaments of adult rabbits. *Medical & Biological Engineering & Computing*. 34:227-231, 1996.

Bray, R. C., D. J. Butterwick, M. R. Doschak and J. V. Tyberg. Coloured microsphere assessment of blood flow to knee ligaments in adult rabbits: Effects of injury. *Journal Of Orthopaedic Research*. 14:618-625, 1996.

Bremer, H. J., A. Anninos and B. Schulz. Amino Acid Composition Of Food Products Used In the Treatment Of Patients With Disorders Of the Amino Acid and Protein Metabolism. *European Journal of Pediatrics*. 155:S 108-S 114, 1996.

Brown, W. E., M. G. Magno, P. D. Buckman, M. F. Di, D. R. Gale and J. D. Mannion. The coronary collateral circulation in normal goats. *J. Surg. Res.* 51:54-9, 1991.

Brown, W. R., D. M. Moody, D. A. Stump, D. D. Deal and R. L. Anderson. Dog model for cerebrovascular studies of the proximal-to-distal distribution of sequentially injected emboli. *Microvasc Res*. 50:105-12., 1995.

Brunston, R. L., W. K. Tao, A. Bidani, D. L. Traber and J. B. Zwischenberger. Organ blood flow during arteriovenous carbon dioxide removal. *Asaio Journal*. 43:M821-M824, 1997.

Brust, P., R. Bauer, G. Vorwieger, B. Walter, R. Bergmann, F. Fuchtner, J. Steinbach, U. Zwiener and B. Johannsen. Upregulation of the aromatic amino acid decarboxylase under neonatal asphyxia. *Neurobiology of Disease*. 6:131-139, 1999.

Buchwalder, L. F., M. Lin, T. J. McDonald and P. W. Nathanielsz. Fetal sheep adrenal blood flow responses to hypoxemia after splanchnicotomy using fluorescent microspheres. *Journal Of Applied Physiology*. 84:82-89, 1998.

Buckberg, G. D., J. C. Luck, D. B. Payne, J. I. E. Hoffman, J. P. Archie and D. E. Fixler. Some sources of error in measuring regional blood flow with radioactive microspheres. *J. Appl. Physiol.* 31:598-604, 1971.

Burchfield, D. J., A. Pena, A. J. M. Peters, R. M. Abrams and D. Phillips. Cocaine does not compromise cerebral or myocardial oxygen delivery in fetal sheep. *Reproduction Fertility And Development*. 8:383-389, 1996.

Caldarone, C. A., I. B. Krukenkamp, B. D. Misare and S. Levitsky. Perfusion deficits with retrograde warm blood cardioplegia. *Ann Thorac Surg*. 57:403-6., 1994.

Carlson, G. D., Y. Minato, A. Okada, C. D. Gorden, K. E. Warden, J. M. Barbeau, C. L. Biro, E. Bahnuik, H. H. Bohlman and J. C. Lamanna. Early time-dependent decompression for spinal cord injury: Vascular mechanisms of recovery. *JOURNAL OF NEUROTRAUMA*. 14:951-962, 1997.

Carlson, G. D., K. E. Warden, J. M. Barbeau, E. Bahniuk, K. L. KutinaNelson, C. L. Biro, H. H. Bohlman and J. C. LaManna. Viscoelastic relaxation and regional blood flow response to spinal cord compression and decompression. *Spine*. 22:1285-1291, 1997.

Cerda, S. E., C. Y. Tong, D. D. Deal and J. C. Eisenach. A physiologic assessment of intrathecal amitriptyline in sheep. *Anesthesiology*. 86:1094-1103, 1997.

Chase, P. B., K. B. Kern, A. B. Sanders, C. W. Otto and G. A. Ewy. Effects of graded doses of epinephrine on both noninvasive and invasive measures of myocardial perfusion and blood flow during cardiopulmonary resuscitation. *Crit Care Med*. 21:413-9., 1993.

Chien, G. L., C. G. Anselone, R. F. Davis and D. M. Van-Winkle. Fluorescent vs. radioactive microsphere measurement of regional myocardial blood flow. *Cardiovasc Res*. 30:405-12, 1995.

Chiou, G. C. and Y. J. Chen. Effects of D- and L-isomers of timolol on retinal and choroidal blood flow in ocular hypertensive rabbit eyes. *J Ocul Pharmacol*. 8:183-90., 1992.

Chiou, G. C. and Y. J. Chen. Improvement of ocular blood flow with dopamine antagonists on ocular-hypertensive rabbit eyes. *Chung Kuo Yao Li Hsueh Pao*. 13:481-4., 1992.

Cicutti, N. and K. Rakusan. The effect of hypoxia on capillary flow direction in the isolated perfused rat heart. *Can J Cardiol*. 10:367-73, 1994.

Cicutti, N., K. Rakusan and H. F. Downey. Colored microspheres reveal interarterial microvascular anastomoses in canine myocardium. *Basic Res Cardiol*. 87:400-9, 1992.

Cicutti, N., K. Rakusan and H. F. Downey. Coronary artery occlusion extends perfusion territory boundaries through microvascular collaterals. *Basic Res Cardiol*. 89:427-37., 1994.

Cioffi, G. A. and S. Orgul. Intraluminal corrosion casting and colored-microsphere techniques as means to assess optic nerve hemodynamics. *Ocular Blood Flow*. 226:1996.

Cochran, R. P., K. S. Kunzelman, C. R. Vocelka, H. Akimoto, R. Thomas, L. O. Soltow and B. D. Spiess. Perfluorocarbon emulsion in the cardiopulmonary bypass prime reduces neurologic injury. *Annals Of Thoracic Surgery*. 63:1326-1332, 1997.

Conhaim, R. L. and L. A. Rodenkirch. Estimated functional diameter of alveolar septal microvessels in zone 1. *Am J Physiol*. 271:H996-1003., 1996.

Consigny, P. M., E. D. Verrier, B. D. Payne, G. Edelist, J. Jester, R. W. Baer, G. J. Vlahakes and J. I. Hoffman. Acute and chronic microsphere loss from canine left ventricular myocardium. *Am J Physiol*. 242:H392-404, 1982.

Daldrup, H. E., D. M. Shames, W. Husseini, M. F. Wendland, Y. Okuhata and R. C. Brasch. Quantification of the extraction fraction for gadopentetate across breast cancer capillaries. *MAGNETIC RESONANCE IN MEDICINE*. 40:537-543, 1998.

DeBehnke, D. J., M. G. Angelos and J. E. Leasure. Use of cardiopulmonary bypass, high-dose epinephrine, and standard-dose epinephrine in resuscitation from post-countershock electromechanical dissociation. *Ann Emerg Med*. 21:1051-7., 1992.

Deem, S., M. J. Bishop and M. K. Alberts. Effect of anemia on intrapulmonary shunt during atelectasis in rabbits. *Journal Of Applied Physiology*. 79:1951-1957, 1995.

Degens, H., A. J. Craven, J. C. Jarvis and S. Salmons. The use of coloured dye-extraction microspheres to measure blood flow in rabbit skeletal muscle: A validation study with special emphasis on repeated measurements. *Experimental Physiology*. 81:239-249, 1996.

Deka, C., L. A. Sklar and J. A. Steinkamp. Fluorescence lifetime measurements in a flow cytometer by amplitude demodulation using digital data acquisition technique. *Cytometry*. 17:94-101, 1994.

Deveci, D. and S. Egginton. Development of the fluorescent microsphere technique for quantifying regional blood flow in small mammals. *EXPERIMENTAL-PHYSIOLOGY*. 84:615-630, 1999.

Diebel, L. N., J. G. Tyburski and S. A. Dulchavsky. Effect of hypertonic saline solution and dextran on ventricular blood flow and heart-lung interaction after hemorrhagic shock. *Surgery*. 124:642-650, 1998.

Domenech, R. J., J. I. Hoffman, M. I. Noble, K. B. Saunders, J. R. Henson and S. Subijanto. Total and regional coronary blood flow measured by radioactive microspheres in conscious and anesthetized dogs. *Circ Res*. 25:581-96, 1969.

Eckstein, E. C., J. F. Koleski and C. M. Waters. Concentration profiles of 1 and 2.5 microns beads during blood flow. Hematocrit effects. *Asaio Trans*. 35:188-90, 1989.

Ehring, T., D. Baumgart, M. Krajcar, M. Hummelgen, S. Kompa and G. Heusch. Attenuation of myocardial stunning by the ACE inhibitor ramiprilat through a signal cascade of bradykinin and prostaglandins but not nitric oxide. *Circulation*. 90:1368-85., 1994.

Ehring, T., M. Bohm and G. Heusch. The calcium antagonist nisoldipine improves the functional recovery of reperfused myocardium only when given before ischemia. *J Cardiovasc Pharmacol*. 20:63-74., 1992.

Eising, G. P., L. Mao, G. W. SchmidSchonbein, R. L. Engler and J. Ross. Effects of induced tolerance to bacterial lipopolysaccharide on myocardial infarct size in rats. *Cardiovascular Research*. 31:73-81, 1996.

Elgjo, G. I., B. P. Mathew, L. F. P. deFigueiredo, P. J. Schenarts, J. W. Horton, M. A. Dubick and G. C. Kramer. Resuscitation with hypertonic saline dextran improves cardiac function in vivo and ex vivo after burn injury in sheep. *SHOCK*. 9:375-383, 1998.

Erickson, H. H., S. L. Bernard, R. W. Glenny, M. R. Fedde, N. L. Polissar, R. J. Basaraba, S. M. Walther, E. M. Gaughan, R. McMurphy and M. P. Hlastala. Effect of furosemide on pulmonary blood flow distribution in resting and exercising horses. *Journal Of Applied Physiology*. 86:2034-2043, 1999.

Fan, F. C., G. B. Schuessler, R. Y. Z. Chen and S. Chien. Determination of blood flow and shunting of 9- and 15- µm spheres in regional beds. *Am. J. Physiol.* 237:H25-H33, 1979.

Fenton, B. M., R. T. Carr and G. R. Cokelet. Nonuniform red cell distribution in 20 to 100 micrometers bifurcations. *Microvasc Res*. 29:103-26, 1985.

Flynn, A. E., D. L. Coggins, R. E. Austin, D. D. Muehrcke, G. S. Aldea, M. Goto, J. W. Doucette and J. I. Hoffman. Nonuniform blood flow in the canine left ventricle. *J Surg Res*. 49:379-84, 1990.

Forrester, K., M. Doschak and R. Bray. In vivo comparison of scanning technique and wavelength in laser Doppler perfusion imaging: measurement in knee ligaments of adult rabbits. *MEDICAL & BIOLOGICAL ENGINEERING & COMPUTING*. 35:581-586, 1997.

Frangioni, G. and G. Borgioli. Data on haemodynamics of splenic circulation in the newt. *Journal Of Zoology*. 238:149-155, 1996.

Fujiki, H., T. Mori, K. Yoshida, T. Imaizumi and M. Tominaga. OPC-18790, a novel positive inotropic agent, has both arterial and venous vascular dilating actions in the dog. *European Journal Of Pharmacology*. 313:191-200, 1996.

Funato, H., M. Watanabe and A. Uemura. Therapeutic effects of a calcium antagonist, lacidipine, on stroke-prone spontaneously hypertensive rats with cerebrovascular lesions. *JAPANESE-JOURNAL-OF-PHARMACOLOGY*. 80:199-208, 1999.

Gagnon, R., J. Challis, L. Johnston and L. Fraher. Fetal endocrine responses to chronic placental embolization in the late-gestation ovine fetus. *Am J Obstet Gynecol*. 170:929-38., 1994.

Galiuto, L., A. N. DeMaria, K. MayNewman, U. DelBalzo, K. Ohmori, V. Bhargava, S. F. Flaim and S. Iliceto. Evaluation of dynamic changes in microvascular flow during ischemia-reperfusion by myocardial contrast echocardiography. *Journal of the American College of Cardiology*. 32:1096-1101, 1998.

Gates, R. N., J. G. Lee, H. Laks, D. C. Drinkwater, E. Rhudis, A. S. Aharon, J. Y. Chung and P. A. Chang. Evidence of improved microvascular perfusion when using antegrade and retrograde cardioplegia. *Annals Of Thoracic Surgery*. 62:1388-1391, 1996.

Gervais, M., P. Demolis, V. Domergue, M. Lesage, C. Richer and J. F. Giudicelli. Systemic and regional hemodynamics assessment in rats with fluorescent microspheres. *Journal of Cardiovascular Pharmacology*. 33:425-432, 1999.

Glenny, R. W. Blood flow measurements using fluorescent microspheres. Second Oxford Conference on Spectrometry. 1995.

Glenny, R. W., S. Bernard and M. Brinkley. Validation of fluorescent-labeled microspheres for measurement of regional organ perfusion. *J Appl Physiol*. 74:2585-97, 1993.

Glenny, R. W., S. Bernard, H. T. Robertson and M. P. Hlastala. Gravity is an important but secondary determinant of regional pulmonary blood flow in upright primates. *Journal of Applied Physiology*. 86:623-632, 1999.

Glenny, R. W., S. McKinney and K. T. Robertson. Spatial pattern of pulmonary blood flow distribution is stable ever days. *Journal Of Applied Physiology*. 82:902-907, 1997.

Glenny, R. W., N. L. Polissar, S. McKinney and H. T. Robertson. Temporal heterogeneity of regional pulmonary perfusion is spatially clustered. *J Appl Physiol*. 79:986-1001., 1995.

Glenny, R. W. and H. T. Robertson. A computer simulation of pulmonary perfusion in three dimensions. *J Appl Physiol*. 79:357-69., 1995.

Gottlieb, G. J., S. H. Kubo and D. R. Alonso. Ultrastructural characterization of the border zone surrounding early experimental myocardial infarcts in dogs. *Am J Pathol*. 103:292-303, 1981.

Granetzny, A., U. Schwanke, C. Schmitz, G. Arnold, D. Schafer, H. D. Schulte, E. Gams and J. D. Schipke. Pharmacologic heart rate reduction: Effect of a novel, specific bradycardic agent on the heart. *THORACIC AND CARDIOVASCULAR SURGEON*. 46:63-69, 1998.

Granetzny, A., U. Schwanke, C. Schmitz, S. SchmitzSpanke, G. Arnold, H. D. Schulte and J. D. Schipke. Effects of a new bradycardic agent on the isolated rabbit heart. *Zeitschrift Fur Kardiologie*. 85:953-960, 1996.

Greve, G. and T. Saetersdal. Problems related to infarct size measurements in the rat heart. *Acta Anat Basel*. 142:366-73, 1991.

Groban, L., D. A. Zvara, D. D. Deal, J. C. Vernon, C. W. Flye, X. L. Ma and J. VintenJohansen. Cloricromene reduces infarct size and alters postischaemic blood flow defects in dog myocardium. *CLINICAL AND EXPERIMENTAL PHARMACOLOGY AND PHYSIOLOGY*. 25:417-423, 1998.

Gross, T. S., A. A. Damji, S. Judex, R. C. Bray and R. F. Zernicke. Bone hyperemia precedes disuse-induced intracortical bone resorption. *Journal of Applied Physiology*. 86:230-235, 1999.

Gross, W., P. Zeller, U. Kreimeier and K. Messmer. Pseudocolor display of regional organ blood flow determined by means of the radioactive microsphere technique. *Comput Med Imaging Graph*. 14:1-11, 1990.

Grund, F., H. T. Sommerschild, T. Lyberg, K. A. Kirkeboen and A. Ilebekk. Microembolization in pigs: effects on coronary blood flow and myocardial ischemic tolerance. *AMERICAN-JOURNAL-OF-PHYSIOLOGY-HEART-AND-CIRCULATORY-PHYSIOLOGY*. 46:H533-H542, 1999.

Guilbault, G. G. Practical Fluorescence. Modern Monographs in Analytical Chemistry. 3: 1990.

Haga, Y., R. Nordlander, P. O. Sjoquist and L. Ryd'en. Influence of coronary venous retroinfusion and vasodilatation on regional myocardial blood flow measurement with microspheres. An analysis of 'microsphere loss' from ischaemic and reperfused porcine hearts. *Acta Physiol Scand*. 153:13-20, 1995.

Hagendorff, A., C. Dettmers, P. Danos, M. Hummelgen, C. Vahlhaus, C. Martin, G. Heusch and B. Luderitz. Cerebral vasoconstriction during sustained ventricular tachycardia induces an ischemic stress response of brain tissue in rats. *Journal of Molecular and Cellular Cardiology*. 30:2081-2094, 1998.

Hagendorff, A., C. Vahlhaus, W. Jung, C. Martin, G. Heusch and B. Luderitz. Association between hemodynamic parameters and the degeneration of sustained ventricular tachycardias into ventricular fibrillation in rats. *JOURNAL OF MOLECULAR AND CELLULAR CARDIOLOGY*. 29:3091-3103, 1997.

Hakkinen, J. P., M. W. Miller, A. H. Smith and D. R. Knight. Measurement of organ blood flow with coloured microspheres in the rat. *Cardiovasc Res*. 29:74-9, 1995.

Hale, S. L., K. J. Alker and R. A. Kloner. Evaluation of nonradioactive, colored microspheres for measurement of regional myocardial blood flow in dogs. *Circulation*. 78:428-34, 1988.

Hale, S. L. and R. A. Kloner. Effect of early coronary artery reperfusion on infarct development in a model of low collateral flow. *Cardiovasc Res*. 21:668-73, 1987.

Hale, S. L., M. T. Vivaldi and R. A. Kloner. Fluorescent microspheres: a new tool for visualization of ischemic myocardium in rats. *Am J Physiol*. 251:H863-8, 1986.

Hales, J. R. S. and W. J. Cliff. Direct observation of the behavior of microspheres in microvasculature. *Bibl. Anat.* 15:87-91, 1977.

Hall, J. L., L. A. Hernandez, J. Henderson, L. A. Kellerman and W. C. Stanley. Decreased interstitial glucose and transmural gradient in lactate during ischemia. *Basic Res Cardiol*. 89:468-86, 1994.

Hanger, C. C., S. C. Hillier, R. G. Presson, Jr., R. W. Glenny and W. W. Wagner, Jr. Measuring pulmonary microvessel diameters using video image analysis. *J Appl Physiol*. 79:526-32., 1995.

Hardy, J., A. L. Bertone and W. W. Muir. Joint pressure influences synovial tissue blood flow as determined by colored microspheres. *Journal Of Applied Physiology*. 80:1225-1232, 1996.

Hariawala, M. D., J. R. Horowitz, D. Esakof, D. D. Sheriff, D. Walter, B. Keyt, J. M. Isner and J. F. Symes. VEGF improves myocardial blood flow but produces EDRF-mediated hypotension in porcine hearts. *Journal Of Surgical Research*. 63:77-82, 1996.

Harris, D. A. Spectrophotometry and Spectrofluorimetry a Practical Approach, Washington, D.C.: IRL Press, 1987

Hasegawa, T., A. Kimura, R. Miyataka, M. Inagaki and K. Ishikawa. Basic fibroblast growth factor increases regional myocardial blood flow and salvages myocardium in the infarct border zone in a rabbit model of acute myocardial infarction. *Angiology*. 50:487-495, 1999.

Hatori, N., Y. Uriuda, K. Isozima, T. Isono, E. Okuda, K. Hamada, I. Nakahoshi, A. Kurita, H. Yoshizu and S. Tanaka. Short-term treatment with synchronized coronary venous retroperfusion before full reperfusion significantly reduces myocardial infarct size. *Am Heart J*. 123:1166-74., 1992.

Herijgers, P., V. Leunens, T. B. Tjandramaga, K. Mubagwa and W. Flameng. Changes in organ perfusion after brain death in the rat and its relation to circulating catecholamines. *Transplantation*. 62:330-335, 1996.

Heyman, M. A., B. D. Payne, J. I. Hoffman and A. M. Rudolf. Blood flow measurements with radionuclide-labeled particles. *Prog. Cardiovasc. Dis.* 20:55-79, 1977.

Hiller, K. H., P. Adami, S. Voll, F. Roder, P. Kowallik, W. R. Bauer, A. Haase and G. Ertl. In vivo colored microspheres in the isolated rat heart for use in NMR. *Journal Of Molecular And Cellular Cardiology*. 28:571-577, 1996.

Hiller, K. H., F. Roder, P. Adami, S. Voll, P. Kowallik, A. Haase, G. Ertl and W. R. Bauer. Study of microcirculation by coloured microspheres and NMR-microscopy in isolated rat heart: Effect of ischaemia, endothelin-1 and endothelin-1 antagonist BQ 610. *JOURNAL OF MOLECULAR AND CELLULAR CARDIOLOGY*. 29:3115-3122, 1997.

Hillier, S. C., J. A. Graham, C. C. Hanger, P. S. Godbey, R. W. Glenny and W. W. Wagner. Hypoxic vasoconstriction in pulmonary arterioles and venules. *Journal Of Applied Physiology*. 82:1084-1090, 1997.

Hlastala, M. P., S. L. Bernard, H. H. Erickson, M. R. Fedde, E. M. Gaughan, R. McMurphy, M. J. Emery, N. Polissar and R. W. Glenny. Pulmonary blood flow distribution in standing horses is not dominated by gravity. *Journal Of Applied Physiology*. 81:1051-1061, 1996.

Hlastala, M. P., M. A. Chornuk, D. A. Self, H. J. Kallas, J. W. Burns, S. Bernard, N. L. Polissar and R. W. Glenny. Pulmonary blood flow redistribution by increased gravitational force. *JOURNAL OF APPLIED PHYSIOLOGY*. 84:1278-1288, 1998.

Hodeige, D., P.-M. De, W. Eechaute, J. Weyne and G. R. Heyndrickx. On the validity of blood flow measurement using colored microspheres. *American Journal of Physiology-Heart and Circulatory Physiology*. 45:H1150-H1158, 1999.

Hoffbrand, B. I. and R. P. Forsyth. Validity studies of the radioactive microsphere method for the study of the distribution of cardiac output, organ blood flow, and resistance in the conscious rhesus monkey. *Cardiovasc. Res.* 3:426-432, 1969.

Hong, S. J., K. Y. Wu and I. J. Chen. Ocular hypotensive and vasodilative effects of two beta-adrenergic blockers with intrinsic sympathomimetic activity. *CURRENT EYE RESEARCH*. 17:700-707, 1998.

Hood, D. D., J. C. Eisenach, C. Tong, E. Tommasi and T. L. Yaksh. Cardiorespiratory and spinal cord blood flow effects of intrathecal neostigmine methylsulfate, clonidine, and their combination in sheep [see comments]. *Anesthesiology*. 82:428-35., 1995.

Hooper, S. B. Role of luminal volume changes in the increase in pulmonary blood flow at birth in sheep. *Experimental Physiology*. 83:833-842, 1998.

Hoshida, S., T. Kuzuya, M. Nishida, N. Yamashita, H. Oe, M. Hori, T. Kamada and M. Tada. Adenosine blockade during reperfusion reverses the infarct limiting effect in preconditioned canine hearts. *Cardiovasc Res*. 28:1083-8, 1994.

Hoshida, S., T. Kuzuya, N. Yamashita, M. Nishida, S. Kitahara, M. Hori, T. Kamada and M. Tada. gamma-Glutamylcysteine ethyl ester for myocardial protection in dogs during ischemia and reperfusion. *J Am Coll Cardiol*. 1. 24:1391-7., 1994.

Hu, N., T. D. Ngo and E. B. Clark. Distribution of blood flow between embryo and vitelline bed in the stage 18, 21 and 24 chick embryo. *Cardiovascular Research*. 31:131, 1996.

Huijbregts, P., E. J. M. Feskens, L. Rasanen, A. Albertifidanza, M. Mutanen, F. Fidanza and D. Kromhout. Dietary Intake In Five Ageing Cohorts Of Men In Finland, Italy and the Netherlands. *European Journal of Clinical Nutrition*. 49:852-860, 1995.

Iglesiasbarreira, V., M. T. Ahn, B. Reusens, S. Dahri, J. J. Hoet and C. Remacle. Pre- and postnatal low protein diet affect pancreatic islet blood flow and insulin release in adult rats. *Endocrinology*. 137:3797-3801, 1996.

Ikeda, T., Y. Murata, E. J. Quilligan, P. Cifuentes, S. Doi and S. D. Park. Two sinusoidal heart rate patterns in fetal lambs undergoing extracorporeal membrane oxygenation. *American Journal of Obstetrics and Gynecology*. 180:462-468, 1999.

Inada, Y., S. Tamai, S. Mizumoto, H. Ono, K. Kawanishi and A. Fukui. Non-radioactive coloured microsphere measurement of regional tissue blood flow for axial pattern flaps in rabbits. *Br J Plast Surg*. 46:127-31, 1993.

Ishikawa, K., N. Kamata, S. Nakai, H. Akiyama, H. Koka, I. Ogawa and R. Katori. Preservation of high regional blood flow at epicardial rim after coronary occlusion in dogs. *Am J Physiol*. 267:H528-34, 1994.

Ishikawa, K., I. Ogawa, M. Shimizu, H. Koka, N. Kamata, S. Nakai, H. Akiyama, T. Shimamoto, N. Ishida and K. Kanamasa. The importance of good endocardial reflow immediately after reperfusion for myocardial salvage in dogs. *Jpn. Circ. J.* 55:983-93, 1991.

Ishikawa, K., I. Ogawa, M. Shimizu, H. Koka, N. Kamata, S. Nakai and R. Katori. Residual critical coronary stenosis during myocardial reperfusion is deleterious to myocardial salvage in dogs. *Jpn Circ J*. 56:921-8., 1992.

Ishikawa, M., T. Mori, S. Itoh, H. Fujiki, K. Koga, M. Tominaga and Y. Yabuuchi. Effects of OPC-18790, a new positive inotropic agent, on energetics in the ischaemic canine heart: a 31P-MRS study. *Cardiovasc Res*. 30:299-306., 1995.

Jasper, M. S., P. McDermott, D. S. Gann and W. C. Engeland. Measurement of blood flow to the adrenal capsule, cortex and medulla in dogs after hemorrhage by fluorescent microspheres. *J Auton Nerv Syst*. 30:159-67, 1990.

Johansen, B., M. N. Melsom, T. Flatebo and G. Nicolaysen. Time course and pattern of pulmonary flow distribution following unilateral airway occlusion in sheep. *CLINICAL SCIENCE*. 94:453-460, 1998.

Kaihara, S., P. D. Heerden, T. Migita and H. N. Wagner Jr. Measurement of distribution of cardiac output. *Journal of Applied Physiology*. 25:696-700, 1968.

Kallas, H. J., K. B. Domino, R. W. Glenny, E. A. Anderson and M. P. Hlastala. Pulmonary blood flow redistribution with low levels of positive end-expiratory pressure. *ANESTHESIOLOGY*. 88:1291-1299, 1998.

Kamimura, T., H. Sakamoto and K. Misumi. Regional blood flow distribution from the proximal arterial cannula during veno-arterial extracorporeal membrane oxygenation in neonatal dog. *Journal of Veterinary Medical Science*. 61:311-315, 1999.

Kanagawa, R., T. Wada, T. Sanada, M. Ojima and Y. Inada. Regional hemodynamic effects of candesartan cilexetil (TCV-116), an angiotensin II AT(1)-receptor antagonist, in conscious spontaneously hypertensive rats. *Japanese Journal Of Pharmacology*. 73:185-190, 1997.

Kapadia, S. J., J. S. Terlato and A. S. Most. Presence of a critical coronary artery stenosis does not abolish the protective effect of ischemic preconditioning. *Circulation*. 95:1286-1292, 1997.

Kawagoe, Y., S. Permutt and H. E. Fessler. Hyperinflation with intrinsic PEEP and respiratory muscle blood flow. *J Appl Physiol*. 77:2440-8., 1994.

Kelly, R. F., T. L. Hursey, R. B. Patel, J. E. Parrillo and G. L. Schaer. Effect of poloxamer 188 on collateral blood flow, myocardial infarct size, and left ventricular function in a canine model of prolonged (3-hour) coronary occlusion and reperfusion. *JOURNAL OF THROMBOSIS AND THROMBOLYSIS*. 5:239-247, 1998.

Kelly, R. F., T. L. Hursey, G. L. Schaer, M. J. Piotrowski, S. V. Dee, J. E. Parrillo and S. M. Hollenberg. Cardiac endothelin release and infarct size, myocardial blood flow, and ventricular function in canine infarction and reperfusion. *Journal Of Investigative Medicine*. 44:575-582, 1996.

Kemp, P. A., S. M. Gardiner, J. E. March, P. C. Rubin and T. Bennett. Assessment of the effects of endothelin-1 and magnesium sulphate on regional blood flows in conscious rats, by the coloured microsphere reference technique. *British Journal of Pharmacology*. 126:621-626, 1999.

Kern, K. B. and G. A. Ewy. Minimal coronary stenoses and left ventricular blood flow during CPR [published erratum appears in Ann Emerg Med 1993 Jan;22(1):124]. *Ann Emerg Med*. 21:1066-72., 1992.

Kern, K. B., L. Lancaster, S. Goldman and G. A. Ewy. The effect of coronary artery lesions on the relationship between coronary perfusion pressure and myocardial blood flow during cardiopulmonary resuscitation in pigs. *Am. Heart J.* 120:324-33, 1990.

Khoobehi, B., B. Shoelson, Y. Z. Zhang and G. A. Peyman. Fluorescent microsphere imaging: A particle-tracking approach to the hemodynamic assessment of the retina and choroid. *Ophthalmic Surgery And Lasers*. 28:937-947, 1997.

Kimura, A., K. Ishikawa and I. Ogawa. Myocardial salvage by reperfusion 12 hours after coronary ligation in dogs. *JAPANESE CIRCULATION JOURNAL-ENGLISH EDITION*. 62:294-298, 1998.

Kinoshita, H., I. Ijiri, S. Ameno, C. Fuke, Y. Fujisawa and K. Ameno. Inhibitory mechanism of intestinal ethanol absorption induced by high acetaldehyde concentrations: Effect of intestinal blood flow and substance specificity. *Alcoholism Clinical And Experimental Research*. 20:510-513, 1996.

Kinoshita, K., D. J. Hearse, M. V. Braimbridge and A. S. Manning. 'Early' ischemia and reperfusion-induced arrhythmias: antiarrhythmic effects of diltiazem in the conscious rat. *Can J Cardiol*. 4:37-43, 1988.

Klabunde, R. E., W. A. Anderson, M. Locke, S. E. Ianuzzo and C. D. Ianuzzo. Regional blood flows in the goat latissimus dorsi muscle before and after chronic stimulation. *Journal Of Applied Physiology*. 81:2365-2372, 1996.

Klemm, K. and F. G. Moody. Regional intestinal blood flow and nitric oxide synthase inhibition during sepsis in the rat. *Annals of Surgery*. 227:126-133, 1998.

Kobayashi, N., K. Kobayashi, K. Hara, T. Higashi, H. Yanaka, S. Yagi and H. Matsuoka. Benidipine stimulates nitric oxide synthase and improves coronary circulation in hypertensive rats. *American Journal of Hypertension*. 12:483-491, 1999.

Kobayashi, N., K. Kobayashi, K. Kono, T. Akabane, H. Kaneko, M. Takada, N. Tsuchiya and S. Yagi. Effects of microsphere suspension agents on systemic hemodynamics in rats. Comparison of nonradioactive colored and radioactive microspheres. *Jpn Heart J*. 35:467-75, 1994.

Kobayashi, N., K. Kobayashi, K. Kouno, S. Horinaka and S. Yagi. Effects of intra-atrial injection of colored microspheres on systemic hemodynamics and regional blood flow in rats. *Am J Physiol*. 266:H1910-7., 1994.

Kobayashi, N., K. Kobayashi, K. Kouno, S. Yagi and H. Matsuoka. Effect of benidipine on microvascular remodeling and coronary flow reserve in two-kidney, one clip Goldblatt hypertension. *Journal Of Hypertension*. 15:1285-1294, 1997.

Kohmoto, T., P. E. Fisher, A. Gu, S. M. Zhu, C. M. DeRosa, C. R. Smith and D. Burkhoff. Physiology, histology, and 2-week morphology of acute transmyocardial channels made with a CO2 laser. *Annals Of Thoracic Surgery*. 63:1275-1283, 1997.

Kohmoto, T., P. E. Fisher, A. Gu, S. M. Zhu, O. J. Yano, H. M. Spotnitz, C. R. Smith and D. Burkhoff. Does blood flow through holmium:YAG transmyocardial laser channels? *Annals Of Thoracic Surgery*. 61:861-868, 1996.

Kohmoto, T., G. Uzun, A. Gu, S. M. Zhu, C. R. Smith and D. Burkhoff. Blood flow capacity via direct acute myocardial revascularization. *Basic Research In Cardiology*. 92:45-51, 1997.

Kowallik, P., D. Baumgart, A. Skyschally, T. Ehring and G. Heusch. Three-dimensional analysis of regional mechanical function, blood flow and electrophysiological parameters during early myocardial ischemia in dogs. *Basic Res Cardiol*. 87:215-26., 1992.

Kowallik, P., R. Schulz, B. D. Guth, A. Schade, W. Paffhausen, R. Gross and G. Heusch. Measurement of regional myocardial blood flow with multiple colored microspheres. *Circulation*. 83:974-82, 1991.

Kramer, C. M., P. D. Nicol, W. J. Rogers, M. M. Suzuki, A. Shaffer, T. M. Theobald and N. Reichek. Reduced sympathetic innervation underlies adjacent noninfarcted region dysfunction during left ventricular remodeling. *Journal Of The American College Of Cardiology*. 30:1079-1085, 1997.

Kreidstein, M. L., R. H. Levine, R. J. Knowlton and C. Y. Pang. Serial fluorometric assessments of skin perfusion in isolated perfused human skin flaps. *Br J Plast Surg*. 48:288-93, 1995.

Kuhle, W. G., G. Porenta, S. C. Huang, D. Buxton, S. S. Gambhir, H. Hansen, M. E. Phelps and H. R. Schelbert. Quantification of regional myocardial blood flow using 13N-ammonia and reoriented dynamic positron emission tomographic imaging. *Circulation*. 86:1004-17, 1992.

Kurdak, S. S., B. Grassi, P. D. Wagner and M. C. Hogan. Blood flow distribution in working in situ canine muscle during blood flow reduction. *Journal Of Applied Physiology*. 80:1978-1983, 1996.

Kuwahira, I., N. C. Gonzalez, N. Heisler and J. Piiper. Regional blood flow in conscious resting rats determined by microsphere distribution. *J Appl Physiol*. 74:203-10, 1993.

Kuwahira, I., H. Mori, Y. Moue, Y. Shinozaki, Y. Ohta, H. Yamabayashi, H. Okino, N. C. Gonzalez, N. Heisler and J. Piiper. Cardiac output and regional blood flow measurement with nonradioactive microspheres by X-ray fluorescence spectrometry in rats. *Adv Exp Med Biol*. 345:877-84, 1994.

Kuwahira, I., Y. Moue, Y. Ohta and N. C. Gonzalez. Chronic hypoxia decreases heterogeneity of pulmonary blood flow distribution in rats. *Respiration Physiology*. 104:2-3, 1996.

Kvinnsland, S., K. Heyeraas and E. S. Ofjord. Effect of experimental tooth movement on periodontal and pulpal blood flow. *Eur J Orthod*. 11:200-5, 1989.

Kvinnsland, S., A. B. Kristiansen, I. Kvinnsland and K. J. Heyeraas. Effect of experimental traumatic occlusion on periodontal and pulpal blood flow. *Acta Odontol Scand*. 50:211-9, 1992.

Kvinnsland, S., I. Kvinnsland and A. B. Kristiansen. Effect of experimental traumatic occlusion on blood flow in the temporomandibular joint of the rat. *Acta Odontol Scand*. 51:293-8, 1993.

Laham, R. J., M. Simons, M. Tofukuji, D. Hung and F. W. Sellke. Modulation of myocardial perfusion and vascular reactivity by pericardial basic fibroblast growth factor: Insight into ischemia-induced reduction in endothelium-dependent vasodilatation. *Journal of Thoracic and Cardiovascular Surgery*. 116:1022-1028, 1998.

Lee, J., R. N. Gates, H. Laks, D. C. Drinkwater, E. Rhudis, A. Aharon, A. Ardehali and P. Chang. A comparison of distribution between simultaneously or sequentially delivered antegrade/retrograde blood cardioplegia. *Journal Of Cardiac Surgery*. 11:111-115, 1996.

Li, D. S., A. C. Yong and D. Kilpatrick. Validation of a subendocardial ischaemic sheep model by intracoronary fluorescent microspheres. *Clinical & Experimental Pharmacology & Physiology*. 23:111-118, 1996.

Liu, S. X. L., C. H. Chiang, Q. S. Yao and G. C. Y. Chiou. Increase of ocular blood flow by some phytogenic compounds. *Journal Of Ocular Pharmacology And Therapeutics*. 12:95-101, 1996.

Liu, Y. H., R. C. Bahn and E. L. Ritman. Microvascular blood volume-to-flow relationships in porcine heart wall: whole body CT evaluation in vivo. *Am J Physiol*. 269:H1820-6., 1995.

Liu, Y. M., P. H. Guth, K. Kaneko, E. H. Livingston and F. C. Brunicardi. Dynamic in vivo observation of rat islet microcirculation. *Pancreas*. 8:15-21, 1993.

Lossec, G., C. Duchamp, Y. Lebreton and P. Herpin-. Postnatal changes in regional blood flow during cold-induced shivering in sow-reared piglets. *CANADIAN-JOURNAL-OF-PHYSIOLOGY-AND-PHARMACOLOGY*. 77:414-421, 1999.

Luchtel, D. L., J. C. Boykin, S. L. Bernard and R. W. Glenny. Histological methods to determine blood flow distribution with fluorescent microspheres. *Biotech Histochem.* 73:291-309, 1998.

Mahgoub, M. A., J. H. Guo, S. P. Gao, M. M. Taher, D. D. Salter, A. S. Wechsler and A. S. Abd-Elfattah. Hyperdynamic circulation of arteriovenous fistula preconditions the heart and limits infarct size. *ANNALS-OF-THORACIC-SURGERY*. 68:22-28, 1999.

Main, M. L., J. F. Escobar, S. A. Hall, A. L. Killam and P. A. Grayburn. Detection of myocardial perfusion defects by contrast echocardiography in the setting of acute myocardial ischemia with residual antegrade flow. *JOURNAL OF THE AMERICAN SOCIETY OF ECHOCARDIOGRAPHY.* 11:228-235, 1998.

Mann, C. M., K. B. Domino, S. M. Walther, R. W. Glenny, N. L. Polissar and M. P. Hlastala. Redistribution of pulmonary blood flow during unilateral hypoxia in prone and supine dogs. *JOURNAL OF APPLIED PHYSIOLOGY*. 84:2010-2019, 1998.

Mannion, J. D., P. D. Buckman, M. G. Magno and F. Dimeo. Collateral blood flow from skeletal muscle to normal myocardium. *J Surg Res*. 53:578-87., 1992.

Mannion, J. D., M. G. Magno, P. D. Buckman, F. DiMeo, R. Greene, M. Bowers, M. McHugh and H. Menduke. Acute electrical stimulation increases extramyocardial collateral blood flow after a cardiomyoplasty. *Ann Thorac Surg*. 56:1351-8., 1993.

Marber, M. S., D. M. Walker, D. J. Eveson, J. M. Walker and D. M. Yellon. A single five minute period of rapid atrial pacing fails to limit infarct size in the in situ rabbit heart. *Cardiovasc Res*. 27:597-601, 1993.

Marshall, W. G., G. B. Boatman, G. Dickerson, A. Perlin, E. P. Todd and J. R. Utley. Shunting, release, and distribution of nine and fifteen micron spheres in myocardium. *Surgery*. 79:631-7, 1976.

Masuda, Y., M. Ozaki and T. Oguma. Alteration of hepatic microcirculation by oxethazaine and some vasoconstrictors in the perfused rat liver. *Biochemical Pharmacology*. 53:1779-1787, 1997.

Maxwell, A. J., E. Schauble, D. Bernstein and J. P. Cooke. Limb blood flow during exercise is dependent on nitric oxide. *CIRCULATION*. 98:369-374, 1998.

Maxwell, L. C., A. P. Shepherd, G. L. Riedel and M. D. Morris. Effect of microsphere size on apparent intramural distribution of intestinal blood flow. *Am J Physiol*. 241:H408-14, 1981.

Mazhari, R., J. H. Omens, L. K. Waldman and A. D. McCulloch. Regional myocardial perfusion and mechanics: A model-based method of analysis. *ANNALS OF BIOMEDICAL ENGINEERING*. 26:743-755, 1998.

Mazoit, J. X., R. LeGuen, A. Decaux, P. Albaladejo and K. Samii. Application of HPLC to counting of colored microspheres in determination of regional blood flow-Special Communication. *AMERICAN JOURNAL OF PHYSIOLOGY-HEART AND CIRCULATORY PHYSIOLOGY*. 45:H1041-H1047, 1998.

McCrabb, G. J. and R. Harding. Cerebral blood flow is increased throughout 12 h of hypoxaemia in the mid-gestation ovine fetus. *Reprod Fertil Dev*. 7:463-7, 1995.

McCrabb, G. J. and R. Harding. Role of nitric oxide in the regulation of cerebral blood flow in the ovine foetus. *Clinical And Experimental Pharmacology And Physiology*. 23:10-11, 1996.

McCrabb, G. J. and R. Harding. Cerebral oxygen delivery is reduced during the acidaemia associated with prolonged hypoxaemia in the immature ovine fetus. *Biology Of The Neonate*. 71:385-394, 1997.

McCulloch, A. D., D. Sung, J. M. Wilson, R. S. Pavelec and J. H. Omens. Flow-function relations during graded coronary occlusions in the dog: effects of transmural location and segment orientation. *CARDIOVASCULAR RESEARCH*. 37:636-645, 1998.

McHugh, N. A., A. Solowiej, R. E. Klabunde and G. F. Merrill. Acute coronary vascular and myocardial perfusion effects of conjugated equine estrogen in the anesthetized dog. *Basic Research in Cardiology*. 93:470-476, 1998.

McMahan, C. A., L. C. Maxwell and A. P. Shepherd. Estimation of the distribution of blood vessel diameters from the arteriovenous passage of microspheres. *Biometrics*. 42:371-80, 1986.

Medvedev, O. S., E. R. Martynova, R. S. Akchurin and V. Y. Khalatov. Experimental estimation of chronic microsphere loss from the rat myocardium. *Biull. Eksp. Biol. Med.* 103:8-10, 1987.

Meissner, A., T. P. Weber, H. VanAken, K. Zbieranek and N. Rolf. Clonidine improves recovery from myocardial stunning in conscious chronically instrumented dogs. *Anesthesia and Analgesia*. 87:1009-1014, 1998.

Melsom, M. N., T. Flatebo and G. Nicolaysen. Hypoxia and hyperoxia both transiently affect distribution of pulmonary perfusion but not ventilation in awake sheep. *ACTA-PHYSIOLOGICA-SCANDINAVICA*. 166:151-158, 1999.

Melsom, M. N., T. Flatebo, O. V. Sjaastad, A. Aulie and G. Nicolaysen. Minor redistribution of ventilation and perfusion within the lung during exercise in sheep [In Process Citation]. *Acta Physiol Scand*. 165:283-92, 1999.

Melsom, M. N., J. Kramer-Johansen, T. Flatebo, C. Muller and G. Nicolaysen. Distribution of pulmonary ventilation and perfusion measured simultaneously in awake goats [published erratum appears in Acta Physiol Scand 1997 Jul;160(3):297]. *Acta Physiol Scand*. 159:199-208, 1997.

Mercer, D. W., K. Klemm, J. M. Cross, G. S. Smith, M. Cashman and T. A. Miller. Cholecystokinin-induced protection against gastric injury is independent of endogenous somatostatin. *American Journal Of Physiology Gastrointestinal And Liver Physiology*. 34:G692-G700, 1996.

Meyns, B., Y. Nishimura, R. Racz, R. Jashari and W. Flameng. Organ perfusion with hemopump device assistance with and without intraaortic balloon pumping. *Journal Of Thoracic And Cardiovascular Surgery*. 114:243-253, 1997.

Miglierina, R. Some applications of microspheres in flow cytometry. *Biol Cell*. 58:127-30, 1986.

Miller, S. L., K. Dickson, G. Jenkin and D. W. Walker. Physiological evidence for arteriovenous anastomoses in the uterine circulation of late-pregnant ewes. *CLINICAL AND EXPERIMENTAL PHARMACOLOGY AND PHYSIOLOGY*. 25:92-98, 1998.

Mitsumaru, A., R. Yozu, Y. Inoue, S. Tanaka, H. Yoshito, K. Kanda, Y. Tsutsui, N. Tsutsui and S. Kawada. Experimental study of combination of extraaortic balloon counterpulsation and ventricular assist cup to acute heart failure in dogs. *Asaio Journal*. 43:187-192, 1997.

Miyamae, M., H. Fujiwara, M. Kida, R. Yokota, M. Tanaka, M. Katsuragawa, K. Hasegawa, M. Ohura, K. Koga, Y. Yabuuchi and et al. Preconditioning improves energy metabolism during reperfusion but does not attenuate myocardial stunning in porcine hearts. *Circulation*. 88:223-34., 1993.

Miyataka, M., K. Ishikawa and R. Katori. Basic fibroblast growth factor increased regional myocardial blood flow and limited infarct size of acutely infarcted myocardium in dogs. *ANGIOLOGY*. 49:381-390, 1998.

Moore, R. M., J. Hardy and W. W. Muir. Mural blood flow distribution in the large colon of horses during low-flow ischemia and reperfusion. *Am J Vet Res*. 56:812-8, 1995.

Mor-Avi, V., D. David, S. Akselrod, Y. Bitton and I. Choshniak. Myocardial regional blood flow: quantitative measurement by computer analysis of contrast enhanced echocardiographic images. *Ultrasound Med Biol*. 19:619-33, 1993.

Mori, H., M. Chujo, S. Haruyama, H. Sakamoto, Y. Shinozaki, M. Uddin-Mohammed, A. Iida and H. Nakazawa. Local continuity of myocardial blood flow studied by monochromatic synchrotron radiation-excited x-ray fluorescence spectrometry. *Circ Res*. 76:1088-100, 1995.

Mori, H., S. Haruyama, Y. Shinozaki, H. Okino, A. Iida, R. Takanashi, I. Sakuma, W. K. Husseini, B. D. Payne and J. I. Hoffman. New nonradioactive microspheres and more sensitive X-ray fluorescence to measure regional blood flow. *Am J Physiol*. 263:H1946-57, 1992.

Mori, H., S. Haruyama, Y. Shinozaki, H. Sakamoto, M. Chujyo and I. Kuwahira. [Practice of the flow measurement using nonradioactive microspheres and X-ray fluorescence spectrometer]. *Kokyu To Junkan*. 41:447-50, 1993.

Mori, H., S. Haruyama, Y. Shinozaki, H. Sakamoto, H. Okino, R. Takanashi and I. Sakuma. [Regional blood flow measurement with nonradioactive microspheres]. *Kokyu To Junkan*. 40:957-61., 1992.

Morita, Y., B. D. Payne, G. S. Aldea, C. McWatters, W. Husseini, H. Mori, J. I. Hoffman and L. Kaufman. Local blood flow measured by fluorescence excitation of nonradioactive microspheres. *Am J Physiol*. 258:H1573-84, 1990.

Moros, E. G., A. W. Dutton, R. B. Roemer, M. Burton and K. Hynynen. Experimental evaluation of two simple thermal models using hyperthermia in muscle in vivo. *Int J Hyperthermia*. 9:581-98., 1993.

Mortola, J. P., D. Merazzi and L. Naso. Blood flow to the brown adipose tissue of conscious young rabbits during hypoxia in cold and warm conditions. *Pflugers Archiv-European Journal of Physiology*. 437:255-260, 1999.

Mulder, A. L. M., J. C. vanGolde, F. W. Prinzen and C. E. Blanco. Cardiac output distribution in response to hypoxia in the chick embryo in the second half of the incubation time. *JOURNAL OF PHYSIOLOGY-LONDON*. 508:281-287, 1998.

Mulder, T. L. M., J. C. vanGolde, F. W. Prinzen and C. E. Blanco. Cardiac output distribution in the chick embryo from stage 36 to 45. *Cardiovascular Research*. 34:525-528, 1997.

MunchEllingsen, J., E. Bugge and K. Ytrehus. Blockade of the K-ATP-channel by glibenclamide aggravates ischemic injury, and counteracts ischemic preconditioning. *Basic Research In Cardiology*. 91:382-388, 1996.

Murata, Y., K. Fujimori, E. J. Quilligan, N. Nagata, S. Ibara, T. Hirano and T. Kamimura. Cardiac oxygenation by extracorporeal membrane oxygenation in exteriorized fetal lambs. *American Journal Of Obstetrics And Gynecology*. 174:864-870, 1996.

Nabavi, D. G., A. Cenic, J. Dool, R. M. L. Smith, F. Espinosa, R. A. Craen, A. W. Gelb and T. Y. Lee. Quantitative assessment of cerebral hemodynamics using CT: Stability, accuracy, and precision studies in dogs. *JOURNAL-OF-COMPUTER-ASSISTED-TOMOGRAPHY*. 234:506-515, 1999.

Nagai, H., T. Nakashima, T. Suzuki and N. Yanagita. Effect of increased middle ear pressure on blood flow to the middle ear, inner ear and facial nerve in guinea pigs. *Acta Oto Laryngologica*. 116:439-442, 1996.

Nakai, S., K. Ishikawa, I. Ogawa, H. Koka, N. Kamata, H. Akiyama and R. Katori. New collateral flow increasing early after coronary occlusion prevented myocardial necrosis in dogs. *Heart Vessels*. 10:171-7, 1995.

Nakashima, T., K. Asami, K. Akanabe, K. Kuno, H. Nagai and N. Yanagita. Effect of carbon dioxide on facial nerve blood flow in rabbits. *Acta Otolaryngol Stockh*. 115:40-3., 1995.

Nakashima, T., T. Suzuki, H. Morisaki and N. Yanagita. Blood flow in the cochlea, vestibular apparatus and facial nerve. *Acta Otolaryngol Stockh*. 111:738-42, 1991.

Nakashima, T., T. Suzuki and N. Yanagita. Cochlear blood flow under increased inner ear pressure. *Ann Otol Rhinol Laryngol*. 100:394-7., 1991.

Naredi, P., J. Mattson, L. Hafstrom and L. Jacobsson. Evaluation of blood flow measurements with microspheres and rubidium--an experimental study in rats. *Int J Microcirc Clin Exp*. 9:423-37, 1990.

Nellis, S. H., K. L. Carroll and A. M. Eggleston. Measurement of phasic velocities in vessels of intact freely beating hearts. *Am J Physiol*. 260:H1264-75, 1991.

Neumann, T. and G. Heusch. Myocardial, skeletal muscle, and renal blood flow during exercise in conscious dogs with heart failure. *American Journal Of Physiology Heart And Circulatory Physiology*. 42:H2452-H2457, 1997.

Nohara, R., K. Okuda, M. Ogino, R. Hosokawa, N. Tamaki, J. Konishi, Y. Fujibayashi, Y. Yonekura, M. Fujita and S. Sasayama. Evaluation of myocardial viability with iodine-123-BMIPP in a canine model. *Journal Of Nuclear Medicine*. 37:1403-1407, 1996.

Nose, Y., T. Nakamura and M. Nakamura. The microsphere method facilitates statistical assessment of regional blood flow. *Basic Res Cardiol*. 80:417-29, 1985.

Okuda, K., R. Nohara, M. Fujita, N. Tamaki, J. Konishi and S. Sasayama. Technetium-99m-pyrophosphate uptake as an indicator of myocardial injury without infarct. *J Nucl Med*. 35:1366-70., 1994.

Oohara, K., A. Usui, M. Murase, M. Tanaka and T. Abe. Regional cerebral tissue blood flow measured by the colored microsphere method during retrograde cerebral perfusion. *J Thorac Cardiovasc Surg*. 109:772-9., 1995.

Oohara, K., A. Usui, M. Tanaka, T. Abe and M. Murase. Determination of organ blood flows during retrograde inferior vena caval perfusion. *Ann Thorac Surg*. 58:139-45., 1994.

Ooiwa, H., T. Miura, T. Iwamoto, T. Ogawa, R. Ishimoto, T. Adachi and O. Iimura. Superoxide dismutase attenuated post-ischaemic contractile dysfunction in a myocardial xanthine oxidase deficient species. *Clin Exp Pharmacol Physiol*. 19:119-25., 1992.

Orgul, S., G. A. Cioffi, D. R. Bacon, A. Bhandari and E. M. VanBuskirk. Measurement of optic nerve blood flow with nonradioactive colored microspheres in rabbits. *Microvascular Research*. 51:175-186, 1996.

Orgul, S., G. A. Cioffi, D. R. Bacon and E. M. VanBuskirk. An endothelin-1-induced model of chronic optic nerve ischemia in rhesus monkeys. *Journal Of Glaucoma*. 5:135-138, 1996.

Orgul, S., G. A. Cioffi, D. J. Wilson, D. R. Bacon and E. M. VanBuskirk. An endothelin-1 induced model of optic nerve ischemia in the rabbit. *Investigative Ophthalmology & Visual Science*. 37:1860-1869, 1996.

Pinkerton, K. E., J. T. Gallen, R. R. Mercer, V. C. Wong, C. G. Plopper and B. K. Tarkington. Aerosolized fluorescent microspheres detected in the lung using confocal scanning laser microscopy. *Microsc Res Tech*. 26:437-43, 1993.

Pisarri, T. E., H. M. Coleridge and J. C. Coleridge. Reflex bronchial vasodilation in dogs evoked by injection of a small volume of water into a bronchus. *J Appl Physiol*. 75:2195-202., 1993.

Polissar, N. L., D. Stanford and R. W. Glenny. The 400 microsphere per piece "rule" does not apply to all blood flow studies. Am. J. Physiol. in press.

Powers, K. M., C. Schimmel, R. W. Glenny and C. M. Bernards. Cerebral blood flow determinations using fluorescent microspheres: variations on the sedimentation method validated. *Journal of Neuroscience Methods*. 87:159-165, 1999.

Preckel, B., W. Schlack, D. Obal, H. Barthel, D. Ebel, S. Grunert and V. Thamer. Effect of acidotic blood reperfusion on reperfusion injury after coronary artery occlusion in the dog heart. *JOURNAL OF CARDIOVASCULAR PHARMACOLOGY*. 31:179-186, 1998.

Presson, R. G., Jr., J. A. Graham, C. C. Hanger, P. S. Godbey, S. A. Gebb, R. A. Sidner, R. W. Glenny and W. W. Wagner, Jr. Distribution of pulmonary capillary red blood cell transit times. *J Appl Physiol*. 79:382-8, 1995.

Pries, A. R., K. Ley, M. Claassen and P. Gaehtgens. Red cell distribution at microvascular bifurcations. *Microvasc Res*. 38:81-101, 1989.

Prinzen, F. W. and R. W. Glenny. Developments in non-radioactive microsphere techniques for blood flow measurement. *Cardiovasc Res*. 28:1467-75, 1994.

Quinones, A. and B. J. Cheirif. New perspectives for perfusion imaging in echocardiography. *Circulation*. 83:III104-10, 1991.

Raab, S., E. Thein, A. G. Harris and K. Messmer. A new sample-processing unit for the fluorescent microsphere method. *American Journal of Physiology-Heart and Circulatory Physiology*. 45:H1801-H1806, 1999.

Rao, P. V., R. F. Stahl, B. R. Soller, K. G. Shortt, C. Hsi, K. J. Cotter, J. M. BelleIsle and J. M. Moran. Retrograde abdominal visceral perfusion: Is it beneficial? *Annals Of Thoracic Surgery*. 60:1704-1708, 1995.

Rasmussen, O., F. F. Lauszus, C. Christiansen, C. Thomsen and K. Hermansen. Differential Effects Of Saturated and Monounsaturated Fat On Blood Glucose and Insulin Responses In Subjects With Non-Insulin-Dependent Diabetes Mellitus. *American Journal of Clinical Nutrition*. 63:249-253, 1996.

Rattigan, S., G. J. Appleby, K. A. Miller, J. T. Steen, K. A. Dora, E. Q. Colquhoun and M. G. Clark. Serotonin inhibition of 1-methylxanthine metabolism parallels its vasoconstrictor activity and inhibition of oxygen in perfused rat hindlimb. *Acta Physiologica Scandinavica*. 161:161-169, 1997.

Reeves, W. J. and K. Rakusan. Myocardial capillary flow pattern as determined by the method of coloured microspheres. *Adv. Exp. Med. Biol.* 222:447-53, 1988.

Revelly, J. P., T. Ayuse, N. Brienza, H. E. Fessler and J. L. Robotham. Endotoxic shock alters distribution of blood flow within the intestinal wall. *Critical Care Medicine*. 24:1345-1351, 1996.

Ring, G. C., A. S. Blum, T. Kurbatov, W. G. Moss and W. Smith. Size of microspheres passing through pulmonary circuit in the dog. *American Journal of Applied Physiology*. 200:1191-1196, 1961.

Robertson, H. T., R. W. Glenny, D. Stanford, L. M. McInnes, D. L. Luchtel and D. Covert. High-resolution maps of regional ventilation utilizing inhaled fluorescent microspheres. *Journal Of Applied Physiology*. 82:943-953, 1997.

Rolf, N., A. Meissner, H. VanAken, T. P. Weber, D. Hammel and T. Mollhoff. The effects of thoracic epidural anesthesia on functional recovery from myocardial stunning in propofol-anesthetized dogs. *Anesthesia And Analgesia*. 84:723-729, 1997.

Rolf, N., M. VandeVelde, P. F. Wouters, T. Mollhoff, T. P. Weber and H. K. VanAken. Thoracic epidural anesthesia improves functional recovery from myocardial stunning in conscious dogs. *Anesthesia And Analgesia*. 83:935-940, 1996.

Rose, J., T. Ehring, S. G. Sakka, A. Skyschally and G. Heusch. Aspirin does not prevent the attenuation of myocardial stunning by the ACE inhibitor ramiprilat. *Journal Of Molecular And Cellular Cardiology*. 28:603-613, 1996.

Rovainen, C. M., T. A. Woolsey, N. C. Blocher, D. B. Wang and O. F. Robinson. Blood flow in single surface arterioles and venules on the mouse somatosensory cortex measured with videomicroscopy, fluorescent dextrans, nonoccluding fluorescent beads, and computer-assisted image analysis. *J Cereb Blood Flow Metab*. 13:359-71, 1993.

Rudis, E., R. N. Gates, H. Laks, D. C. Drinkwater, A. Ardehali, A. Aharon and P. Chang. Coronary sinus ostial occlusion during retrograde delivery of cardioplegic solution significantly improves cardioplegic distribution and efficacy [see comments]. *J Thorac Cardiovasc Surg*. 109:941-6; discussion 946-7., 1995.

Rudolph, A. M. and M. A. Heymann. The circulation of the fetus in utero. Methods for studying distribution of blood flow, cardiac output and organ blood flow. *Circ Res*. 21:163-84, 1967.

Saida, A., H. Ito, T. Shibuya and Y. Watanabe. Time-course alterations of monoamine levels and cerebral blood flow in brain regions after subarachnoid hemorrhage in rats. *Brain Research Bulletin*. 43:69-80, 1997.

Saitou, H., T. Watanabe, J. W. Zhang, N. Oshikiri, Y. Iijima, K. Inui, S. Kuraoka and Y. Shimazaki. Regional tissue blood flow and pH in the brain during deep hypothermic retrograde brain perfusion. *Journal Of Surgical Research*. 72:135-140, 1997.

Sakaki, M., Y. Taenaka, E. Tatsumi, T. Nakatani, M. Kinoshita, H. Akagi, T. Masuzawa, Y. Matsuo, K. Inoue, Y. Baba and et al. Pulmonary function in a non-pulsatile pulmonary circulation. *Asaio J*. 38:M366-9., 1992.

Sakka, S. G., D. R. Wallbridge and G. Heusch. Methods for the measurement of coronary blood flow and myocardial perfusion - Glossary. *Basic Research In Cardiology*. 91:155-178, 1996.

Sakurai, H., L. D. Traber and D. L. Traber. Altered systemic organ blood flow after combined injury with burn and smoke inhalation. *SHOCK*. 9:369-374, 1998.

Salmons, S., A. T. M. Tang, J. C. Jarvis, H. Degens, M. Hastings and T. L. Hooper. Morphological and functional evidence, and clinical importance, of vascular anastomoses in the latissimus dorsi muscle of the sheep. *JOURNAL OF ANATOMY*. 193:93-104, 1998.

Sato, M., T. Saito, M. Mitsugi, S. I. Saitoh, T. Niitsuma, K. Maehara and Y. Maruyama. Effects of cardiac contraction and coronary sinus pressure elevation on collateral circulation. *American Journal Of Physiology Heart And Circulatory Physiology*. 40:H1433-H1440, 1996.

Saxena, P. R. and P. D. Verdouw. Tissue blood flow and localization of arteriovenous anastomoses in pigs with microspheres of four different sizes. *Pflugers Arch*. 403:128-35, 1985.

Schenarts, P. J., H. G. Bone, L. D. Traber and D. L. Traber. Effect of severe smoke inhalation injury on systemic microvascular blood flow in sheep. *Shock*. 6:201-205, 1996.

Schimmel, C., D. Frazer and R.W. Glenny. Extending Flourescent Microsphere Methods for Regional Organ Blood Flow to 13 Simultaneous Colors. *Am J Physiol Heart Circ Physiol.* 280: H2496-506, 2001.

Schimmel, C, D. Frazer, S.R. Huckins and R.W. Glenny. Validation of Automated Spectroflurimetry for Measurement of Regional Organ Perfusion Using Fluorescent Microspheres. *Comput Methods Programs Biomed.* 62:115-25, 2000.

Schlack, W., D. Ebel, S. Grunert, S. Halilovic, O. Meyer and V. Thamer. Effect of heart rate reduction by 4-(N-ethyl-N-phenylamino)-1,2-dimethyl-6- (methylamino)pyrimidinium chloride on infarct size in dog. *ARZNEIMITTEL-FORSCHUNG/DRUG RESEARCH*. 48:26-33, 1998.

Schmid-Schonbein, G. W., R. Skalak, S. Usami and S. Chien. Cell distribution in capillary networks. *Microvasc Res*. 19:18-44, 1980.

Schosser, R., K. E. Arfors and K. Messmer. MIC-II - a program for the determination of cardiac output, arterio-venous shunt and regional blood flow using the radioactive microsphere method. *Comput Programs Biomed*. 9:19-38, 1979.

Schwanke, U., H. Strauss, G. Arnold and J. D. Schipke. Analysis of respiratory water - A new method for evaluation of myocardial energy metabolism. *J Appl Physiol*. 81:2115-2122, 1996.

Shabsigh, A., D. T. Chang, D. F. Heitjan, A. Kiss, C. A. Olsson, P. J. Puchner and R. Buttyan. Rapid reduction in blood flow to the rat ventral prostate gland after castration: Preliminary evidence that androgens influence prostate size by regulating blood flow to the prostate gland and prostatic endothelial cell survival. *PROSTATE*. 36:201-206, 1998.

Shimada, K., K. Yoshida, H. Tadokoro, S. Kitsukawa, A. Takami, K. Suzuki, S. Tanada and Y. Masuda. High-resolution cardiac PET in rabbits: Imaging and quantitation of myocardial blood flow. *Journal of Nuclear Medicine*. 39:2022-2027, 1998.

Shin, C., M. P. Kinsky, J. A. Thomas, D. L. Traber and G. C. Kramer. Effect of cutaneous burn injury and resuscitation on the cerebral circulation in an ovine model. *BURNS*. 24:39-45, 1998.

Sidi, A. and W. Rush. An alternative to radioactive microspheres for measuring regional myocardial blood flow .1. colored microspheres. *Journal of Cardiothoracic & Vascular Anesthesia*. 10:368-373, 1996.

Sidi, A. and W. Rush. An alternative to radioactive microspheres for measuring regional myocardial blood flow .2. laser-doppler perfusion monitor. *Journal of Cardiothoracic & Vascular Anesthesia*. 10:374-377, 1996.

Simor, T., W. J. Chu, L. Johnson, A. Safranko, M. Doyle, G. M. Pohost and G. A. Elgavish. In vivo MRI visualization of acute myocardial ischemia and reperfusion in ferrets by the persistent action of the contrast agent Gd(BME-DTTA). *Circulation*. 92:3549-3559, 1995.

Smith, M. V., R. F. Stahl, C. Cronin, C. Hsi, J. M. Li, J. BelleIsle, M. Knox and T. J. Vander-Salm. Retrograde coronary sinus perfusion provides non-homogeneous myocardial blood flow. *Cardiology*. 83:331-8, 1993.

Souders, J. E., S. C. George, N. L. Polissar, E. R. Swenson and M. P. Hlastala. Tracheal gas exchange: perfusion-related differences in inert gas elimination. *J Appl Physiol*. 79:918-28, 1995.

Spinale, F. G., R. Tanaka, F. A. Crawford and M. R. Zile. Changes in myocardial blood flow during development of and recovery from tachycardia-induced cardiomyopathy. *Circulation*. 85:717-29, 1992.

Steinhausen, M., B. Zimmerhackl, H. Thederan, R. Dussel, N. Parekh, H. U. Esslinger, G. von-Hagens, D. Komitowski and F. D. Dallenbach. Intraglomerular microcirculation: measurements of single glomerular loop flow in rats. *Kidney Int*. 20:230-9, 1981.

Stryer, L. and R. P. Haugland. Energy transfer: A spectroscopic ruler. *Proc. Natnl. Acad. Sci.* 58:719-726, 1967.

Suckfull, M., S. Holtmann and R. Hecht. A new method for measuring internal ear circulation using colored microspheres. *Laryngorhinootologie*. 74:141-4., 1995.

Suckfull-M., Winkler-G., Thein-E., Raab-S., Schorn-K. and Mees-K. Changes in serum osmolarity influence the function of outer hair cells. *Acta Oto-Laryngologica*. 119:316-321, 1999.

Suo, Z. M., J. Humphrey, A. Kundtz, F. Sethi, A. Placzek, F. Crawford and M. Mullan. Soluble Alzheimers beta-amyloid constricts the cerebral vasculature in vivo. *Neuroscience Letters*. 257:77-80, 1998.

Suzuki, T., T. Nakashima and N. Yanagita. Effects of increased cerebrospinal fluid pressure on cochlear and cerebral blood flow. *Eur Arch Otorhinolaryngol*. 250:332-6, 1993.

Svensson, A. M., C. G. Ostenson, S. Sandler, S. Efendic and L. Jansson. Inhibition of nitric oxide synthase by NG-nitro-L-arginine causes a preferential decrease in pancreatic islet blood flow in normal rats and spontaneously diabetic GK rats. *Endocrinology*. 135:849-53., 1994.

Symons, J. D., S. D. Correa and S. Schaefer. Na-H exchange inhibition with cariporide limits functional impairment caused by repetitive ischemia. *Journal of Cardiovascular Pharmacology*. 32:853-862, 1998.

Tabor, O. B., M. J. Bosse, K. G. Greene, H. E. Gruber, K. Kaysinger, S. H. Sims, S. R. Blumenthal and J. E. Kellam. Effects of surgical approaches for acetabular fractures with associated gluteal vascular injury. *JOURNAL OF ORTHOPAEDIC TRAUMA*. 12:78-84, 1998.

Takahata, O., K. Ichihara, Y. Abiko and H. Ogawa. Sevoflurane preserves endocardial blood flow during coronary ligation in dogs: comparison with adenosine. *ACTA ANAESTHESIOLOGICA SCANDINAVICA*. 42:225-231, 1998.

Takanashi, H. and M. Akima. Protective effects of arbaprostil against indomethacin-induced gastric lesions in rats: significance of maintained gastric blood flow. *Jpn J Pharmacol*. 59:349-55., 1992.

Takao, S., M. Maeda, M. Inoue, T. Fukushima, M. Tomonaga and Y. Hayashida. Spinal cord blood flow decreases following microinjection of sodium nitroprusside into the nucleus tractus solitarii of anesthetized rats. *Neuroscience Research*. 25:285-291, 1996.

Tamaki, Y., E. Kawamoto, M. Araie, S. Eguchi and H. Fujii. [Noninvasive two-dimensional analysis of retinal microcirculation using the laser speckle phenomenon--II. Comparison of results with those obtained with the microsphere technique]. *Nippon Ganka Gakkai Zasshi*. 98:169-74., 1994.

Tan, D. Y., M. R. Cernadas, P. Aragoncillo, M. A. Castilla, M. V. A. Arroyo, A. J. L. Farre, S. Casado and C. Caramelo. Role of nitric oxide-related mechanisms in renal function in ageing rats. *NEPHROLOGY DIALYSIS TRANSPLANTATION*. 13:594-601, 1998.

Tan, W. P., K. W. Riggs, R. L. Thies and D. W. Rurak. Use of an automated fluorescent microsphere method to measure regional blood flow in the fetal lamb. *Canadian Journal Of Physiology And Pharmacology*. 75:959-968, 1997.

Tanabe, T., T. Iwamoto, O. Iwata, M. Aikawa, S. Kusuzaki, S. Handa, Y. Shinozaki and H. Mori. Electrophysiologic and blood-flow responses in the endocardium and epicardium to disopyramide and MS-551 during myocardial ischemia in the dog. *JOURNAL-OF-CARDIOVASCULAR-PHARMACOLOGY*. 34:275-286, 1999.

Tang, A. T. M., J. C. Jarvis, T. L. Hooper and S. Salmons. Observation and basis of improved blood flow to the distal latissimus dorsi muscle: a case for electrical stimulation prior to grafting. *Cardiovascular Research*. 40:131-137, 1998.

Tatsumi, E., K. Miyazaki, K. Toda, Y. Taenaka, T. Nakatani, Y. Baba, T. Masuzawa, Y. Wakisaka, K. Eya, T. Nishimura, Y. Takewa, T. Ohno and H. Takano. Influence of non pulsatile systemic circulation on tissue blood flow and oxygen metabolism. *Asaio Journal*. 42:M757-M762, 1996.

Tokuda, N. and R. B. Levy. 1,25-dihydroxyvitamin D-3 stimulates phagocytosis but suppresses HLA-DR and CD13 antigen expression in human mononuclear phagocytes. *Proceedings Of The Society For Experimental Biology And Medicine*. 211:244-250, 1996.

Tretli, S. and M. Gaard. Lifestyle Changes During Adolescence and Risk Of Breast Cancer - an Ecologic Study Of the Effect Of World War Ii In Norway. *Cancer Causes & Control*. 7:507-512, 1996.

Tsuchida, Y., N. Aoki, O. Fukuda, M. Nakano and H. Igarashi. Changes in hemodynamics in jejunal flaps of rabbits due to ischemia, venous congestion, and reperfusion as measured by means of colored microspheres., 1998

Tsumoto, S., S. Kawashima and T. Iwasaki. Unaltered size of right ventricular infarct in dogs with right ventricular hypertrophy induced by pressure overload. *Am J Physiol*. 268:H1781-7, 1995.

Usui, K., T. Tanabe, S. Handa, Y. Shinozaki and H. Mori. Disproportional response between refractory period and blood flow to alpha(1) and beta-andrenoceptor blockade in canine ischemic myocardium. *Cardiovascular Drugs and Therapy*. 12:561-571, 1998.

Utley, J., E. L. Carlson, J. I. Hoffman, H. M. Martinez and G. D. Buckberg. Total and regional myocardial blood flow measurements with 25 micron, 15 micron, 9 micron, and filtered 1-10 micron diameter microspheres and antipyrine in dogs and sheep. *Circ Res*. 34:391-405, 1974.

van Golde, J. M., T. A. Mulder, E. Scheve, F. W. Prinzen and C. E. Blanco. Hyperoxia and local organ blood flow in the developing chick embryo. *J Physiol (Lond)*. 515:243-248, 1999.

van Oosterhout, M. F., H. M. Willigers, R. S. Reneman and F. W. Prinzen. Fluorescent microspheres to measure organ perfusion: validation of a simplified sample processing technique. *Am J Physiol*. 269:H725-33, 1995.

van Oosterhout, M. F. M. and F. W. Prinzen. The fluorescent microsphere method for determination of organ blood flow. *FASEB J.* 8:A854, 1994.

van Oosterhout, M. F. M., F. W. Prinzen, S. Sakurada, R. W. Glenny and J. R. S. Hales. Fluorescent microspheres are superior to radioactive microspheres in chronic blood flow measurements. *AMERICAN JOURNAL OF PHYSIOLOGY-HEART AND CIRCULATORY PHYSIOLOGY*. 44:H110-H115, 1998.

Vandevska-Radunovic, V., A. B. Kristiansen, K. J. Heyeraas and S. Kvinnsland. Changes in blood circulation in teeth and supporting tissues incident to experimental tooth movement. *Eur J Orthod*. 16:361-9, 1994.

Vandevska-Radunovic, V., I. H. Kvinnsland and S. Kvinnsland. Effect of inferior alveolar nerve axotomy on periodontal and pulpal blood flow subsequent to experimental tooth movement in rats. *ACTA ODONTOLOGICA SCANDINAVICA*. 56:57-64, 1998.

vanDoorn, C. A. M., H. Degens, M. S. Bhabra, C. B. W. Till, T. E. Shaw, J. C. Jarvis, S. Salmons and T. L. Hooper. Intramural blood flow of skeletal muscle ventricles functioning as aortic counterpulsators. *Annals Of Thoracic Surgery*. 64:86-93, 1997.

Vescovo, G., C. Ceconi, P. Bernocchi, R. Ferrari, U. Carraro, G. B. Ambrosio and L. DallaLibera. Skeletal muscle myosin heavy chain expression in rats with monocrotaline-induced cardiac hypertrophy and failure. Relation to blood flow and degree of muscle atrophy. *CARDIOVASCULAR RESEARCH*. 39:233-241, 1998.

Viroonchatapan, E., H. Sato, M. Ueno, I. Adachi, K. Tazawa and I. Horikoshi. Magnetic targeting of thermosensitive magnetoliposomes to mouse livers in an in situ on-line perfusion system. *Life Sciences*. 58:2251-2261, 1996.

Walker, D. M., J. M. Walker and D. M. Yellon. Global myocardial ischemia protects the myocardium from subsequent regional ischemia. *Cardioscience*. 4:263-6., 1993.

Walland, A., H. Weihs and E. Mutschler. Perfusion pressure and transmural flow distribution in the left ventricles of isolated rat hearts. *Clin Exp Pharmacol Physiol*. 20:723-9, 1993.

Walter, B., R. Bauer, E. Gaser and U. Zwiener. Validation of the multiple colored microsphere technique for regional blood flow measurements in newborn piglets. *Basic Research In Cardiology*. 92:191-200, 1997.

Walter, D. H., U. Hink, T. Asahara, E. VanBelle, J. Horowitz, Y. Tsurumi, R. Vandlen, H. Heinsohn, B. Keyt, N. Ferrara, J. F. Symes and J. M. Isner. The in vivo bioactivity of vascular endothelial growth factor vascular permeability factor is independent of N-linked glycosylation. *Laboratory Investigation*. 74:546-556, 1996.

Walther, S., K. Domino, R. Glenny, N. Polissar and M. Hlastala. Pulmonary blood flow distribution has a hilar-to-peripheral gradient in awake, prone sheep. *J. Appl. Physiol.* 82:678-685, 1997.

Walther, S. M., K. B. Domino, R. W. Glenny and M. P. Hlastala. Pulmonary blood flow distribution in sheep: Effects of anesthesia, mechanical ventilation, and change in posture. *Anesthesiology*. 87:335-342, 1997.

Walther, S. M., K. B. Domino, R. W. Glenny and M. P. Hlastala. Positive end-expiratory pressure redistributes perfusion to dependent lung regions in supine but not in prone lambs. *Critical Care Medicine*. 27:37-45, 1999.

Wang, X. J., F. Q. Li, S. Said, J. M. Capasso and A. M. Gerdes. Measurement of regional myocardial blood flow in rats by unlabeled microspheres and Coulter Channelyzer. *American Journal Of Physiology Heart And Circulatory Physiology*. 40:H1656-H1665, 1996.

Weihs, H., E. Mutschler and A. Walland. Alinidine prevents hypoperfusion-induced transmural flow redistribution in isolated paced rat hearts. *Clin Exp Pharmacol Physiol*. 21:471-6, 1994.

Wiedeman, M. P. Dimensions of Blood Vessels from Distributing Artery to Collecting Vein. *Circulation Research*. XII:375-378, 1963.

Wieland, W., P. F. Wouters, H. Van Aken and W. Flameng. Measurement of Organ Blood Flow with Coloured Microspheres: a First Time-Saving Improvement using Automated Spectrophotometry. *Proceedings of Computers in Cardiology*. 691-694, 1993.

Wouters, P. F., M. VandeVelde, H. VanAken and W. Flameng. Ischemic event characteristics determine the extent of myocardial stunning in conscious dogs. *Basic Research In Cardiology*. 91:140-146, 1996.

Wu, C. H., D. C. Lindsey, D. L. Traber, C. E. Cross, D. N. Herndon and G. C. Kramer. Measurement of bronchial blood flow with radioactive microspheres in awake sheep. *J Appl Physiol*. 65:1131-9, 1988.

Xuan, B., Y. H. Zhou, R. Varma and G. C. Y. Chiou. Effects of some N-nitropyrazole derivatives on ocular blood flow and retinal function recovery after ischemic insult. *Journal of Ocular Pharmacology and Therapeutics*. 15:135-142, 1999.

Yamamoto, N., T. Kohmoto, A. G. Gu, C. DeRosa, C. R. Smith and D. Burkhoff. Angiogenesis is enhanced in ischemic canine myocardium by transmyocardial laser revascularization. *JOURNAL OF THE AMERICAN COLLEGE OF CARDIOLOGY*. 31:1426-1433, 1998.

Yamasaki, T. and T. Tsutsui. Spontaneous emission from fluorescent molecules embedded in photonic crystals consisting of polystyrene microspheres. *APPLIED PHYSICS LETTERS*. 72:1957-1959, 1998.

Yanagi, S., K. Takeuchi, T. Takeda, M. Ishikawa and I. Miura. Effects of inotropic stimulation on phosphate compounds in ischaemic canine hearts. *Cardiovasc Res*. 27:1435-43., 1993.

Yanagi, S., K. Takeuchi, T. Takeda, M. Ishikawa and I. Miura. Comparison of the effects of dobutamine and isoproterenol in ischemic hearts by phosphorus-31 nuclear magnetic resonance spectroscopy. *Jpn Circ J*. 58:338-50., 1994.

Yang, R., Q. Liu, J. L. Unthank, M. D. Pescovitz and J. L. Grosfeld. Preservation of postprandial intestinal hyperemic response after small bowel transplantation. *J Pediatr Surg*. 30:1090-2., 1995.

Yen, R. T. and Y. C. Fung. Effect of velocity of distribution on red cell distribution in capillary blood vessels. *J R Coll Gen Pract Occas Pap*. 235:H251-7, 1978.

Yipintsoi, T., W. A. Dobbs, Jr., P. D. Scanlon, T. J. Knopp and J. B. Bassingthwaighte. Regional distribution of diffusible tracers and carbonized microspheres in the left ventricle of isolated dog hearts. *Circ Res*. 33:573-87, 1973.

Zeltner, T. B., T. D. Sweeney, W. A. Skornik, H. A. Feldman and J. D. Brain. Retention and clearance of 0.9-micron particles inhaled by hamsters during rest or exercise. *J Appl Physiol*. 70:1137-45, 1991.

Zink, B. J., C. H. Schultz, X. Wang, M. Mertz, S. A. Stern and A. L. Betz. Effects of ethanol on brain lactate in experimental traumatic brain injury with hemorrhagic shock. *BRAIN-RESEARCH*. 837:1-7, 1999.

Zippel, K. C., H. B. Lillywhite and C. R. J. Mladinich. Contribution of the vertebral artery to cerebral circulation in the rat snake Elaphe obsoleta. *JOURNAL OF MORPHOLOGY*. 238:39-51, 1998.

Zwissler, B., R. Schosser, C. Weiss, V. Iber, M. Weiss, C. Schwickert, P. Spengler and K. Messmer. Methodological error and spatial variability of organ blood flow measurements using radiolabeled microspheres. *Res Exp Med Berl*. 191:47-63, 1991.

# Appendix A: List of Suppliers

| Item | Catalog# | Price | Company | Address | Telephone # |
|---|---|---|---|---|---|
| **Plastics** | | | | | |
| CRYOSURE VIALS 1.5ML NO CAPS 1000/PKG | 220-3902-080 | $51.75 | EVERGREEN SCIENTIFIC | 2300 E 49th St. PO Box 58238 Los Angeles, CA 90058-0248 | 800-421-6261 |
| CRYOSURE VIALS 3.5ML NO CAPS 1000/PKG | 220-3905-080 | $59.80 | EVERGREEN SCIENTIFIC | | |
| CRYOSURE VIALS CAPS 200/PKG | 300-3900-020<br>300-3900-B20<br>300-3900-E20<br>300-3900-G20<br>300-3900-L20<br>300-3900-R20<br>300-3900-Y20 | $6.00<br>$6.00<br>$6.00<br>$6.00<br>$6.00<br>$6.00<br>$6.00 | EVERGREEN SCIENTIFIC | | |
| CRYOSURE VIALS 1.5ML WITH CAPS 1000/PKG | 240-3902-G80 | $91.50 | EVERGREEN SCIENTIFIC | | |
| CRYOSURE VIAL TRAY 1/EA | 240-3919-W80 | $13.00 | EVERGREEN SCIENTIFIC | | |
| CRYOSURE VIALS 3.5ML WITH CAPS 1000/PKG | 240-3905-G80 | $99.50 | EVERGREEN SCIENTIFIC | | |
| CENTRIFUGE TUBE 50ML 1000/CS | 300-3541-G20 | $65.00 | EVERGREEN SCIENTIFIC | | |
| CENTRIFUGE 50ML TUBE CAPS 1000/CS | 220-3550-030 | $65.00 | EVERGREEN SCIENTIFIC | | |
| POLYPROPYLENE 96 WELL MICROTITER PLATES | | pending (case) | WILKS PLASTICS | 4800 Green Valley RD. Union Bridge, MD 21791 | 410-775-7917 |
| POLYAMIDE WOVEN FILTERS | | $500.00 (case) | PERKIN ELMER | 761 Main Ave. Norwalk, CT 06859-0156 | 800-762-8288 |

| Item | Catalog# | Price | Company | Address | Telephone # |
|---|---|---|---|---|---|
| **Filtration** | | | | | |
| STAINLESS SCREEN | 92255 | $23.00 | PORETICS CORP | 111 Lindburgh Ave Livermore, CA 94550 | 415-373-0500 |
| TEFLON GASKET | 92260 | $4.00 | PORETICS | | |
| GLASS HOLDER 25mm SS SCREEN | 92250 | $139.00 | PORETICS | | |
| FILTER FORCEPS | 99090 | $18.00 | PORETICS | | |
| 25mm MEMBRANES 100/PKG | 11078 | $43.00 | PORETICS | | |
| **Microspheres** | | | | | |
| 15-µm FLUORESCENT MICROSPHERES(10Million/vial) | | | MOLECULAR PROBES | 4849 Pitchford Ave Eugene, OR 97402 | 541-344-3007 |
| 15µm | | | | | |
| BLUE | F8837 | $175.00 | | | |
| BLUE- GREEN | F8838 | $175.00 | | | |
| GREEN | F8840 | $175.00 | | | |
| YELLOW GREEN | F8844 | $175.00 | | | |
| CRIMSON | F8839 | $175.00 | | | |
| RED | F8842 | $175.00 | | | |
| SCARLET | F8843 | $175.00 | | | |
| 15-µm FLUORESCENT MICROSPHERES (20Million/vial) | | | TRITON TECH | 4616 Sante Fe St San Diego, CA 92109 | 800-872-1251 |
| BLUE | 255-9890 | $275.00 | | | |
| YELLOW GREEN | 255-9891 | $275.00 | | | |
| RED | 255-9893 | $275.00 | | | |
| CRIMSON | 255-9894 | $275.00 | | | |
| FAR RED | 255-9895 | $275.00 | | | |
| BLUE-GREEN | 255-9896 | $275.00 | | | |
| GREEN | 255-9897 | $275.00 | | | |
| SCARLET | 255-9895 | $275.00 | | | |
| **Misc. Supplies** | | | | | |
| REPEATER PIPETTER EFFENDORF | P5063-20 | $355.00 | BAXTER | Baxter Scientific Pdts 1430 Waukegan Rd McGaw Park, IL 60085-6787 | 708-689-8410 |
| EPPENDORF COMBITIP SYRINGES 12.5ML 100/PK | P5063-27 | $98.00 | BAXTER | | |

| Item | Catalog# | Price | Company | Address | Telephone # |
|---|---|---|---|---|---|
| **Chemicals** | | | | | |
| TWEEN 80 (POLYOXY-ETHYLENE SORBITAL MONOOLEATE) | P1754 | $51.35 (gallon) | SIGMA CHEMICAL | PO Box 14508 St. Louis, MO 63178-9916 | 800-325-3010 |
| METHANOL ABSOLUTE | | | | | |
| **Fluorimeter Supplies** | | | | | |
| CUVETTE | 18-F | $99.00 | STARNA CELLS INC. | PO Box 1919 Atascadero, CA 93423 | 805-466-8855 |
| CUVETTE RACK | 58020-105 | $13.45 | VWR | Regional Offices | 800-333-6336 |
| CUVETTE WASHER | KT459961 | $127.00 | VWR | | 800-333-6336 |
| NEOPRENE GASKET 12/PKG | KT459951 | $22.40 | VWR | | 800-333-6336 |
| ES™ 7X | 76-671-94 | | ICN Biomedical Inc. | 3300 Hyland Ave Costa Masa, CA 92626 | |
| **Fluorimeter** | | | | | |
| LUMINESCENT SPECTROMETER LS50B | L225-0115 | $28,615.00 | PERKIN ELMER | 761 Main Ave. Norwalk, CT 06859-0156 | 800-762-8288 |

# Appendix B: Contributors to Manual


Dowon An
University of Washington

Susan Bernard, D.V.M.
University of Washington

Michael Brinkley, Ph.D.
Emerald Diagnostics

Pam Campbell
University of Washington

Robb Glenny, M.D.
University of Washington

Dan Luchtel, Ph.D.
University of Washington

Karen Powers
University of Washington

Fritz Prinzen, Ph.D.
CVRI, Maastricht, The Netherlands

H. Thomas Robertson, M.D.
University of Washington

Erin Shade
University of Washington

Carmel Schimmel
University of Washington

Jeffery Taylor, Ph.D.
Perkin Elmer

Matthijs F.M. van Oosterhout, M.D.
CVRI, Maastricht, The Netherlands